
Electronic Thesis and Dissertation Repository

8-10-2017 12:00 AM

The Effect of Radial and Ulnar Length Change on Distal Forearm Loading

Ahaoiza D. Isa, *The University of Western Ontario*

Supervisor: Dr. GJW King, *The University of Western Ontario*

Joint Supervisor: Dr. JA Johnson, *The University of Western Ontario*

A thesis submitted in partial fulfillment of the requirements for the Master of Science degree in Surgery

© Ahaoiza D. Isa 2017

Follow this and additional works at: <https://ir.lib.uwo.ca/etd>



Part of the [Biomechanics and Biotransport Commons](#), and the [Other Biomedical Engineering and Bioengineering Commons](#)

Recommended Citation

Isa, Ahaoiza D., "The Effect of Radial and Ulnar Length Change on Distal Forearm Loading" (2017). *Electronic Thesis and Dissertation Repository*. 4707.
<https://ir.lib.uwo.ca/etd/4707>

This Dissertation/Thesis is brought to you for free and open access by Scholarship@Western. It has been accepted for inclusion in Electronic Thesis and Dissertation Repository by an authorized administrator of Scholarship@Western. For more information, please contact wlsadmin@uwo.ca.

ABSTRACT

The effect of distal radial and ulnar length change on forearm bone loading is not well understood during simulated dynamic wrist loading. This thesis presents two studies which investigate the effect of these length changes on distal forearm loading under simulated dynamic wrist motion. The first study investigates the effect of radial length change on axial loading at the distal radius and ulna and relationship between ulnar variance and distal forearm loading. The complex variation in axial loads in the distal radius and during length change and dynamic wrist motion were studied and discussed. There was no correlation between native variance and distal loads. The second study investigates the effect of ulnar change on axial loading at the distal radius and ulna and the effect of triangular fibrocartilage ligament complex (TFCC) on this relationship. Variation in axial loads during ulnar lengthening followed similar trends to radial shortening and vice versa.

Keywords: Axial loading, distal radius and ulna, kienbock's disease, ulnocarpal impaction, ulnar variance, triangular fibrocartilage ligament complex (TFCC), wrist, forearm, biomechanics, *in-vitro*, simulator, simulated dynamic motion.

Co- Authorship Statement

Chapter 1

Sole Author: Diana Isa

Manuscript Review: Nina Suh, Jim Johnson, Graham King

Chapter 2

Study Design: Diana Isa, Martine McGregor, Jim Johnson, Graham King

Specimen Preparation: Diana Isa, Martine McGregor

Data Collection: Diana Isa, Martine McGregor, Clare Padmore, Mark Welsh, Dan Langhor

Data Analysis: Diana Isa

Statistical Analysis: Diana Isa

Manuscript Preparation: Diana Isa

Manuscript Review: Nina Suh, Jim Johnson, Graham King

Chapter 3

Study Design: Diana Isa, Martine McGregor, Jim Johnson, Graham King

Specimen Preparation: Diana Isa, Martine McGregor

Data Collection: Diana Isa, Martine McGregor, Clare Padmore, Mark Welsh, Dan Langhor

Data Analysis: Diana Isa

Statistical Analysis: Diana Isa

Manuscript Preparation: Diana Isa

Manuscript Review: Nina Suh, Jim Johnson, Graham King

Chapter 4

Sole Author: Diana Isa

Manuscript Review: Nina Suh, Jim Johnson, Graham King

Acknowledgements

I would first like to express my sincere gratitude to my supervisors, Dr. G. King and Dr. J. Johnson for the incredible opportunity to be a part of the world class research coming out of the RothlMcFarlane Hand and Upper Limb Centre. Their patience, motivation, enthusiasm and dedication to excellence in research has created an environment that made this research project a success. I would also like to thank the contribution of Dr. N. Suh whose participation and input as part of the supervisory committee was invaluable.

I would like to express my gratitude to my research partner Martine McGregor for designing the length change implant used in this study and exposing me not only to the nuances of engineering, but the vast world of Spotify. I appreciated her energy and upbeat attitude in the face of setbacks and extensive testing days.

I am grateful to the members of the HULC Bioengineering team with whom I had the pleasure of working with during this project and whose involvement was pivotal to the success of this project: Dan Langhor, Clare Padmore, Duncan Iglesias Jordan O'Brien and Mark Welsh. I am grateful to Dan for not only the wealth of knowledge contributed, but uncanny ability to pick out great take-out food, to Clare for her support with operating the motion simulator, to Duncan who developed the novel wrist simulator this testing took place on and who was always available for troubleshooting, to Jordan, for providing technical assistance and to Mark for his valuable participation, exemplary work ethic and constant supply of wittiness.

To my parents and siblings who have extended their support and love even from the distance. I am forever indebted to them.

Finally, to my amazing, kind, all kinds of wonderful husband Deji Ayoola, for being an incredible pillar of support, for taking the time to learn all about forearm biomechanics just so he could be a sounding board, for supporting my dreams and putting my needs and the needs of our children always before his. To our beautiful children Dami and Seyi, for being so understanding when I had to work long hours and my attention was diverted to the writing of this thesis.

The completion of this project was a combined achievement by all the aforementioned to whom I am truly grateful.

TABLE OF CONTENTS

ABSTRACT	I
CO- AUTHORSHIP STATEMENT	II
ACKNOWLEDGEMENTS	III
TABLE OF CONTENTS	V
1. INTRODUCTION	1
1.1 OSSEOUS ANATOMY OF THE FOREARM	1
1.1.1 OSTEOLGY OF THE RADIUS	1
1.1.2 OSTEOLGY OF THE ULNA	6
1.1.3 DISTAL RADIO-ULNAR JOINT OSTEOLGY	8
1.2 SOFT TISSUE ANATOMY AND STABILIZERS OF THE FOREARM.....	11
1.2.1 LIGAMENTS OF THE DRUJ	11
1.2.2 INTEROSSEOUS MEMBRANE	14
1.2.3 MUSCLES OF THE FOREARM.....	16
1.3 BIOMECHANICS OF THE FOREARM AND DRUJ	20
1.3.1 BIOMECHANICS OF THE IOM	20
1.3.2 BIOMECHANICS OF THE DRUJ	23
1.3.3 FOREARM LOAD TRANSMISSION	25
1.4 DISTAL RADIUS SHORTENING	26
1.4.1 SHORTENING IN DISTAL RADIUS FRACTURES	26
1.4.2 RADIAL SHORTENING OSTEOTOMY IN KIENBOCK’S	28
1.4.3 CLINICAL EFFECTS OF ULNAR POSITIVE VARIANCE.....	32
1.5 CURRENT BIOMECHANICAL STUDIES ON FOREARM LOAD TRANSMISSION	34
1.6 RATIONALE	39
1.7 OBJECTIVES AND HYPOTHESIS.....	42
1.8 THESIS OVERVIEW	43
1.9 REFERENCES	44

2. EFFECT OF RADIAL LENGTH CHANGE ON DISTAL FOREARM LOADING DURING SIMULATED WRIST MOTION.....	58
2.1 OVERVIEW	58
2.2 INTRODUCTION	58
2.3 METHODS	61
2.3.1 IMPLANT DESIGN.....	61
2.3.2 AXIAL LOAD MEASUREMENT	64
2.3.3 SPECIMEN PREPARATION	65
2.3.4 SIMULATION OF MOTION AND TESTING PROTOCOL.....	72
2.3.5 METHODS AND DATA ANALYSIS	74
2.4 RESULTS.....	75
2.4.1 NATIVE LOADS AND ULNAR VARIANCE.....	75
2.4.2 FLEXION.....	76
2.4.3 ULNAR DEVIATION	80
2.4.4 DART THROW MOTION	84
2.5 DISCUSSION	88
2.6 REFERENCES.....	96
3. THE EFFECT OF ULNAR LENGTH CHANGE AND TFC INTEGRITY ON DISTAL FOREARM LOADING DURING SIMULATED WRIST MOTION.....	102
3.1 OVERVIEW	102
3.2 INTRODUCTION.....	102
3.3 METHODS.....	105
3.3.1 IMPLANT DESIGN	105
3.3.2 AXIAL LOAD MEASUREMENT	107
3.3.3 SPECIMEN PREPARATION	107
3.3.4 SIMULATION OF MOTION AND TESTING PROTOCOL.....	110
3.3.5 METHODS AND DATA ANALYSIS.....	111
3.4 RESULTS	112
3.4.1 FLEXION.....	112
3.4.2 ULNAR DEVIATION	117
3.4.3 DART THROW.....	121

3.5 DISCUSSION	125
3.6 REFERENCES	132
4. CONCLUSIONS AND FUTURE DIRECTIONS.....	136
4.1 OVERVIEW	136
4.2 OBJECTIVES AND HYPOTHESES	136
4.3 EFFECT OF RADIAL LENGTH CHANGE ON DISTAL FOREARM LOADING DURING SIMULATED WRIST MOTION.....	137
4.4 THE EFFECT OF ULNAR LENGTH CHANGE AND TFC INTEGRITY ON DISTAL FOREARM LOADING DURING SIMULATED WRIST MOTION	138
4.5 FUTURE DIRECTIONS.....	141
4.6 REFERENCES	142
APPENDICES.....	143
CURRICULUM VITAE.....	154

List of Figures

Figure 1. 1 Radius and Ulna.	2
Figure 1. 2 Articulating surfaces of the Distal Radius.....	3
Figure 1. 3 Anatomic radiographic parameters of the distal radius.....	4
Figure 1. 4 Measurement of radiographic bow of radial shaft in coronal and sagittal planes.....	5
Figure 1. 5 Distal ulna osteology.....	6
Figure 1. 6 Bony osteology of the ulnar shaft.....	7
Figure 1. 7 Proximal ulna osteology.....	8
Figure 1. 8 Axial view of the DRUJ.....	9
Figure 1. 9 Categories of sigmoid notches.....	10
Figure 1. 10 Configurations of DRUJ in the coronal plane.....	11
Figure 1. 11 The Triangular Fibrocartilaginous Cartilage Complex (TFCC).....	12
Figure 1. 12 Superficial and deep limbs of the dorsal and volar radioulnar ligaments.....	13
Figure 1. 13 The anatomic components of the IOM.....	15
Figure 1. 14 Muscles of the volar compartment of the forearm.....	20
Figure 1. 15 Muscles of the dorsal compartment of the forearm.....	20
Figure 1. 16 Axis of rotation of the forearm (AOR).....	21
Figure 1. 17 Change in axis of rotation(AOR) during forearm rotation.....	24
Figure 1. 18 Distal Radius Malunion.....	27
Figure 1. 19 Distal radius shortening osteotomy for Kienbock's disease.....	30
Figure 1. 20 Ulnocarpal impaction Syndrome.....	33
Figure 2. 1 Custom Radial Implants.....	62
Figure 2. 2 Custom Ulnar Implant.....	64

Figure 2. 3 FCR approach. Pronator quadratus over the distal radius.	66
Figure 2. 4 Bone bridge technique radius	67
Figure 2. 5 Radial and ulnar spacers in cadaver specimens.....	69
Figure 2. 6 Running locking stitch through tendon	70
Figure 2. 7 Wrist motion simulator.....	71
Figure 2. 8 Radiographic image of radial and ulnar implants in-situ.	72
Figure 2. 9 Wrist motions evaluated.....	74
Figure 2. 10 Radial and ulnar loads during wrist flexion n=8.	78
Figure 2. 11 Radial and ulnar loads with radial length change during simulated wrist motion from extension to flexion n = 8.	79
Figure 2. 12 Radial and ulnar loads during wrist ulnar deviation n = 7.	82
Figure 2. 13 Radial and ulnar loads with radial length change during simulated wrist motion from radial to ulnar deviation n = 7.	83
Figure 2. 14 Radial and ulnar loads with radial length change during simulated wrist dart throw motion n = 6.....	86
Figure 2. 15 Radial and ulnar loads with radial length change during simulated wrist dart throw motion n = 6.....	87
Figure 3. 1 Approach to Subcutaneous Border of the Ulna demonstrating Bone Bridge.....	108
Figure 3. 2 Radial and ulnar loads during wrist flexion n = 8.	115
Figure 3. 3 Radial and ulnar loads with ulnar length change during simulated wrist flexion with and without the TFC intact n = 8.	116
Figure 3. 4 Radial and ulnar loads during ulnar deviation n = 7.	119

Figure 3. 5 Radial and ulnar loads with ulnar length change during simulated ulnar deviation with and without the TFC intact n = 7.....	120
Figure 3. 6 Radial and ulnar loads during dart throw n = 6.....	123
Figure 3. 7 Radial and ulnar loads with ulnar length change during simulated dart thrower's motion with and without the TFC intact n = 6.....	124

List of Tables

Table 1. The volar/anterior compartment of the forearm	17
Table 2. The dorsal/posterior compartment of the forearm	18
Table 3. Litchman Classification for Kienbock’s Disease.....	31

List of Appendices

Appendix 1 Glossary of Terms.....	143
Appendix 2. 1 Graph showing radial and ulnar loads with radial length change during flexion (Mean ± SD).	144
Appendix 2. 2 Graph showing radial and ulnar loads with radial length change during ulnar deviation (Mean ± SD).....	144
Appendix 2. 3 Graph showing radial and ulnar loads with radial length change during dart throw (Mean ± SD).	145

Appendix 2. 4 Graph showing radial and ulnar loads with radial length change during dynamic wrist motion (Mean \pm SD).....	145
Appendix 2. 5 Graph showing radial and ulnar loads with ulnar length change during flexion with and without the TFC intact (Mean \pm SD).	146
Appendix 2. 6 Graph showing radial and ulnar loads with radial length change during ulnar deviation with and without the TFC intact (Mean \pm SD).	146
Appendix 2. 7 Graph showing radial and ulnar loads with radial length change during dart throw with and without the TFC intact (Mean \pm SD).	147
Appendix 2. 8 Graph showing radial and ulnar loads with radial length change during dynamic wrist motion with and without the TFC intact (Mean \pm SD).....	147
Appendix 2. 9 Radial and ulnar loads during wrist flexion with the TFC excised n = 8.	148
Appendix 2. 10 Radial and ulnar loads during ulnar deviation with the TFC excised n = 7	149
Appendix 2. 11 Radial and ulnar loads during dart throw with the TFC excised n = 6.	150
Appendix 2. 12 Percentage load sharing with radial length change during flexion expressed as a percentage of forearm compressive loads.....	151
Appendix 2. 13 Percentage load sharing with radial length change during ulnar deviation expressed as a percentage of forearm compressive loads	151
Appendix 2. 14 Percentage load sharing with radial length change during ulnar deviation expressed as a percentage of forearm compressive loads.....	151
Appendix 2. 15 Percentage load sharing with ulnar length change with and without an intact TFC during flexion expressed as a percentage of forearm compressive loads	152
Appendix 2. 16 Percentage load sharing with ulnar length change with and without an intact TFC during ulnar deviation expressed as a percentage of forearm compressive loads	152

Appendix 2. 17 Percentage load sharing with ulnar length change with and without an intact TFC
during ulnar deviation expressed as a percentage of forearm compressive loads. 153

Appendix 2. 18 Ulnar and radial implants in cadaver forearms 153

Chapter 1

1. INTRODUCTION

This chapter reviews the anatomy, function and biomechanics of the radiocarpal joint, distal radioulnar joint and forearm. The clinical and biomechanical effects of radial shortening in a malunited distal radius fracture, ulnar positive variance in ulnocarpal impaction syndrome and ulnar negative variance in Kienbock's disease are discussed followed by the study rationale, objectives and hypotheses.

1.1 OSSEOUS ANATOMY OF THE FOREARM

1.1.1 OSTEOLOGY OF THE RADIUS

The radius articulates with the ulna at its proximal and distal extent causing the radius to rotate on the ulna producing forearm supination (palm up) and pronation (palm down) in addition to flexion and extension of the wrist. The proximal articulation is referred to as the proximal radioulnar joint (PRUJ) and the distal articulation is referred to as the distal radioulnar joint (DRUJ) (Figure 1.1). The distal radius consists of three articulating surfaces: the scaphoid and lunate facets which articulate with the scaphoid and lunate respectively (Figure 1.2) and the sigmoid notch which articulates with the distal ulna.

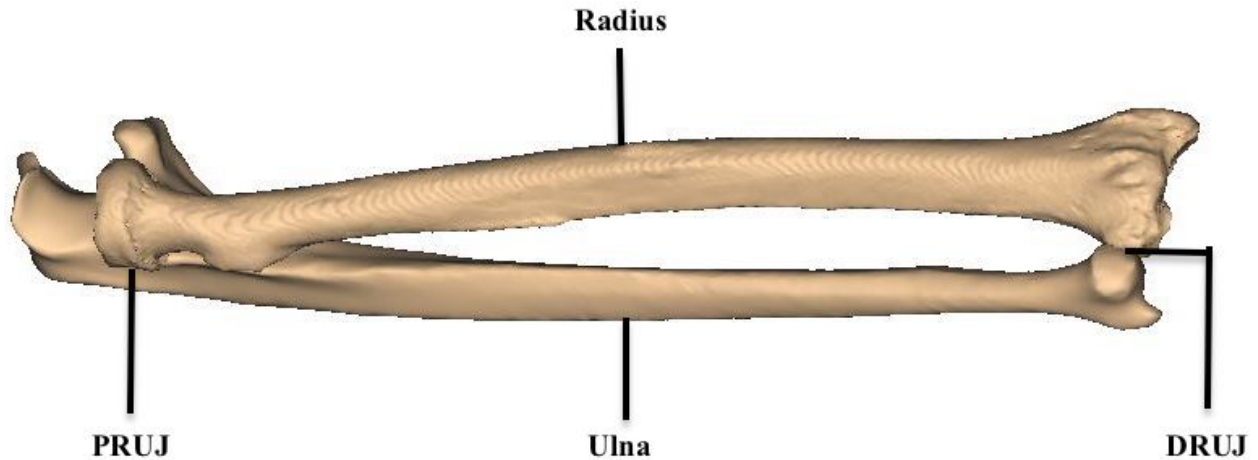


Figure 1. 1 Radius and Ulna.
Radius and Ulna articulating at the proximal radioulnar joint (PRUJ) and the distal radioulnar joint (DRUJ) (© D Isa).

The anatomy of the distal radius is commonly described in terms of plain radiographic measurements: radial inclination, radial length, ulnar variance and volar tilt (Figure 1.3). The radial inclination of the distal radius articular surface averages 22° on posteroanterior (PA) radiographs, radial length averages 11-22mm, and volar tilt averages 11° .¹

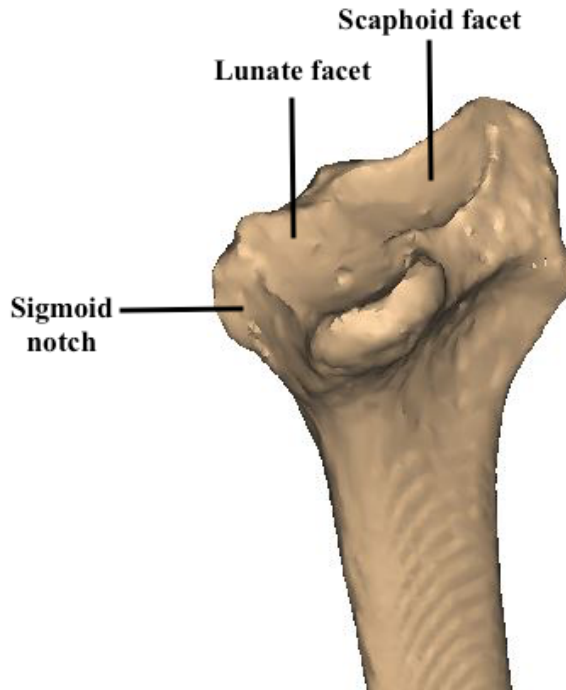


Figure 1. 2 Articulating surfaces of the Distal Radius.
The scaphoid and lunate facets and the sigmoid notch (© D Isa).

The radial diaphysis also possesses a bow in both the coronal and sagittal plane. Schemitsch and Richards² devised a radiographic measurement to quantify the position and magnitude of radial bow. With the forearm in neutral rotation on radiographs, a line is drawn from the radial tuberosity to the ulnar border of the distal radius. A second line perpendicular to this is drawn from the point of maximal radial bow. The height of this line is measured and compared to the contralateral side. The radial bow is described by noting the length and position of this line (see line X in figure 1.4). Alternatively, the bow can be described by the location of the apex of maximal bow at the middle third of the radius and measures on average 10° which corresponds to the position of line X.^{3,4}

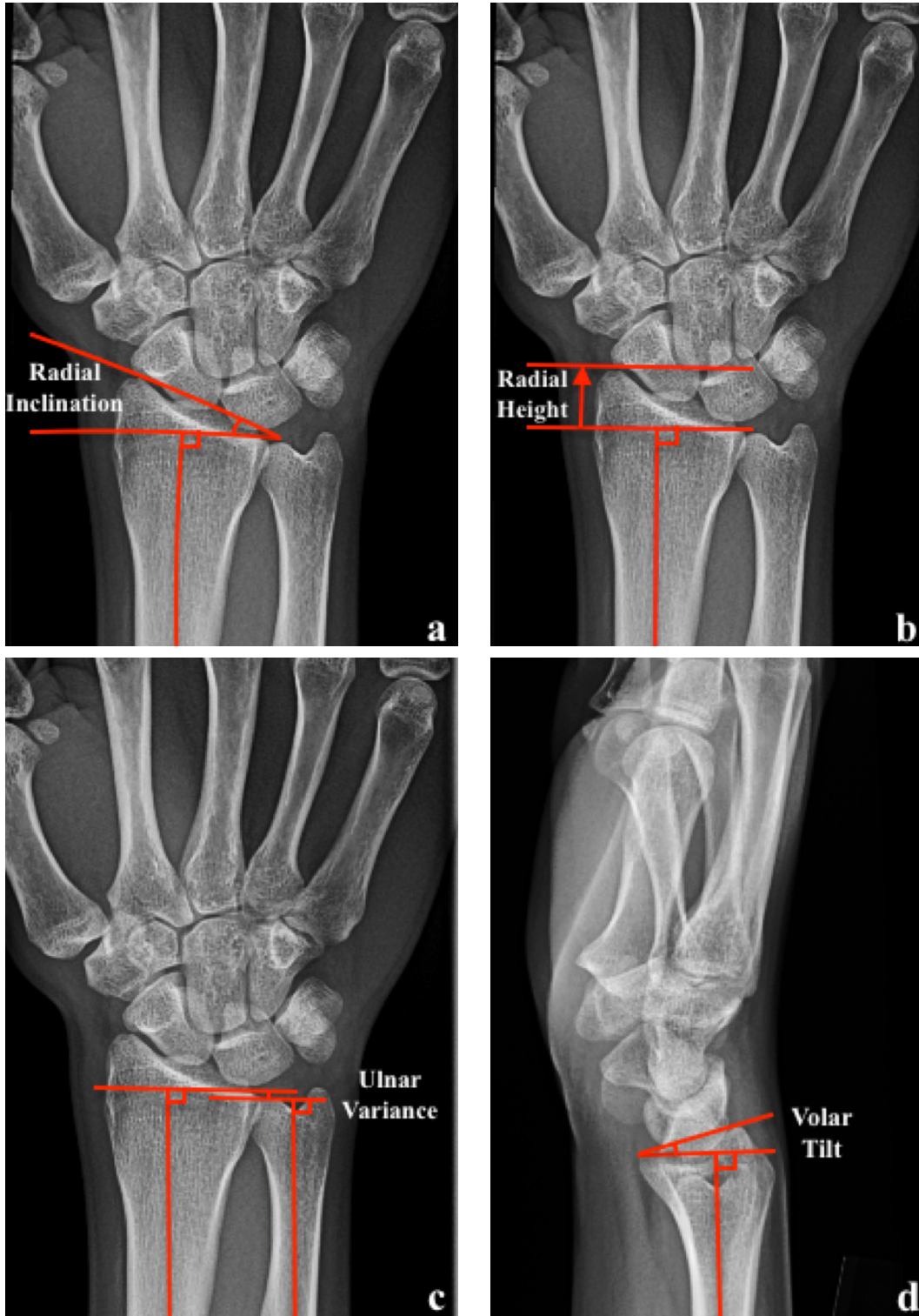


Figure 1. 3 Anatomic radiographic parameters of the distal radius.
 PA radiographs showing radiographic measurements of (a) Radial inclination (b) Radial height and (c) Ulnar variance. Lateral radiograph showing radiographic measurement of (d) Volar tilt (© D Isa).

In the coronal plane, the radial bow measures 10° with an apex radial bow at the middle third of the radius. In the sagittal plane, the apex dorsal bow is on average 12cm distal to the radial head and located within the proximal two-thirds of the radius averaging 5° .⁴ (Figure 1.4)

The proximal radius consists of the radial head, neck and tuberosity. The radial head is elliptical with the concavity of the radial head articulating with the capitellum offset in a radial direction from the radial neck axis.

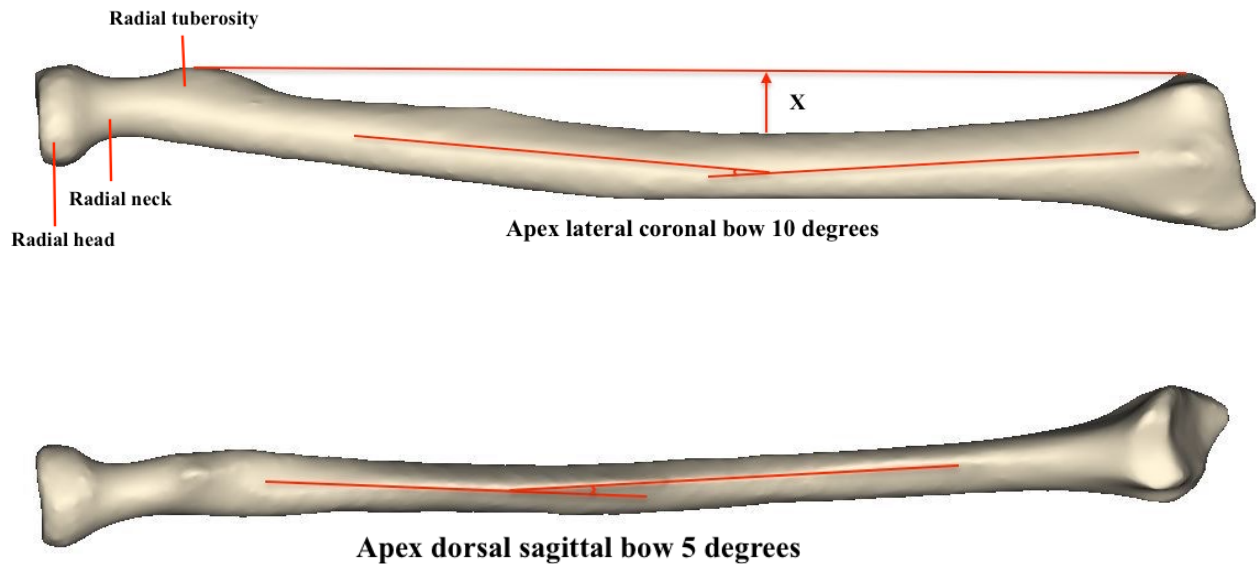


Figure 1. 4 Measurement of radiographic bow of radial shaft in coronal and sagittal planes. (© D Isa).

The radial bow is described by noting the length and position of the line "X"

1.1.2 OSTEOLOGY OF THE ULNA

The distal ulna articulates with the sigmoid notch around which the radius rotates. The dorsomedial extension of the subcutaneous border of the ulna is called the ulnar styloid. The base of the ulnar styloid is devoid of cartilage and is called the fovea which is the geometric center of rotation of the DRUJ. The ulna head articulates with the articular disc of the TFCC. The dorsal groove of the ulnar head accommodates the extensor carpi ulnaris (ECU) tendon. (Figure 1.5).

Ulnar variance is a common radiographic parameter used to assess the height of the ulna relative to the ulnar corner of the lunate fossa on the distal radius (or relative to the length of the distal radius) measured on PA radiographs with the wrist in neutral rotation (Figure 1.3 c). Ulnar variance averages -0.9 mm.⁵ Changes in ulnar variance with forearm position and grip has been described accounting for subtle variations on radiographs.^{6,7,8} Mean maximum dynamic increase in ulnar variance of 1.3 ± 0.5 mm occurs with gripping in pronation compared with ulnar variance with the forearm relaxed in pronation.⁷

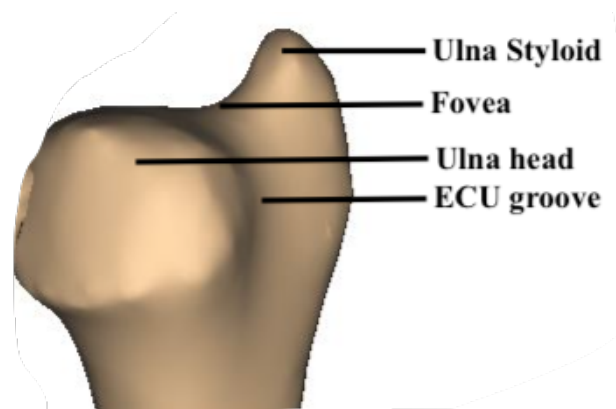


Figure 1. 5 Distal ulna osteology.
(© D Isa)

The ulna diaphysis is relatively straight in the sagittal and coronal plane at the distal and middle third of the ulna. At the proximal third, there is a varus bow of approximately 17.7° ⁹ as well as proximal ulna dorsal angulation averaging $5.7 \pm 2.4^\circ$ an average of 47 ± 6 mm from the olecranon tip in the sagittal plane.¹⁰ (Figure 1.6)

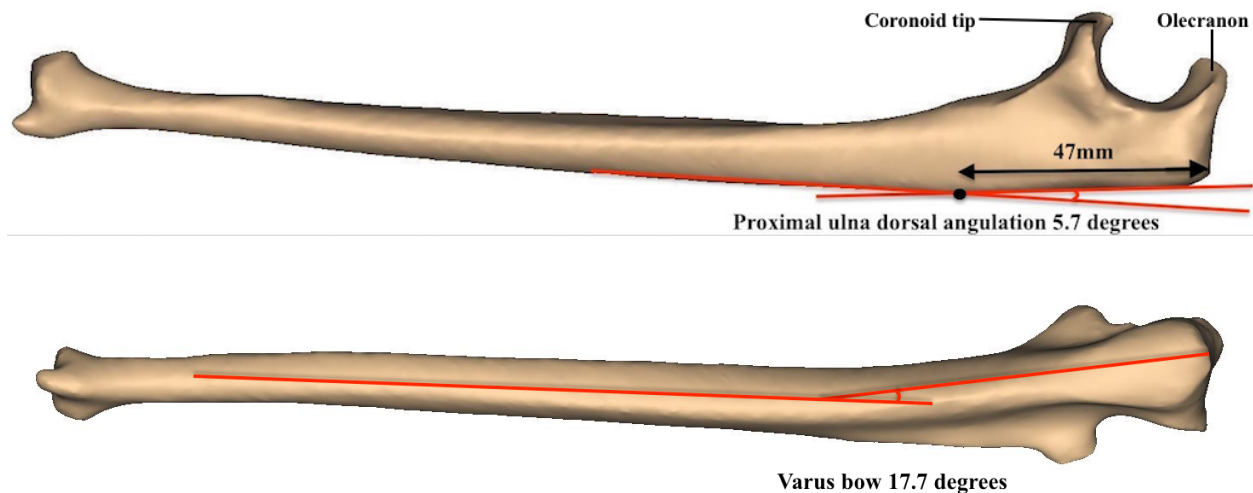


Figure 1. 6 Bony osteology of the ulnar shaft.

(© D Isa)

Osteology depicting the proximal ulna dorsal angulation (PUDA) and the proximal varus bow

The most proximal section of the ulna is referred to as the olecranon. The olecranon and coronoid process form the greater sigmoid notch which articulates with the distal humerus. The coronoid consists of the anteromedial facet, the coronoid tip, the base and the lesser sigmoid notch which articulates with the radial head (Figure 1.7).

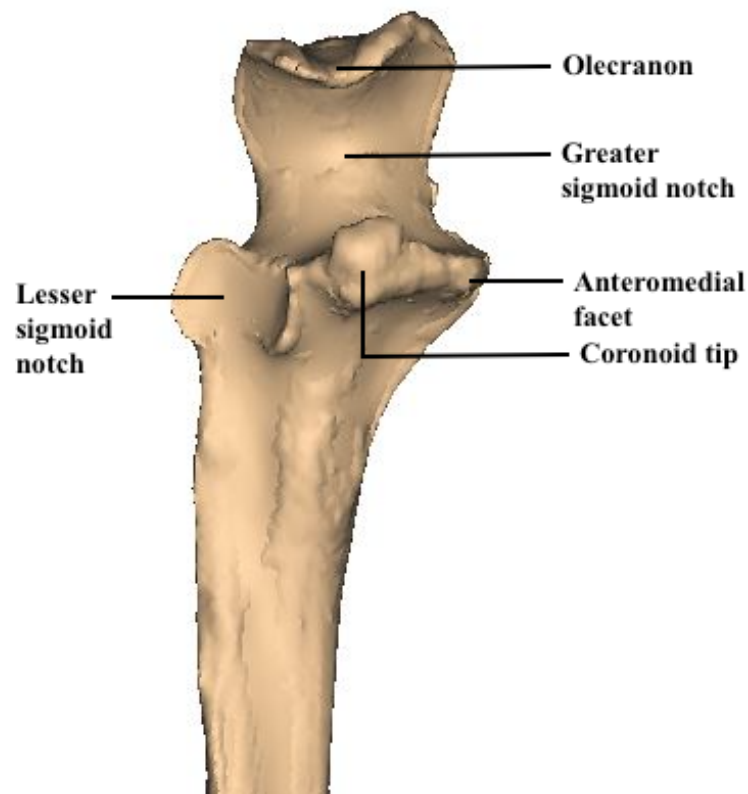


Figure 1. 7 Proximal ulna osteology
(© D Isa).

1.1.3 DISTAL RADIO-ULNAR JOINT OSTEOLOGY

Distally, the DRUJ articulation constitutes the sigmoid notch of the distal radius and the ulnar head. The bony architecture confers 20% stability to the DRUJ.¹¹ The majority of stability comes from the soft tissue stabilizers which are described later in section 1.1.2.1.

The radius of curvature of the sigmoid notch is approximately 15 mm with a 47°- 80° arc of cartilaginous surface. The radius of curvature of the articulating portion of the distal ulna is

approximately 10mm with $90^\circ - 135^\circ$ of cartilaginous coverage creating a lack of congruency between the two surfaces.¹² (Figure 1.8)

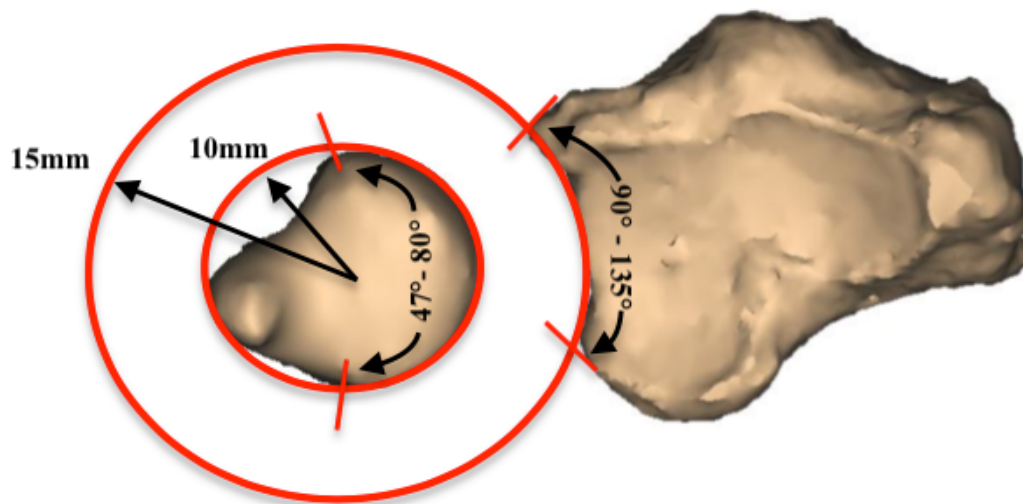


Figure 1. 8 Axial view of the DRUJ.
The radius of curvature of the sigmoid notch is greater than that of the ulnar head (© D Isa).

The morphology of the sigmoid notch was first described by Tolat and colleagues¹³ Four categories of sigmoid notches were described in order of descending prevalence: Flat face, ski slope, “C” type and “S” types, with flat face type influencing the predisposition to instability (Figure 1.9).

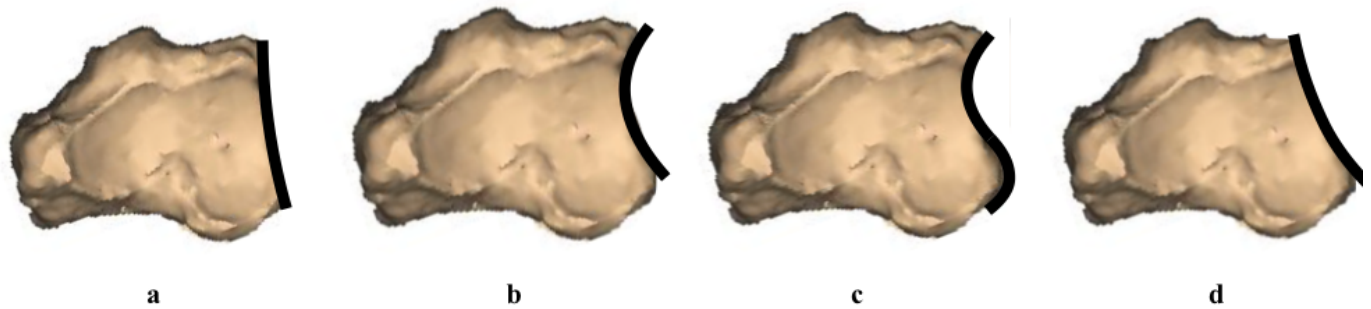


Figure 1. 9 Categories of sigmoid notches.

(© D Isa).

In order of descending prevalence: a. Flat face, b. “C” type, c. “S” type and d. Ski slope

Three basic configurations of the DRUJ in the coronal plane exist: type I vertical (38%); type II oblique (50%); or type III reverse obliquity (12%) described by Tolat and colleagues.¹³ Type I has opposing surfaces parallel, in type II, the opposing joint surfaces are oblique and in type III, the opposing joint surfaces are oriented in a reverse oblique orientation (Figure 1.10). A strong correlation exists between obliquity and ulna variance; the more positive the ulna variance, the less the DRUJ obliquity, eventually becoming reverse oblique.^{14,15,16}

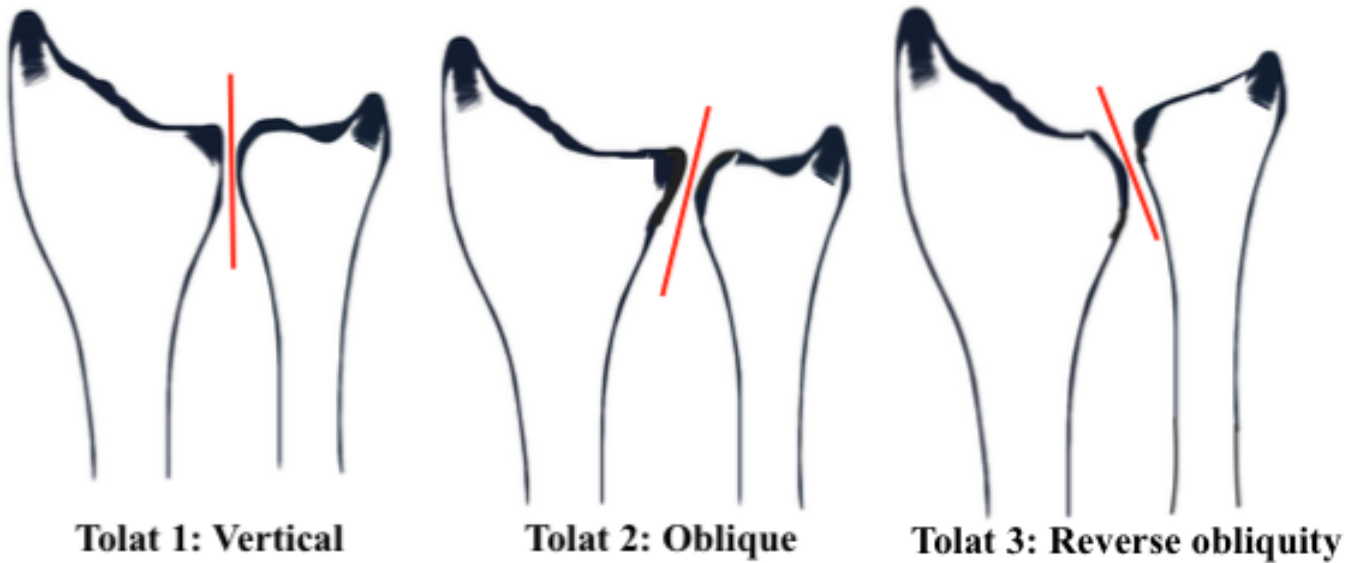


Figure 1. 10 Configurations of DRUJ in the coronal plane

(© D Isa)

Types of DRUJ configurations in the coronal plane as described by Tolat.

1.2 SOFT TISSUE ANATOMY AND STABILIZERS OF THE FOREARM

The radius and ulna are linked by the annular ligament at the PRUJ proximally, the interosseous membrane (IOM) along the diaphysis and the TFCC at the DRUJ.

1.2.1 LIGAMENTS OF THE DRUJ

Static stabilizers of the DRUJ include the TFCC and the IOM. Dynamic stabilizers of the DRUJ include the ECU and pronator quadratus (deep head). The main soft tissue stabilizer of the DRUJ is the TFCC. The term TFCC was coined by Palmer and Werner in 1981¹⁷ and is comprised of a

series of anatomically confluent structures, each with distinct functions. The TFCC consists of the volar and dorsal radioulnar ligaments (VRUL and DRUL), the ulnocarpal ligaments, the ECU tendon subsheath, the articular disc and the meniscus homologue. (Figure 1.11)

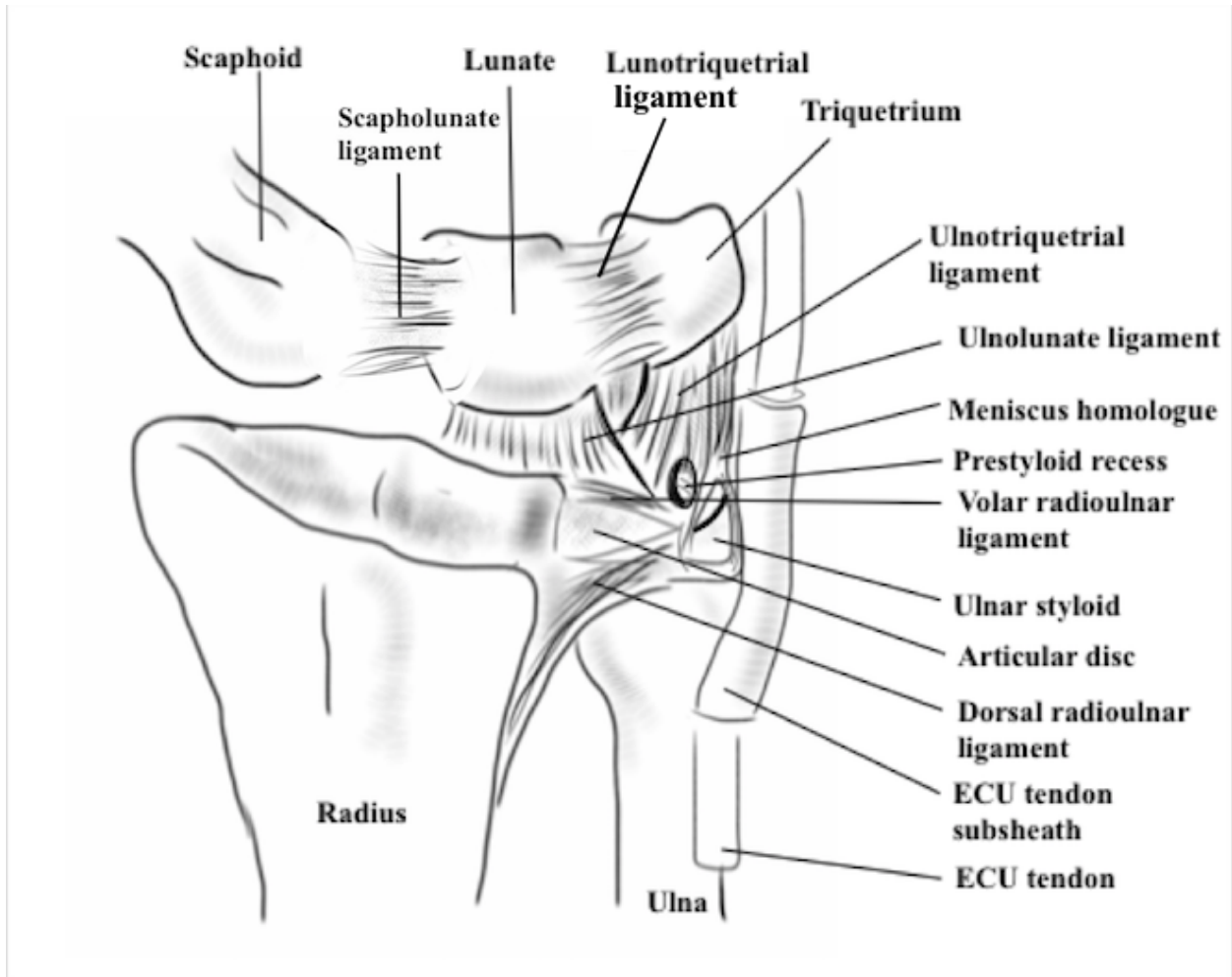


Figure 1. 11 The Triangular Fibrocartilaginous Cartilage Complex (TFCC)
 (© D Isa)

The primary ligamentous stabilizers of the DRUJ are the volar and dorsal radioulnar ligaments which extend from the volar and dorsal aspects of the sigmoid notch respectively and converge

and attach to the ulna in a triangular fashion (Figure 1.12). As these ligaments extend ulnarly, they each divide into two limbs (superficial and deep). The deep limbs attach to the fovea and the superficial limbs extend distally and insert at the base and mid portion of the ulnar styloid. Fractures of the ulnar styloid typically involve injury to the superficial limbs of the radioulnar ligaments but the DRUJ remains stable if the deep fibers remain intact (Figure 1.12). The foveal attachments are the most important components conferring stability.¹⁸

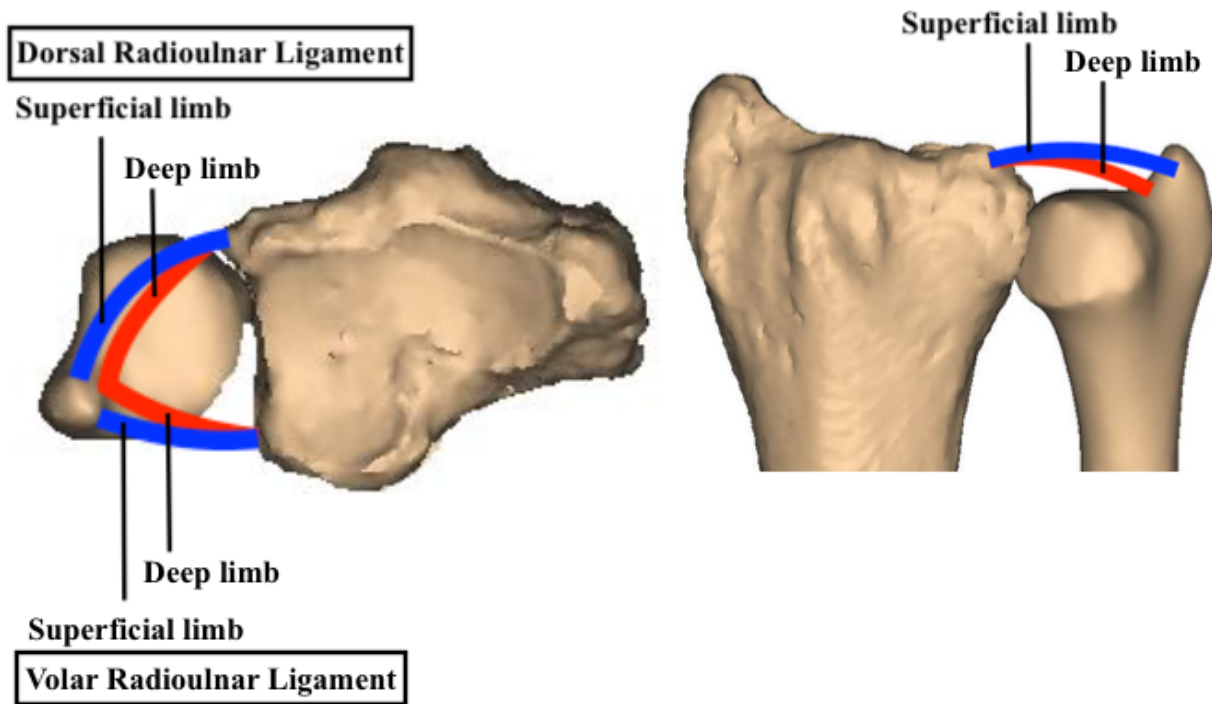


Figure 1. 12 Superficial and deep limbs of the dorsal and volar radioulnar ligaments.
 (© D Isa)

The articular disc, also known as the triangular fibrocartilage disc, serves as a supporting platform for the carpus and is predominantly static during wrist motion (Figure 1.11).¹⁹ The disc

functions to extend the lunate facet's articular surface providing a continuous gliding surface and acts as part of a mobile platform for the ulnar carpus.²⁰ There is a correlation between ulnar variance and articular disc TFCC thickness. The more positive the ulnar variance the thinner the articular disc/triangular fibrocartilage.^{21,22}

The meniscus homologue (Figure 1.11) is a fold of synovium located between the articular disc, ulnocarpal capsule, DRUL, VRUL and triquetrum and is taught in radial deviation and loose in ulnar deviation.^{19,23} It helps to exert a sling effect and has been referred to as a hammock structure stabilizing the ulnar carpus.²⁴

The ulnocarpal ligaments consist of the ulnolunate and ulnotriquetral ligaments which originate off the VRUL and articular disc and insert into the lunate and triquetrium respectively (Figure 1.11). The ulnocarpal collateral ligament, sometimes referred to as the subsheath of the ECU is located ulnar to the ulnocarpal ligaments and has been shown to stabilize the ulnocarpal joint during forearm rotation.²⁵

1.2.2 INTEROSSEOUS MEMBRANE

The interosseous membrane (IOM) of the forearm is a robust ligamentous complex linking the radius to the ulna. The IOM consists of a several components which include a distal membranous portion (distal oblique bundle [DOB]),²⁶ middle ligamentous complex (accessory band [AB] and central band [CB]) and proximal membranous portion (dorsal oblique accessory cord and proximal oblique cord)^{26,27} (See Figure 1.13). The DOB is present in 40% of individuals.^{26,28}

When present, the DOB constrains volar and dorsal instability of the radius at the DRUJ in all

forearm rotation positions and contributes to DRUJ stability.^{28,29,30} The CB contributes to longitudinal stability of the forearm and prevents divergence of the radius and ulna thus maintaining the forearm axis of rotation by tethering the bones together during pronation and supination^{27,31,32} The function of the proximal membranous portion is controversial and unconfirmed in the literature.^{33,34,35} The biomechanics of the IOM is discussed in further detail in section 1.3.1.

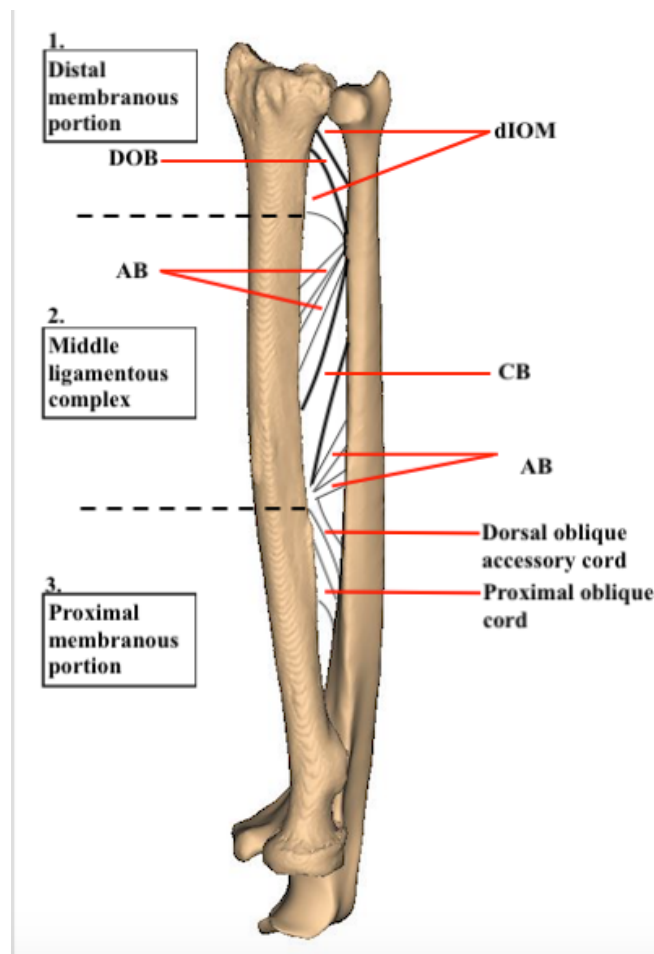


Figure 1. 13 The anatomic components of the IOM.

The distal membranous portion/distal interosseous membrane (dIOM) which consists of the dorsal oblique bundle (DOB), (2) the middle ligamentous complex which consists of the central band (CB) and accessory band (AB) and (3) the proximal membranous portion which consists of the dorsal oblique accessory cord and proximal oblique cord (© D Isa).

1.2.3 MUSCLES OF THE FOREARM

Muscles of the anterior compartment of the forearm are primarily involved in wrist and finger flexion and forearm pronation.

The superficial volar compartment consists of the flexor carpi radialis (FCR), palmaris longus (PL), flexor carpi ulnaris (FCU) and pronator teres (PT) from radial to ulnar. The intermediate compartment consists of the flexor digitorum superficialis (FDS). The deep volar compartment includes the flexor digitorum profundus (FDP), flexor pollicis longus (FPL) and pronator quadratus (PQ). (Figure 1.14)

The volar compartment contains muscles which are primarily responsible for wrist, finger and thumb flexion and well as forearm pronation (Table 1).

Table 1. The volar/anterior compartment of the forearm

Muscle	Function
Flexor Carpi Radialis (FCR)	Wrist flexion and radial deviation
Palmaris Longus (PL)	Wrist flexion
Flexor Carpi Ulnaris (FCU)	Wrist flexion and ulnar deviation
Pronator Teres (PT)	Forearm pronation and secondary elbow flexor
Flexor Digitorum Superficialis (FDS)	Flexion of proximal interphalangeal joints and metacarpophalangeal joint of digits 2-5
Flexor Digitorum Profundus (FDP)	Flexion of the distal interphalangeal joints of digits 2-5
Flexor Pollicis Longus (FPL)	Flexion of thumb
Pronator Quadratus (PQ)	Forearm pronation

The dorsal/posterior compartment contains muscles which are primarily responsible for wrist, finger and thumb extension as well as forearm supination (Table 2)

Table 2. The dorsal/posterior compartment of the forearm

Muscle	Function
Brachioradialis	Forearm flexion
Extensor Carpi Radialis Longus (ECRL)	Wrist extension and radial deviation
Extensor Carpi Radialis Brevis (ECRB)	Wrist extension
Extensor Carpi Ulnaris (ECU)	Wrist extension and ulnar deviation
Anconeus	Assists triceps in elbow extension
Extensor Digitorum Communis (EDC)	Extension of the metacarpophalangeal joint of digits 2 - 5 and assists in wrist extension
Extensor Digiti Minimi (EDM)	Extension of the little finger
Abductor Pollicis Longus (APL)	Thumb abduction and extension at carpometacarpal joint
Extensor Pollicis Longus (EPL)	Thumb extension at the interphalangeal joint
Extensor Pollicis Brevis (EPB)	Thumb extension at the metacarpophalangeal joint
Extensor Indicis Proprius (EIP)	Extension of index finger and assists in wrist extension
Supinator	Forearm supination

The superficial dorsal compartment contains the mobile wad (brachioradialis, extensor carpi radialis longus (ECRL) and extensor carpi radialis brevis (ECRB)), extensor carpi ulnaris (ECU) and anconeus. The intermediate compartment consists of the extensor digitorum communis (EDC) and the extensor digiti minimi (EDM). The deep compartment consists of the abductor pollicis longus (APL), extensor pollicis longus (EPL), extensor pollicis brevis (EPB), extensor indicis proprius (EIP) and the supinator. (Figure 1.15)

The ECU and its subsheath are dynamic stabilizers of the DRUJ.³⁶ The ECU stabilizes the DRUJ and the ulnocarpal joint in both supination and neutral forearm rotation; especially when the TFCC is insufficient.³⁷

The PQ is a dynamic stabilizer of the DRUJ^{38,39} especially in pronation.⁴⁰ The superficial head of PQ is an important pronator while the deep head is a dynamic stabilizer of the DRUJ as suggested by continuous activation throughout forearm rotation in electromyographic studies.³⁸

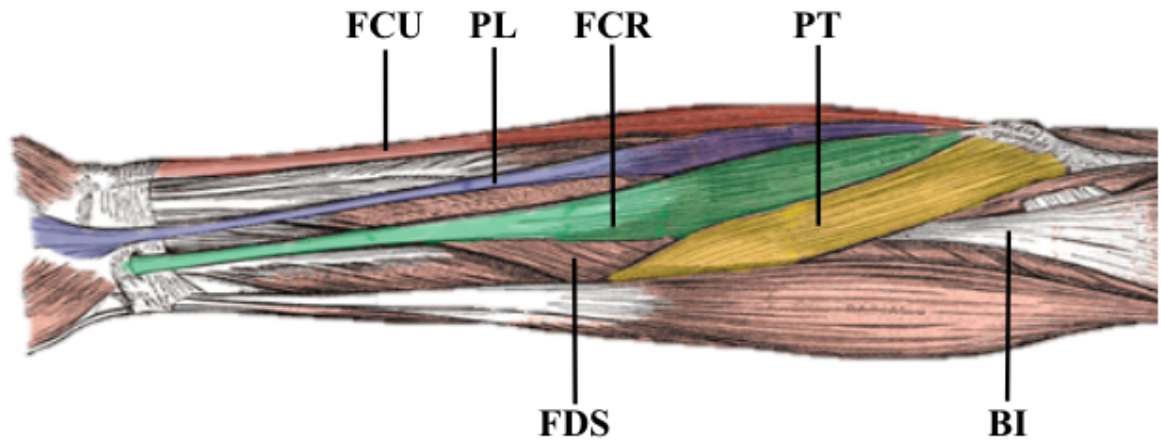


Figure 1. 14 Muscles of the volar compartment of the forearm

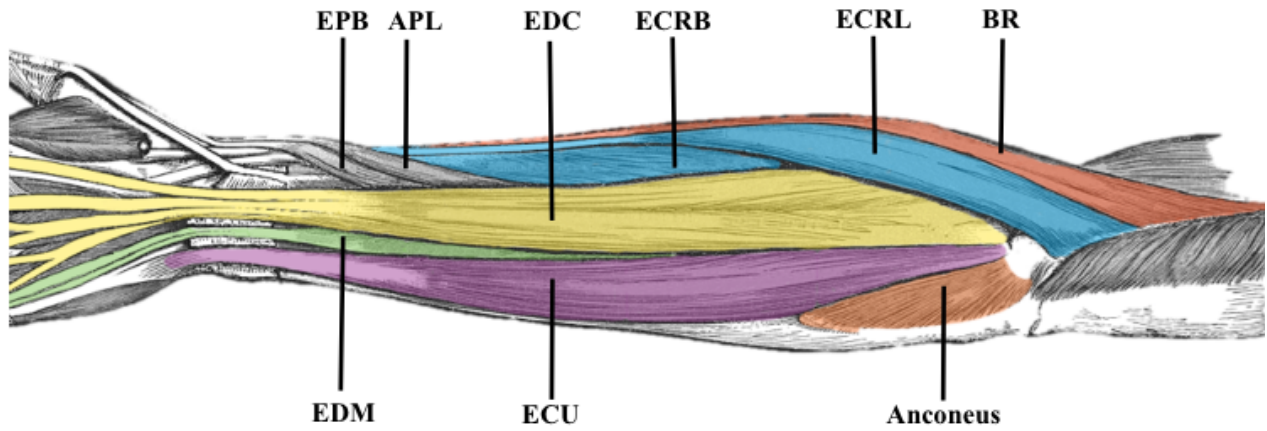


Figure 1. 15 Muscles of the dorsal compartment of the forearm

1.3 BIOMECHANICS OF THE FOREARM AND DRUJ

1.3.1 BIOMECHANICS OF THE IOM

The IOM is a secondary stabilizer of the DRUJ. Its' importance for DRUJ kinematics are most apparent when the primary soft-tissue stabilizers have been compromised at the level of the

DRUJ.^{17,41,42}

The axis of forearm rotation (AOR) runs proximally through the center of the radial head and distally through the fovea of the ulnar head. (Figure 1.16). The change in lengths of the components of the IOM during forearm rotation has been studied.³³ The three most distal ligaments of the IOM (CB, AB and DOB) have negligible length change during pronosupination because the ulnar attachments of these ligaments are located along the course of the AOR thus conceptually supporting these structures as isometric stabilizers of the forearm. The proximal membranous portion lacks isometry and is lengthened (taut) in pronation and lax in supination.^{33,35}

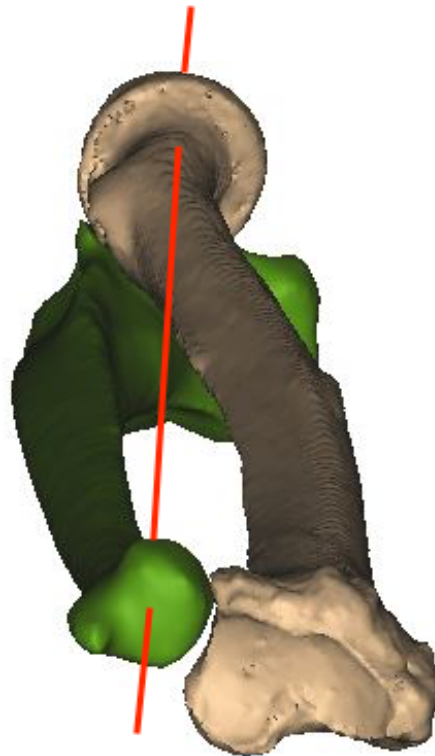


Figure 1. 16 Axis of rotation of the forearm (AOR).

(© D Isa)

AOR passing through the ulnar fovea distally and center of the radial head proximally

If the IOM is sectioned, there is resultant DRUJ instability in the absence of an intact TFCC. In particular, the distal IOM is found to have a key stabilizing role, with the DOB of particular importance when present.^{29,30,43} The distal oblique bundle of the IOM was described by Noda et al²⁶ and its role in DRUJ stability has been demonstrated.^{43,28} The DOB provides longitudinal resistance to ulnar shortening. Arimitsu et al²⁹ reported longitudinal resistance to ulnar shortening was significantly greater when shortening was performed proximal to the DOB compared with a more distal shortening. The presence of a DOB and ulnar shortening proximal to the DOB confers greater DRUJ stability.^{29,30} Moreover, Watanabe et al⁴³ demonstrated the DOB constrained volar and dorsal instability of the radius at the DRUJ in all forearm rotation positions. Several studies have confirmed the DOB contributes to DRUJ stability^{29,30,28} despite its presence in only 40% of individuals.^{26,28} Biomechanical evidence suggests that individuals with a DOB have increased stability of their DRUJ.

The IOM contributes to forearm load sharing between the radius and ulna as dissipation of forces occur via soft tissue stabilizers as the load progresses proximally during axial loading.^{44,45,46} (Discussed in section 1.5 later).

The CB inserts on the proximal radial shaft and runs distally to insert on the distal ulnar shaft. It is frequently discussed in the literature because it is considered the most functional component of the IOM as the result of its stoutness and constancy (Figure 1.13). In particular, the CB becomes the most important contributor to longitudinal stability of the forearm after resection of the radial head.^{27,31} The IOM, especially the CB also prevents divergence of the radius and ulna thus

maintaining the forearm axis of rotation by tethering the bones together during pronation and supination.³² In the absence of a radial head, proximal migration of the radius is resisted by load transference to the ulna through the IOM. Increased strain in the CB of the IOM has been noted in biomechanical studies and is responsible for the majority of longitudinal stiffness of the IOM after radial head excision.^{31,47,48} The load-displacement curve on biomechanical testing demonstrates the CB behaves structurally as a strong ligament.⁴⁹

The proximal membranous portion (the proximal oblique cord and dorsal oblique accessory cord) of the IOM do not represent isometric components and are thought to act as restraints from excessive pronation motion of the forearm; however, the true functions of the proximal membranous portion are controversial and unconfirmed in the literature.^{33,34,35}

1.3.2 BIOMECHANICS OF THE DRUJ

In most normal individuals, the total arc of pronation and supination measures between 150-180°. The differential arc of curvature between the sigmoid notch and ulnar head suggests that prosupination not only involves rotation but also dorsovolar translation due to the cam effect at the DRUJ.¹³ with the ulnar head moving dorsal and distal in pronation and volar and proximal in supination.⁵⁰ Additionally, studies have found that the DRUL is taut in pronation and thus important in stabilizing the DRUJ in pronation while the VRUL is taut in supination and thus more important in stabilizing the DRUJ in supination.^{25,42,51,52} The AOR runs proximally through the center of the radial head and distally through the fovea of the ulnar head (Figure 1.16) and the axis moves from the radial to ulnar at the DRUJ as the forearm moves from pronation to

supination (Figure 1.17).⁵³

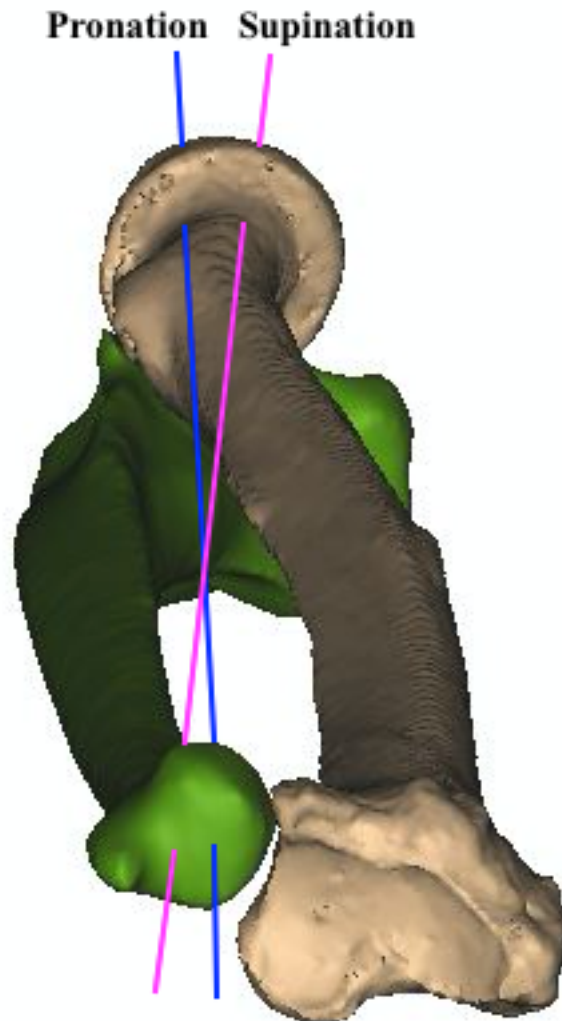


**Figure 1. 17 Change in axis of rotation(AOR) during forearm rotation
AOR moves in an ulnar to radial direction as the forearm moves from pronation to supination.**

1.3.3 FOREARM LOAD TRANSMISSION

In an earlier static biomechanical study,¹⁷ the radius distal was reported to bear 60% of the axial load transmitted through the bones of the forearm and the ulna was thought to bear the remaining 40% in ulnar neutral wrists. TFCC excision resulted in transmission of 95% of the load through the radius and 5% through the ulna. This demonstrates the TFCC also functions to transmit load/load sharing between the radius and ulna. The TFCC not only plays a major role in stability of the DRUJ, but also load transference.⁴⁸

Subsequent static biomechanical studies have examined the axial load distribution between the distal radius and ulna in static positions. It has been reported that 9 – 43 % of the total wrist load passes through the distal ulna in neutral wrist and forearm position^{50,54,55,56,57,58,44} however, the load distribution between the distal radius and ulna varies based on the length of the radius relative to the ulna. When the ulnar length was increased by 2.5 mm, the forearm axial load borne by the distal ulna increased to 42%. Conversely, when ulnar length was decreased by 2.5 mm, the axial load borne by the ulna decreased to 4%.^{50,54} There is a variation in axial load transmission between the radius and ulna throughout the arc of forearm rotation. The axial load transmitted through the distal ulna has been shown to be over 30% at 60° supination during simulated *in-vivo* forearm rotation.^{45,59} This is controversial as some biomechanical studies have demonstrated more load transmitted through the distal ulna at 45° and 75° of pronation.^{22,60} These studies have applied non-physiologic static loads and have not simulated *in-vivo* wrist motion.

However, it is interesting to note that a more positive native ulnar variance does not necessarily

result in more force transmission through the distal ulna than a wrist with a more negative native ulnar variance.^{22,55} This is likely due to the greater thickness of the TFCC in wrists with ulnar negative ulnar variance.^{22,55}

1.4 DISTAL RADIUS SHORTENING

Shortening of the distal radius can occur either as a sequela of distal radial fractures or as a result of distal radius shortening osteotomy as a surgical treatment for Kienbock's disease, avascular necrosis of the lunate.

1.4.1 SHORTENING IN DISTAL RADIUS FRACTURES

The most common cause of axial shortening of the distal radius is due to malunion or growth arrest following distal radius fractures. Distal radius malunion is the most common complication of distal radius fractures with an incidence of 17 - 24%.^{61,62} Radial shortening of 3-6 mm or more affects wrist function, range of motion especially in forearm rotation, and impairs clinical outcome.^{63,64,65} Of the radiographic parameters, radial shortening has been associated most frequently with unsatisfactory outcomes following distal radius fractures.^{66,67,68,69,70} Patients with residual radial shortening develop wrist pain and disability due to ulnar positive variance and subsequent clinical sequelae such as ulnar impaction syndrome (Discussed in section 1.3.3 later). Axial shortening/loss of radial height results in a shift and transfer of load onto the ulna, resulting in pain and limitation of grip strength, which gives rise to poor function (Figure 1.17). Restoration of anatomic parameters improve patient outcomes in distal radius fractures.^{71,72}



Figure 1. 18 Distal Radius Malunion.

(© D Isa).

46 year old woman with previous left (L) distal radius fracture and subsequent malunion with residual shortening and ulnar positive variance after non-operative management. The patient presented with ulnar wrist pain and limited range of motion. X-ray of left wrist shows loss of radial height and bony resorption and osteopenia from chronic regional pain syndrome (CRPS) and disuse. X-ray of the right wrist (R) of the same patient for comparison

Bu et al⁵⁷ investigated the effect of sequential radial length change on distal ulnar loading under static loading conditions. The authors observed differences in the effect of radial shortening on distal ulnar loading on wrists with inherent ulnar positive variance compared with wrists with inherent ulnar negative variance and concluded wrists with an inherent ulnar negative variance may tolerate more radial shortening post-fracture and are less likely to have clinical symptoms of ulnar carpal impaction.⁵⁷

As discussed previously, a biomechanical study of the effect of distal radius shortening reported that when ulnar variance was increased by 2.5 mm, the forearm axial load borne by the ulna increased to 40%. Conversely, when ulnar variance was decreased to 2.5 mm, forearm axial load borne by the ulna decreased to 5%.^{50,54} This suggests considerably altered load distribution with relatively small changes in distal radius length. This altered loading may cause pain and functional impairment and over time, potentially the development of degenerative wrist arthritis.

1.4.2 RADIAL SHORTENING OSTEOTOMY IN KIENBOCK'S

Avascular necrosis of the lunate, also known as Kienbock's disease, is a relatively uncommon disorder of the wrist. Kienbock's disease most commonly affect male laborers aged 20 – 40 years. Both wrists are equally affected. Symptoms include activity related dorsal wrist pain, swelling, decreased motion and reduced grip strength. Existing theories on the cause include the pattern of arterial blood supply,^{73,74} disruption of venous outflow,⁷⁵ ulnar negative variance,^{75,76} and increased/decreased radial inclination.^{77,78} However, no definitive cause has been proven.

The lunate is supplied by dorsal and palmar branches of the radial artery with contributions from

the anterior interosseous artery and palmar intercarpal arch. There are 3 patterns of interosseous branching in the lunate, the “Y,” “X,” or “I,” patterns of blood supply with the ‘I’ pattern demonstrating the highest risk for AVN.⁷³ The extraosseous arterial supply to the lunate arises from branches entering the lunate both palmarly and dorsally. The lunate is supplied by a single palmar artery in 7 – 20% of normal individuals^{73,74} thus in theory placing the lunate at risk of traumatic interruption of its vascular supply. Venous stasis due to disruption of venous outflow is another vascular theory either as a result of the disease process or traumatic insult to vascular outflow.⁷⁵

Negative ulnar variance as a predisposing factor was first described in 1928.⁷⁶ It was noted that 78% of patients with Kienbock’s in this study had negative ulnar variance compared to 23% in the general population. It is theorized that a short distal ulna leads to increased force transmission across the distal radius and lunate facet. However, recent biomechanical studies²² have failed to correlate native ulnar variance with increased load transmission across the distal radius and ulna. Furthermore, other investigators have not observed a correlation between negative native ulnar variance and incidence of Kienbock’s⁷⁹ with no significant difference in ulnar variance between patients with Kienbock’s and the general population.^{78,80,81} This theory of increased load transmission across the distal radius with ulnar negative variance has led to the common practice of treating Kienbock’s disease with radial shortening osteotomies (See figure 1.18).^{57,82,83,84,85} The magnitude of shortening which is optimal and the effect of that shortening under active wrist motion has not been determined.

The theory of radial inclination contributing to Kienbock’s has also been described as a cause for increased force transmission through the lunate facet of the distal radius and has led to various

techniques of radial opening or closing wedge osteotomies to alter inclination.^{86,87,88} However this theory is controversial as radial inclination has been found to be lower than average in most patients with Kienbock's disease.⁷⁸ Conflicting results have been published on the effect of changing radial inclination and unloading of the radiolunate joint thus this is not as popular as radial shortening as a treatment modality.^{77,89,90}

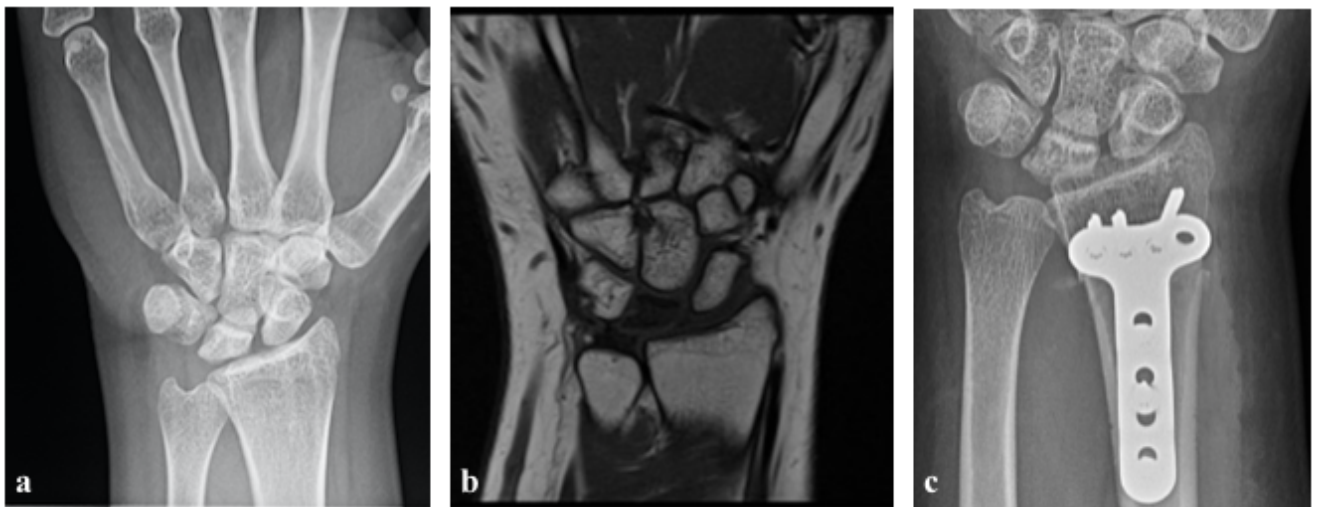


Figure 1. 19 Distal radius shortening osteotomy for Kienbock's disease.

Images of a 24-year-old woman with stage II Kienbock's disease. a) Left wrist x-ray demonstrating sclerosis of the lunate without collapse or fragmentation. Patient has ulnar negative variance b) T1 weighted MRI image of the same wrist demonstrating a hypointense lunate indicating an avascular lunate. c) Post-operative x-ray imaging following radial shortening osteotomy to offload the lunate.

Kienbock's disease has also been reported with various conditions including septic emboli, scleroderma, carpal coalition, sickle cell anemia, systemic lupus erythematosus, and

corticosteroid use. No consistent correlation with any specific etiology has been demonstrated suggesting that multiple factors are likely at play in the etiology of Kienbock’s disease.

As a result of osteonecrosis, the final stages Kienbock’s disease are lunate fragmentation and collapse. Litchman et al⁹¹ described a 4 stage classification system for Kienbock’s disease based on plain radiographs (Table 1) and may be useful to guide treatment.

Table 3. Litchman Classification for Kienbock’s Disease

Muscle	Function
Stage 1	No X-ray changes Signal change on MRI
Stage 2	Lunate sclerosis
Stage 3A	Lunate collapse No scaphoid palmar flexion No loss of carpal height
Stage 3B	Lunate collapse Fixed scaphoid palmar flexion Loss of carpal height
Stage 4	Perilunate arthritis

The treatment of Kienbock's disease is based on the Litchman's classification. In the early stages before lunate collapse (stage 2 or 3a), treatment is aimed at unloading the lunate fossa which includes radial shortening osteotomies or lunate revascularization with the use of vascularized pedicled bone grafts.^{92,93,94} In later stages, treatment is aimed at addressing the carpal malalignment, preventing further collapse and salvage procedures. These procedures include scaphotrapeziotrapezoid fusion, scaphocapitate fusion, proximal row carpectomy, limited intercarpal fusion and total wrist fusion based on amount of degenerative changes and patient goals.^{92,93,94}

1.4.3 CLINICAL EFFECTS OF ULNAR POSITIVE VARIANCE

Positive ulnar variance, can be congenital or acquired. Common causes include distal radius malunion with shortening, radial head excision with subsequent proximal migration of the radius, congenital positive ulnar variance, premature physal closure of the radius or overgrowth of the ulna due to trauma, Madelung's deformity, infection or tumor.

Positive ulnar variance can lead to ulnocarpal impaction. The most common cause of symptomatic ulnocarpal impaction is radial shortening due to a distal radius malunion. Ulnar positive variance is associated with ulnar sided wrist pain, restricted ulnar deviation and forearm rotation and development of degenerative changes due to the impaction of the ulnar head against the ulnar carpus. These changes include erosion and perforation of the TFCC and lunotriquetral ligament and lunate chondromalacia.^{95,96}

Ulnar impaction syndrome is most frequently associated with the ulnar positive variance (Figure 1.20), however, it can also occur in wrists with either ulnar negative or neutral variance.⁹⁷ Pain often occurs with wrist pronation, forceful grip and axial loading with ulnar deviation. The ulnocarpal stress test⁹⁸ places the wrist in ulnar deviation while passively rotating the forearm with an axial load which should reproduce the patients' pain.

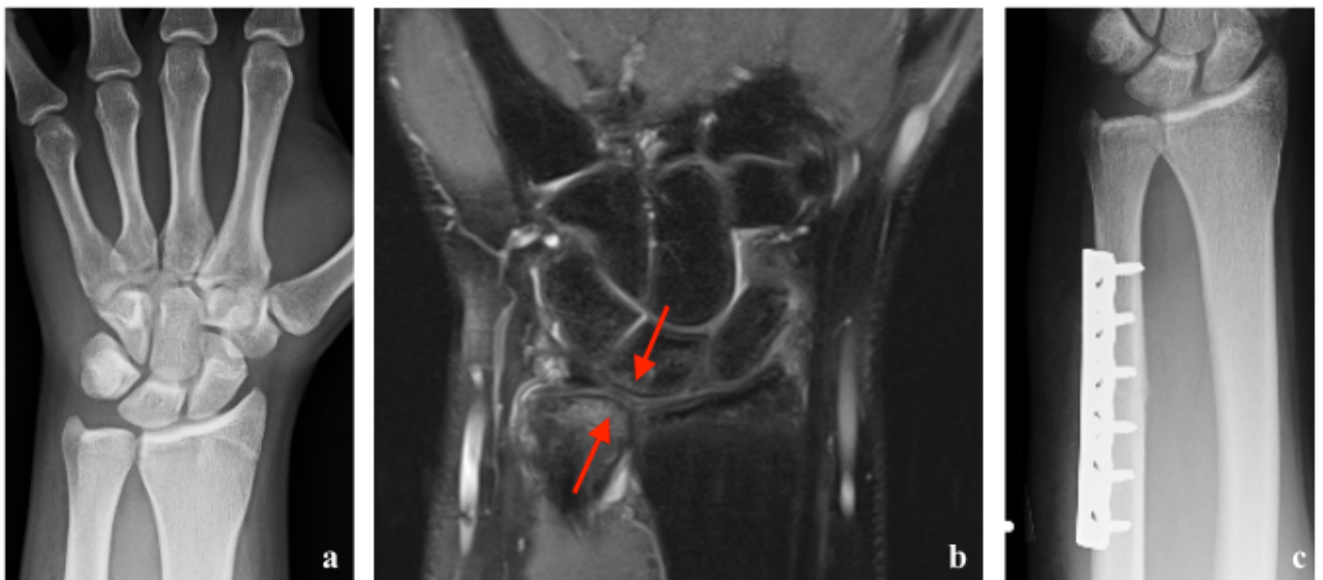


Figure 1. 20 Ulnocarpal impaction Syndrome

Images of a 20-year-old male with ulnar positive variance and symptomatic ulnocarpal impaction. a) Left wrist X-ray demonstrating ulnar positive variance. b) Left wrist T2 weighted coronal cut demonstrating ulnocarpal impaction with subchondral bony edema (red arrows). c) Post-operative X-ray following ulnar shortening osteotomy demonstrating restoration of neutral ulnar variance.

As noted previously, changes in ulnar variance with forearm position and grip has been described accounting for subtle variations on radiographs.^{6,7,8} An increase in ulnar variance of up to 2.5mm can occur on pronated grip view.⁸ This proximal migration/dynamic positive ulnar

variance with increased ulnocarpal load with pronation and grip may explain why patients with ulnocarpal impaction syndrome have pain with the ulnocarpal stress test.

Treatment for symptomatic ulnar impaction includes ulnar shortening osteotomy, wafer resection of the ulnar head,⁹⁹ a hemiresection interposition arthroplasty or an excisional arthroplasty.¹⁰⁰ These procedures have been shown to decrease load transmission through the distal ulna⁵⁶ and provide satisfactory pain relief.^{101,102,103,104} However the optimal magnitude of ulnar shortening is unknown. Excessive ulnar shortening can cause DRUJ incongruity¹⁰⁵ and contribute to the late onset of distal radioulnar joint arthritis which is commonly reported after this procedure.¹⁰⁶

1.5 CURRENT BIOMECHANICAL STUDIES ON FOREARM LOAD TRANSMISSION

A range of 9 – 43 % of the total wrist load has been reported to pass through the distal ulna in neutral wrist and forearm position.^{44,50,54,55,56,57,58,107}

Earlier studies by Palmer and Werner^{21,50,54,95} investigated loading by application of a constant force to cadaveric wrists. The wrists were constrained by cementing a pin in the third metacarpal to a loading frame to prevent radioulnar deviation and flexion/extension of the wrist. A constant load of 22.2 N was applied across the wrist using weights attached to the ECRL, ECRB, ECU, FCR and FCU. Loading of supinators and pronators and their respective contributions were not accounted for and the effects of wrist and forearm positioning on load transmission was not investigated. Axial loads were recorded by means of load cells in the mid-shaft of the radius and ulna which did not account for load dissipation through the IOM as load progresses proximally

and hence did not accurately measure load at the distal radius and ulna.^{44,45} This method of static wrist loading may not accurately simulate distal radius and ulna loading during *in-vivo* wrist motion.

Trumble et al¹⁰⁸ further investigated load sharing in the radius and ulna by static loading of the wrist in 5° and 10° of radial deviation, 5°, 15° and 15° ulnar deviation, 5° flexion and 5°, 10°, 15°, 20°, and 25° extension and 40° of pronation and supination. An arbitrary constrained axial load of 98.1 N was applied to the wrist using an Instron® materials testing machine (servohydraulic testing system). Radial and ulnar loads were measured by load cells affixed to the shaft between the middle and distal thirds of the radius and ulna. An average of 17% of the applied axial load was transmitted through the ulna with an increase observed in wrist extension, ulnar deviation and supination. Although this study expanded on earlier studies by examining the effects of wrist and forearm position on load transmission, their method of static loading does not, in all likelihood, accurately simulate dynamic motion. Load cells were also placed in the radial and ulnar shaft between the middle and distal one third at a distance the distal articular surfaces and the ROM studied was limited to a narrow range especially in flexion and extension.

In the studies listed above, the wrist was fixed in a neutral position while an axial load was applied. The limitation of the methodology was that they did not reproduce active dynamic wrist motion and therefore, did not account for the effect of muscle activation on wrist loading and did not accurately simulate normal wrist kinematics. Thus, their results may not reflect *in-vivo* wrist load transmission in various wrist and forearm positions. Secondly, the load cells were placed in the mid portion of the radius and ulna, measuring the load transmission across the forearm. This may not accurately measure load across the distal radius and ulna as dissipation of forces occur via soft tissue stabilizers, especially the IOM, as the load progresses proximally during axial

loading.^{44,45,46}

The importance of the IOM in load sharing between the radius and ulna has been investigated in two prior biomechanical studies.^{44,45} Loading has been shown to be equal in the proximal and distal aspects of the radius and ulna after IOM sectioning indicating no load transfer from the radius to the ulna after IOM sectioning.⁴⁵ In another study with an intact IOM,⁴⁴ in neutral elbow position, there was an increased load registered in the proximal ulna (11.8%) compared to the distal ulna (2.8%) indicating force transfer via the interosseous membrane.

Markolf et al⁴⁴ further expanded on previous biomechanical studies on forearm load transmission and also investigated the role of the IOM in load sharing by placing load cells in the distal ulna and proximal radius as close as possible to the radial and ulna heads. A static constant constrained load of 134 N was applied to the wrist using a servohydraulic testing machine while manually rotating the forearm. This was the maximum load that could be applied without causing structural failure; the magnitude of loading had no clinical rationale. As with previously mentioned studies, the applied loading was constant and did not take into account variation in loading with supination and pronation. Flexion, extension and radioulnar deviation were not studied. The proportion of load transmission at the distal radius and proximal ulna was calculated indirectly by subtracting the fraction that was registered by the proximal radial load-cell and distal ulnar load cell from 100%. Since the investigators did not directly measure loading in these areas load transfer through the IOM or other structures were not accounted for and thus the actual loading may have been considerably different. The effect of elbow position (full extension, 45° and 90° of flexion and varus/valgus positioning) and radial shortening on load sharing was investigated. At 4mm radial shortening, there was approximately equal load sharing observed between both the radius and ulna. However, the effects of ulnar lengthening/shortening

and radial lengthening on forearm load sharing was not investigated.

There is conflicting evidence regarding the relationship between ulnar variance and load transmitted through the distal ulna.^{22,109} Bu et al⁵⁷ investigated the effects of native ulnar variance and radial shortening on load transmission. The effects of radial lengthening and ulnar length change was not investigated. Loading was performed by application of a static axial load of 143 N applied to dead weights to a ball joint fixed to intramedullary pins in the second and third metacarpal. Load distribution in specimens with native ulnar positive variance was 69% through the radius and 31% through the ulna and in wrists with ulnar negative variance and 94% through the radius and 6% through the ulna.

However, a recent biomechanical study simulating dynamic wrist motion showed no significant relationship between ulnar variance and load transmission.²² Harley et al²² investigated the effects of simulated dynamic ROM on force variation in the distal radius and ulna. Load cells were placed at the junction between the middle and distal third of the radial and ulnar shafts and dynamic wrist motion simulated. There was no significant relationship between native ulnar variance and the proportion of load transmission through the distal ulna. Under quasi-static loading at neutral wrist and forearm positions, 13% of the forearm load was transmitted through the distal ulna and during simulated dynamic motion, peak ulnar forces were 17% during wrist flexion/extension and 20% during ulnar deviation. Loading was also higher through the distal ulna in pronation than supination. Although this study simulated dynamic wrist motion, the forearm muscles were stripped off the bone while the prime mover tendons were left intact distally. The dorsal and volar palmar radioulnar joint ligaments were also sectioned in this study to ensure load was directly applied to the distal radius and ulna. The results from these studies

lack the influence and contribution of forearm muscles and intact ligamentous stabilizers of the wrist to load distribution in the forearm. The effect of multiplanar motion such as dart throw on load transmission was not investigated. Dart throw motion has been shown to be an important functional motion in performing activities of daily living.¹¹⁰ Load cells were placed at a distance from the articular surface of the distal radius and ulna and were not placed in line with the central aspect/mid axis of the radius and ulna thus, absolute loads may not represent true loads at the distal radius and ulna. The effect of radial and ulnar length change on load sharing during simulated dynamic motion was not investigated.

There is a correlation between ulnar variance and articular disc of the TFCC (TFC) thickness with greater thickness of the TFC in wrists with ulnar negative ulnar variance.^{22,55} An earlier study using constrained axial loading by Palmer et al¹⁷ showed resection of the TFC resulted in a redistribution of the axial load so that the radius transmitted 95% and the ulna, 5% as opposed to 60% through the radius and 40% through the ulna with the TFC intact during static wrist loading. A subsequent study showed excision of two thirds or more of the TFC reduced ulnar load to 3% under static loading conditions.¹¹¹

It was previously reported that a more positive ulnar variance resulted in more load being transmitted through the distal ulna in the static loading scenario.^{57,109} However the correlation between ulnar variance and loading at the distal ulna is controversial in more recent literature using more physiologically relevant dynamic wrist motion simulators.^{22,57} The load distribution between the radius and ulna varies based on the length of the radius relative to the ulna. When ulnar variance is decreased to 2.5 mm, forearm axial load borne by the ulna decreased to 4%. The results from this study indicate shortening of only 2.5 mm is sufficient to decompress the

ulnocarpal joint.^{50,54} This load decrease is the rationale behind ulnar shortening osteotomy for ulnar impaction syndrome.

1.6 RATIONALE

Load sharing between the distal radius and ulna remains controversial at native length and following changes in radial and ulnar length. The aforementioned studies investigated load sharing during wrist motion under static loading. Only one study²² has investigated loading during simulated dynamic motion at native forearm bone length.

We chose a method of dynamic loading by suturing the prime mover tendons and connecting them to servomotors. The use of servomotors provide more precise motion control than that of hydraulic or pneumatic actuators used in previous studies²² that have simulated dynamic motion. Proportional loads were applied to the other tendons based on previous electromyographic studies of muscle activation and the relative cross sectional areas of muscles to simulate more physiologic motion.^{112,113}

The purpose of this research is to quantify how changes in radial and ulnar length affects distal forearm loading as the wrist is moved through simulated dynamic wrist motion. Surgeons require an improved knowledge of the normal forces across the distal radius and how this is altered with radial and ulnar shortening and lengthening to influence clinical and surgical decisions.

This study aims to clarify the relationship between radial and ulnar length change and load distribution between the distal radius and ulna during simulated wrist motion. We also aim to

quantify the relationship between native ulnar variance and load distribution across the wrist.

Furthermore, the contribution of the TFC to load transfer in the distal radius and ulna with ulnar length change during simulated dynamic wrist motion to recreate normal wrist mechanics will be investigated.

Although the effects of distal radius and ulna length changes on load transfer between the radius and ulna has been reported in a static situation; it is poorly understood during clinically relevant motions. This study will help surgeons develop a biomechanical rationale for clinical decisions related to management of Kienbock's disease, ulnocarpal impaction syndrome, distal radius and ulnar malunions and will have implications in the design of improved wrist implants. Hence, we plan to quantify the load distribution between the distal radius and ulna under simulated dynamic wrist motion for these various clinical scenarios with and without the TFC intact.

These studies herein are important in adding to the existing body of literature. Firstly, a custom jig with a load cell will be placed close to the distal articulating surface of the radius and ulna with placement of the load cell in line with the central axis of the radius and ulna thus gaining a better understanding of distal radial and ulnar forces than previous studies. Secondly, a dynamic wrist motion simulator will be utilized closely simulating *in-vivo* motion as opposed to static loading methods used in most previous studies. We will add to existing body of literature by also investigating the effects of simulated dart throwers motion on distal forearm loading with length changes of the distal radius and ulna. Thirdly, the soft tissue envelope will be left intact thus closely representing *in-vivo* conditions when compared to previous studies. Lastly, the effects of radial and ulnar lengthening during simulated dynamic motion will be studied which has not been reported in the literature to date. This study will contribute significantly to our understanding of load transmission following simulated surgical procedures and diseased states.

1.7 OBJECTIVES AND HYPOTHESIS

Objectives

1. To determine the relationship between distal forearm loading at the wrist and radial length change during simulated dynamic wrist motion.
2. To determine the relationship between native ulnar variance and distal forearm loading.
3. To determine the relationship between distal forearm loading at the wrist and ulnar length change during simulated dynamic wrist motion.
4. To determine the relationship between the TFC integrity and the force transmission through the distal ulna with ulnar length change.

Hypotheses

1. Distal radial loads will increase and distal ulnar loads will decrease with radial lengthening and vice versa. There will be variation in loads at different wrist positions during simulated dynamic wrist motion.
2. There will be no relationship between native ulnar variance and distal forearm loading.
3. Distal radial loads will decrease and distal ulnar loads will increase with ulnar lengthening and vice versa. There will be variation in loads at different wrist positions during simulated dynamic wrist motion.
4. TFC excision will influence load transmission for each interval of ulnar length change. Excision of the TFC during ulnar length change will decrease load transmission through the distal ulna compared to the TFC intact state.

1.8 THESIS OVERVIEW

Chapter 2 is a study on the effects of distal radial length change with radial lengthening of +1mm, +2mm and +3mm and radial shortening of -1mm, -2mm, -3mm and -4mm on load distribution at the wrist joint between the distal radius and ulna during simulated wrist ROM. This study will clarify the effects of radial shortening osteotomy for reducing load across the radiocarpal joint for treatment of Kienbock's disease. The effect of radial shortening after distal radial fractures on distal forearm loading will also be better understood.

Chapter 3 is a study on distal forearm loading with ulnar lengthening of +1mm, +2mm and +3mm and ulnar shortening of -1mm, -2mm, -3mm and -4mm during simulated wrist ROM to clarify the effects of ulnar shortening osteotomy for reducing load across the ulnocarpal joint for treatment of ulnocarpal impaction. The contribution of the TFC to load sharing will also be studied.

Chapter 4 concludes with a summary of our findings and directions for future research.

1.9 REFERENCES

1. Loredó RA, Sorge DG, García G. Radiographic evaluation of the wrist: A vanishing art. *Semin Roentgenol.* 2005;40(3):248-289. doi:10.1053/j.ro.2005.01.014.
2. Schemitsch EH, Richards RR. The effect of malunion on functional outcome after plate fixation of fractures of both bones of the forearm in adults. *J Bone Joint Surg Am.* 1992;74(7):1068-1078.
3. Firl M, Wunsch L. Measurement of bowing of the radius. *J Bone Joint Surg Br.* 2004;86(7):1047-1049. doi:10.1302/0301-620X.86B7.14294.
4. Rupasinghe SL, Poon PC. Radius morphology and its effects on rotation with contoured and noncontoured plating of the proximal radius. *J Shoulder Elb Surg.* 2012;21(5):568-573. doi:10.1016/j.jse.2011.03.015.
5. Schund FA, Linscheid RL, An KN, Chao EYS. A Normal Data Base of Posteroanterior Roentgenographic Measurements of the Wrist. *Curr Concepts Rev.* 1992.
6. Friedman SL, Palmer AK, Short WH, Mark Levinsohn E, Halperin LS. The change in ulnar variance with grip. *J Hand Surg Am.* 1993;18(4):713-716. doi:10.1016/0363-5023(93)90325-W.
7. Jung JM, Baek GH, Kim JH, Lee YH, Chung MS. Changes in ulnar variance in relation to forearm rotation and grip. *J Bone Joint Surg Br.* 2001.
8. Tomaino MM. The importance of the pronated grip x-ray view in evaluating ulnar variance. *J Hand Surg Am.* 2000;25(2):352-357. doi:10.1053/jhsu.2000.jhsu25a0352.
9. Clement H, Pichler W, Tesch NP, Windisch G. The influence of lateral and anterior angulation of the proximal ulna on the treatment of a Monteggia fracture AN

- ANATOMICAL CADAVER STUDY. :836-838. doi:10.1302/0301-620X.89B6.18975.
10. Rouleau DM, Faber KJ, Athwal GS. The proximal ulna dorsal angulation: A radiographic study. *J Shoulder Elb Surg.* 2010;19(1):26-30. doi:10.1016/j.jse.2009.07.005.
 11. Stuart PR, Berger RA, Linscheid RL, An KN. The dorsopalmar stability of the distal radioulnar joint. *J Hand Surg Am.* 2000;25(4):689-699. doi:10.1053/jhsu.2000.9418.
 12. Ekenstam F a. Anatomy of the distal radioulnar joint. *Clin Orthop Relat Res.* 1992;(275):14-18.
 13. Tolat AR, Stanley JK, Trail IA. A cadaveric study of the anatomy and stability of the distal radioulnar joint in the coronal and transverse planes. *J Hand Surg Br.* 1996;21(5).
 14. Daneshvar P, Willing R, Pahuta M, Grewal R, King GJW. Osseous Anatomy of the Distal Radioulnar Joint: An Assessment Using 3-Dimensional Modeling and Clinical Implications. *J Hand Surg Am.* 2016;41(11):1071-1079. doi:10.1016/j.jhsa.2016.08.012.
 15. Garcia-Elias M, Pitágoras T, Gilabert-Senar A. Relationship between joint laxity and radio-ulno-carpal joint morphology. *J Hand Surg Am.* 2003;28 B(2):158-162. doi:10.1016/S0266-7681(02)00364-9.
 16. Sagerman SD, Zogby RG, Palmer AK, Werner FW, Fortino MD. Relative articular inclination of the distal radioulnar joint: A radiographic study. *J Hand Surg Am.* 1995;20(4):597-601. doi:10.1016/S0363-5023(05)80275-8.
 17. Palmer AK, Werner FW, Eng MM. The triangular fibrocartilage complex of the wrist- Anatomy and function. *J Hand Surg Am.* 1981;6(2):153-162. doi:10.1016/S0363-5023(81)80170-0.
 18. Haugstvedt J-R, Berger RA, Nakamura T, Neale P, Berglund L, An K-N. Relative contributions of the ulnar attachments of the triangular fibrocartilage complex to the

- dynamic stability of the distal radioulnar joint. *J Hand Surg Am.* 2006;31(3):445-451.
doi:10.1016/j.jhsa.2005.11.008.
19. Nakamura T, Yabe Y. Histological anatomy of the triangular fibrocartilage complex of the human wrist. *Ann Anat.* 2000;182(6):567-572. doi:10.1016/S0940-9602(00)80106-5.
 20. Nakamura T, Yabe Y, Horiuchi Y. Dynamic changes in the shape of the triangular fibrocartilage complex during rotation demonstrated with high resolution magnetic resonance imaging. *J Hand Surg Br.* 1999;24(3):338-341. doi:10.1054/jhsb.1998.0216.
 21. Palmer a K, Glisson RR, Werner FW. Relationship between ulnar variance and triangular fibrocartilage complex thickness. *J Hand Surg Am.* 1984;9(5):681-682.
doi:10.1016/S0363-5023(84)80013-1.
 22. Harley BJ, Pereria ML, Werner FW, Kinney DA, Sutton LG. Force variations in the distal radius and ulna: Effect of ulnar variance and forearm motion. *J Hand Surg Am.* 2015;40(2):211-216. doi:10.1016/j.jhsa.2014.10.001.
 23. Ishii S, Palmer a K, Werner FW, Short WH, Fortino MD. An anatomic study of the ligamentous structure of the triangular fibrocartilage complex. *J Hand Surg Am.* 1998;23:977-985. doi:10.1016/S0363-5023(98)80003-8.
 24. Nakamura T, Yabe Y, Horiuchi Y. Functional anatomy of the triangular fibrocartilage complex. *J Hand Surg Br.* 1996;21(5):581-586.
 25. DiTano O, Trumble TE, Tencer AF. Biomechanical function of the distal radioulnar and ulnocarpal wrist ligaments. *J Hand Surg Am.* 2003;28(4):622-627. doi:10.1016/S0363-5023(03)00183-7.
 26. Noda K, Goto A, Murase T, Sugamoto K, Yoshikawa H, Moritomo H. Interosseous Membrane of the Forearm: An Anatomical Study of Ligament Attachment Locations. *J*

- Hand Surg Am.* 2009. doi:10.1016/j.jhsa.2008.10.025.
27. Skahen JR, Palmer AK, Werner FW, Fortino MD. The interosseous membrane of the forearm: anatomy and function. *J Hand Surg Am.* 1997;22(6). doi:10.1016/S0363-5023(97)80036-6.
 28. Kitamura T, Moritomo H, Arimitsu S, et al. The biomechanical effect of the distal interosseous membrane on distal radioulnar joint stability: A preliminary anatomic study. *J Hand Surg Am.* 2011;36(10):1626-1630. doi:10.1016/j.jhsa.2011.07.016.
 29. Arimitsu S, Moritomo H, Kitamura T, et al. The stabilizing effect of the distal interosseous membrane on the distal radioulnar joint in an ulnar shortening procedure: a biomechanical study. *J Bone Joint Surg Am.* 2011;93(21):2022-2030. doi:10.2106/JBJS.J.00411.
 30. Moritomo H. The distal interosseous membrane: Current concepts in wrist anatomy and biomechanics. *J Hand Surg Am.* 2012;37(7):1501-1507. doi:10.1016/j.jhsa.2012.04.037.
 31. Hotchkiss RN, An K-N, Sowa DT, Basta S, Weiland AJ. An anatomic and mechanical study of the interosseous membrane of the forearm: pathomechanics of proximal migration of the radius. *J Hand Surg Am.* 1989;14(2 Pt 1):256-261.
 32. Moritomo H, Murase T, Arimitsu S, Oka K, Yoshikawa H, Sugamoto K. The in vivo isometric point of the lateral ligament of the elbow. *J Bone Joint Surg Am.* 2007;89:2011-2017. doi:10.2106/JBJS.F.00868.
 33. Moritomo H, Noda K, Goto A, Murase T, Yoshikawa H, Sugamoto K. Interosseous Membrane of the Forearm: Length Change of Ligaments During Forearm Rotation. *J Hand Surg Am.* 2009;34(4):685-691. doi:10.1016/j.jhsa.2009.01.015.
 34. Tubbs RS, O'Neil JT, Key CD, et al. The oblique cord of the forearm in man. *Clin Anat.*

- 2007;20(4):411-415. doi:10.1002/ca.20346.
35. Patel BA. Form and function of the oblique cord (chorda obliqua) in anthropoid primates. *Primates*. 2005;46(1):47-57. doi:10.1007/s10329-004-0094-8.
 36. Spinner M, Kaplan E. Extensor carpi ulnaris. Its relationship to the stability of the distal radio-ulnar joint. *Clin Orthop Relat Res*. 1970;68:124-129.
 37. Iida A, Omokawa S, Moritomo H, et al. Biomechanical study of the extensor carpi ulnaris as a dynamic wrist stabilizer. *J Hand Surg Am*. 2012;37(12):2456-2461. doi:10.1016/j.jhssa.2012.07.042.
 38. Stuart PR. Pronator quadratus revisited. *J Hand Surg Eur Vol*. 1996;21(6):714-722. doi:10.1016/S0266-7681(96)80175-6.
 39. Gordon KD, Dunning CE, Johnson JA, King GJW. Influence of the Pronator Quadratus and Supinator Muscle Load on DRUJ Stability. *J Hand Surg Am*. 2003;28(6):943-950. doi:10.1016/S0363-5023(03)00487-8.
 40. King GJW, McMurtry RY, Rubenstein JD, Ogston NG. Computerized tomography of the distal radioulnar joint: correlation with ligamentous pathology in a cadaveric model. *J Hand Surg [Am]*. 1986;11(5):711-717.
 41. Gofton WT, Gordon KD, Dunning CE, Johnson JA, King GJW. Soft-tissue stabilizers of the distal radioulnar joint: An in vitro kinematic study. *J Hand Surg Am*. 2004;29(3):423-431. doi:10.1016/j.jhssa.2004.01.020.
 42. Kihara H, Short WH, Werner FW, Fortino MD, Palmer AK. The stabilizing mechanism of the distal radioulnar joint during pronation and supination. *J Hand Surg Am*. 1995;20(6):930-936. doi:10.1016/S0363-5023(05)80139-X.
 43. Watanabe H, Berger RA, Berglund LJ, Zobitz ME, An KN. Contribution of the

- interosseous membrane to distal radioulnar joint constraint. *J Hand Surg Am*. 2005;30(6):1164-1171. doi:10.1016/j.jhsa.2005.06.013.
44. Markolf KL, Lamey D, Yang S, Meals R, Hotchkiss R. Radioulnar load-sharing in the forearm. A study in cadavera. *J Bone Joint Surg Am*. 1998;80(6):879-888.
 45. Birkbeck DP, Failla JM, Hoshaw SJ, Fyhrie DP, Schaffler M. The interosseous membrane affects load distribution in the forearm. *J Hand Surg Am*. 1997;22(6):975-980. doi:10.1016/S0363-5023(97)80035-4.
 46. Pfaeffle HJ, Fischer KJ, Manson TT, Tomaino MM, Woo SLY, Herndon JH. Role of the forearm interosseous ligament: Is it more than just longitudinal load transfer? *J Hand Surg Am*. 2000;25(4):683-688. doi:10.1053/jhsu.2000.9416.
 47. Skahen JR, Palmer AK, Werner FW, Fortino MD. Reconstruction of the interosseous membrane of the forearm in cadavers. *J Hand Surg Am*. 1997;22(6):986-994. doi:10.1016/S0363-5023(97)80037-8.
 48. Rabinowitz RS, Light TR, Havey RM, et al. The role of the interosseous membrane and triangular fibrocartilage complex in forearm stability. *J Hand Surg Am*. 1994;19(3):385-393. doi:10.1016/0363-5023(94)90050-7.
 49. Wallace AL, Walsh WR, van Rooijen M, Hughes JS, Sonnabend DH. The interosseous membrane in radio-ulnar dissociation. *J Bone Joint Surg Br*. 1997;79(3):422-427. doi:10.1302/0301-620X.79B3.7142.
 50. Palmer AK, Werner FW. Biomechanics of the Distal Radioulnar Joint. *Clin Orthop Relat Res*. 1984;187:26-35.
 51. Schuind F, An KN, Berglund L, et al. The distal radioulnar ligaments: a biomechanical study. *J Hand Surg Am*. 1991;16(6):1106-1114. doi:10.1016/S0363-5023(10)80075-9.

52. Adams BD, Holley KA. Strains in the articular disk of the triangular fibrocartilage complex: A biomechanical study. *J Hand Surg Am.* 1993;18(5):919-925.
doi:10.1016/0363-5023(93)90066-C.
53. Tay SC, van Riet R, Kazunari T, et al. A method for in-vivo kinematic analysis of the forearm. *J Biomech.* 2008;41(1):56-62. doi:10.1016/j.jbiomech.2007.07.019.
54. Werner FW, Glisson RR, Murphy DJ, Palmer AK. Force transmission through the distal radioulnar carpal joint: effect of ulnar lengthening and shortening. *Handchir Mikrochir Plast Chir.* 1986;18(5):304-308.
55. Werner FW, Palmer AK, Fortino MD, Short WH. Force transmission through the distal ulna : Effect of ulnar variance , lunate fossa angulation , and radial and palmar tilt of the distal radius. *J Hand Surg Am.* 1992.
56. Markolf KL, Tejwani SG, Benhaim P. Effects of wafer resection and hemiresection from the distal ulna on load-sharing at the wrist: a cadaveric study. *J Hand Surg [Am].* 2005;30(2):351-358. doi:10.1016/j.jhsa.2004.11.013.
57. Bu J, Patterson RM, Morris R, Yang J, Viegas SF. The Effect of Radial Shortening on Wrist Joint Mechanics in Cadaver Specimens With Inherent Differences in Ulnar Variance. *J Hand Surg Am.* 2006;31(10):1594-1600. doi:10.1016/j.jhsa.2006.09.004.
58. Markolf KL, Dunbar AM, Hannani K. Mechanisms of load transfer in the cadaver forearm: Role of the interosseous membrane. *J Hand Surg Am.* 2000;25(4):674-682.
doi:10.1053/jhsu.2000.8640.
59. Shaaban H, Giakas G, Bolton M, et al. The load-bearing characteristics of the forearm: pattern of axial and bending force transmitted through ulna and radius. *J Hand Surg Am.* 2006;31(3):274-279. doi:10.1016/j.jhsb.2005.12.009.

60. Ekenstam FW, Palmer AK, Glisson RR. The load on the radius and ulna in different positions of the wrist and forearm. A cadaver study. *Acta Orthop Scand*. 1984;55(3):363-365.
61. Amadio PC, Botte MJ. Treatment of malunion of the distal radius. *Hand Clin*. 1987;3(4):541-561.
62. Bushnell BD, Bynum DK. Malunion of the distal radius. *J Am Acad Orthop Surg*. 2007;15(1):27-40. doi:15/1/27 [pii].
63. Melone CP. Articular fractures of the distal radius. *Orthop Clin North Am*. 1984;15(2):217-236. doi:10.1016/j.otsr.2013.11.002.
64. Aro HT, Koivunen T. Minor axial shortening of the radius affects outcome of Colles' fracture treatment. *J Hand Surg Am*. 1991;16(3):392-398. doi:10.1016/0363-5023(91)90003-T.
65. Fernandez DL. Correction of post-traumatic wrist deformity in adults by osteotomy, bone-grafting, and internal fixation. *J Bone Joint Surg Am*. 1982;64(8):1164-1178.
66. Hove LM, Fjeldsgaard K, Skjeie R, Solheim E. Anatomical and functional results five years after remanipulated Colles' fractures. *Scand J Plast Reconstr Hand Surg*. 1995;29(4):349-355. doi:10.3109/02844319509008971.
67. Kopylov P, Johnell O, Redlund-johnell I, Bengner U. Fractures of the distal end of the radius in young adults: A 30-year follow-up. *J Hand Surg Am*. 1993;18(1):45-49. doi:10.1016/0266-7681(93)90195-L.
68. A L. Fracture of the distal end of the radius: a clinical and statistical study of end results. *Acta Orthop Scand*. 1959;41:1-118.
69. Batra S, Gupta A. The effect of fracture-related factors on the functional outcome at 1

- year in distal radius fractures. *Injury*. 2002;33(6):499-502.
70. Leung F, Ozkan M, Chow SP. Conservative treatment of intra-articular fractures of the distal radius--factors affecting functional outcome. *Hand Surg*. 2000;5(2):145-153.
 71. Howard P, Stewart H, Hind R, Burke F. External fixation or plaster for severely displaced comminuted Colles' fractures? A prospective study of anatomical results. *J Hand Surg Br*. 1989;71(1):68-73.
 72. McQueen M, Caspers J. Colles fracture: does the anatomical result affect the final function? *J Bone Joint Surg Br*. 1988;70(4):649-651. doi:10.1016/S0140-6736(61)91292-2.
 73. Gelberman RH, Bauman TD, Menon J, Akeson WH. The vascularity of the lunate bone and Kienböck's disease. *J Hand Surg Am*. 1980;5:272-278. doi:10.1097/00006534-198108000-00069.
 74. Panagis JS, Gelberman RH, Taleisnik J, Baumgaertner M. The arterial anatomy of the human carpus. Part II: The intraosseous vascularity. *J Hand Surg Am*. 1983;8(4):375-382. doi:10.1016/S0363-5023(83)80194-4.
 75. Schiltenswolf M, Martini AK, Mau HC, Eversheim S, Brocai DRC, Jensen CH. Further investigations of the intraosseous pressure characteristics in necrotic lunates (Kienbock's disease). *J Hand Surg Am*. 1996;21(5):754-758. doi:10.1016/S0363-5023(96)80187-0.
 76. Hulten O. Uber anatomische variationen der handgelenkknochen. *Acta Radiol (Old Ser)*. 1928;9:155-168.
 77. Watanabe K, Nakamura R, Horii E, Miura T. Biomechanical analysis of radial wedge osteotomy for the treatment of Kienbock's disease. *J Hand Surg [Am]*. 1993;18(4):686-690.

78. Tsuge S, Nakamura R. Anatomical risk factors for Kienbock's disease. *J Hand Surg - Br Vol.* 1993;18(1):70-75.
79. Nakamura R, Imaeda T, Miura T. Radial shortening for Kienbock's disease: Factors affecting the operative result. *J Hand Surg Am.* 1990;15(1):40-45. doi:10.1016/0266-7681(90)90045-6.
80. D'Hoore K, De Smet L, Verellen K, Vral J, Fabry G. Negative ulnar variance is not a risk factor for Kienbock's disease. *J Hand Surg Am.* 1994;19(2):229-231. doi:10.1016/0363-5023(94)90010-8.
81. Van Leeuwen WF, Oflazoglu K, Menendez ME, Ring D. Negative Ulnar Variance and Kienbock Disease. *J Hand Surg Am.* 2016;41(2):214-218. doi:10.1016/j.jhsa.2015.10.014.
82. Rock MG, Roth JH, Martin L. Radial shortening osteotomy for treatment of Kienbock's disease. *J Hand Surg Am.* 1991;16(3):454-460.
83. Takahara M, Watanabe T, Tsuchida H, Yamahara S, Kikuchi N, Ogino T. Long-term follow-up of radial shortening osteotomy for Kienbock disease. Surgical technique. *J Bone Joint Surg Am.* 2009;91 Suppl 2(Part 2):184-190. doi:10.2106/JBJS.I.00315.
84. Matsui Y, Funakoshi T, Motomiya M, Urita A, Minami M, Iwasaki N. Radial shortening osteotomy for kienbock disease: Minimum 10-year follow-up. *J Hand Surg Am.* 2014;39(4):679-685. doi:10.1016/j.jhsa.2014.01.020.
85. Watanabe T, Takahara M, Tsuchida H, Yamahara S, Kikuchi N, Ogino T. Long-term follow-up of radial shortening osteotomy for Kienbock disease. *J Bone Jt Surg Am.* 2008;90(8):1705-1711. doi:10.2106/JBJS.G.00421.
86. Iwasaki N, Minami A, Ishikawa J, Kato H, Minami M. Radial osteotomies for teenage

- patients with Kienbock disease. *Clin Orthop Relat Res.* 2005;439:116-122.
doi:10.1097/01.blo.0000173254.46899.72.
87. Miura H, Uchida Y, Sugioka Y. Radial closing wedge osteotomy for Kienbock's disease. *J Hand Surg Am.* 1996;21(6):1029-1034. doi:10.1016/S0363-5023(96)80311-X.
 88. Wada A, Miura H, Kubota H, Iwamoto Y, Uchida Y, Kojima T. Radial closing wedge osteotomy for Kienbock's disease: an over 10 year clinical and radiographic follow-up. *J Hand Surg[Br].* 2002;27(0266-7681 SB-IM):175-179. doi:10.1054/jhsb.2001.0621.
 89. Kam B, Topper SM, McLoughlin S, Liu Q. Wedge osteotomies of the radius for Kienböck's disease: A biomechanical analysis. *J Hand Surg Am.* 2002;27(1):37-42.
doi:10.1053/jhsu.2002.29489.
 90. F.W. W, A.K. P. Biomechanical evaluation of operative procedures to treat Kienbock's disease. *Hand Clin.* 1993;9(3):431-443.
 91. Lichtman DM, Mack GR, MacDonald RI, Gunther SF, Wilson JN. Kienböck's disease: the role of silicone replacement arthroplasty. *J Bone Joint Surg Am.* 1977;59(7):899-908.
 92. Iwasaki N, Genda E, Minami a, Kaneda K, Chao EY. Force transmission through the wrist joint in Kienböck's disease: a two-dimensional theoretical study. *J Hand Surg Am.* 1998;23(3):415-424. doi:10.1016/S0363-5023(05)80459-9.
 93. Kolovich GP, Kalu CMK, Ruff ME. Current Trends in Treatment of Kienböck Disease: Table 1. *Hand.* 2016;11(1):113-118. doi:10.1177/1558944715616953.
 94. Cross D, Matullo K. Kienbock's Disease. *Hand Clin.* 2014;45(1):141-152.
 95. Palmer AK. Triangular fibrocartilage complex lesions: A classification. *J Hand Surg Am.* 1989;14(4):594-606. doi:10.1016/0363-5023(89)90174-3.
 96. Nishiwaki M, Nakamura T, Nagura T, Toyama Y, Ikegami H. Ulnar-Shortening Effect on

- Distal Radioulnar Joint Pressure: A Biomechanical Study. *J Hand Surg Am*. 2008;33(2):198-205. doi:10.1016/j.jhsa.2007.11.024.
97. Tomaino MM. Ulnar impaction syndrome in the ulnar negative and neutral wrist: Diagnosis and pathoanatomy. *J Hand Surg Eur Vol*. 1998;23(6):754-757. doi:10.1016/S0266-7681(98)80090-9.
98. Nakamura R, Horii E, Imaeda T, Nakao E, Kato H, Watanabe K. The ulnocarpal stress test in the diagnosis of ulnar-sided wrist pain. *J Hand Surg - Br Vol*. 1997;22(6):719-723.
99. Feldon P, Terrono AL, Belsky MR. Wafer distal ulna resection for triangular fibrocartilage tears and/or ulna impaction syndrome. *J Hand Surg Am*. 1992;17(4):731-737. doi:10.1016/0363-5023(92)90325-J.
100. Bowers WH. Distal radioulnar joint arthroplasty: the hemiresection-interposition technique. *J Hand Surg Am*. 1985;10(2):169-178.
101. Fulton C, Grewal R, Faber KJ, Roth J, Gan BS. Outcome analysis of ulnar shortening osteotomy for ulnar impaction syndrome. *Can J Plast Surg*. 2012;20(1).
102. Kim BS, Song HS. A comparison of Ulnar shortening Osteotomy alone versus combined Arthroscopic Triangular Fibrocartilage complex Debridement and Ulnar Shortening Osteotomy for Ulnar Impaction Syndrome. *Clin Orthop Surg*. 2011;3(3):184-190. doi:10.4055/cios.2011.3.3.184.
103. Tomaino MM, Weiser RW. Combined arthroscopic TFCC debridement and wafer resection of the distal ulna in wrists with triangular fibrocartilage complex tears and positive ulnar variance. *J Hand Surg Am*. 2001;26(6):1047-1052. doi:10.1053/jhsu.2001.28757.
104. Doherty C, Gan BS, Grewal R. Ulnar Shortening Osteotomy for Ulnar Impaction

- Syndrome. *J Wrist Surg*. 2014;3(2):85-90. doi:10.1055/s-0034-1372519.
105. Deshmukh SC, Shanahan D, Coulthard D. Distal radioulnar joint incongruity after shortening of the ulna. *J Hand Surg[Br]*. 2005;25(5). doi:10.1054/jhsb.2000.0456.
 106. Baek GH, Hyuk JL, Hyun SG, et al. Long-term Outcomes of Ulnar Shortening Osteotomy for Idiopathic Ulnar Impaction Syndrome: At Least 5-Years Follow-up. *Clin Orthop Surg*. 2011;3(4):295-301. doi:10.4055/cios.2011.3.4.295.
 107. Greenberg JA, Werner FW, Smith JM. Biomechanical analysis of the distal metaphyseal ulnar shortening osteotomy. *J Hand Surg Am*. 2013;38(10):1919-1924. doi:10.1016/j.jhsa.2013.06.038.
 108. Trumble T, Glisson RR, Seaber A V, Urbaniak JR. Forearm force transmission after surgical treatment of distal radioulnar joint disorders. *J Hand Surg Am*. 1987;12(2):196-202. doi:http://dx.doi.org/10.1016/S0363-5023(87)80270-8.
 109. Bu J, Patterson RM, Morris R, Yang J, Viegas SF. The Effect of Radial Shortening on Wrist Joint Mechanics in Cadaver Specimens With Inherent Differences in Ulnar Variance. *J Hand Surg [Am]*. 2006;31(10):1594-1600. doi:10.1016/j.jhsa.2006.09.004.
 110. Brigstocke GHO, Hearnden A, Holt C, Whatling G. In-vivo confirmation of the use of the dart thrower's motion during activities of daily living. *J Hand Surg Eur Vol*. 2014;39E(4):373-378. doi:10.1177/1753193412460149.
 111. Palmer AK, Werner FW, Glisson RR, Murphy DJ. Partial excision of the triangular fibrocartilage complex. *J Hand Surg Am*. 1988;13(3):391-394. doi:10.1016/S0363-5023(88)80015-7.
 112. Iglesias D, Lockhart J, Johnson J, King GJW. Development of an In-Vitro Passive and Active Motion Simulator for the Investigation of Wrist Function and Kinematics. 2015.

113. Gordon KD, Pardo RD, Johnson JA, King GJW, Miller TA. Electromyographic activity and strength during maximum isometric pronation and supination efforts in healthy adults. *J Orthop Res.* 2004;22(1):208-213. doi:10.1016/S0736-0266(03)00115-3.

2. EFFECT OF RADIAL LENGTH CHANGE ON DISTAL FOREARM LOADING DURING SIMULATED WRIST MOTION

2.1 OVERVIEW

This chapter reports on an in-vitro cadaveric study examining the relationship between changes in radial length and distal forearm forces during simulated wrist motion. Load cells were implanted in the distal radius and ulna to quantify loads, during simulated active motion.

2.2 INTRODUCTION

Distal radius malunion is a frequent cause of wrist pain and disability impairing patient function. It is the most common complication of distal radius fractures with an incidence of 17 - 24%.^{1,2,3} Of the radiographic deformities, radial shortening has been associated most frequently with unsatisfactory outcomes following distal radius fractures.^{4,5,6,7,8} Radial shortening results in a transfer of load onto the ulna, resulting in pain and weakness, which gives rise to poor function. The treatment of distal radius malunion aims to restore normal radial length and correct associated deformities. Understanding the biomechanical implications of radial shortening will aid in surgical decision making when performing distal radial osteotomies by clarifying the importance of restoring normal anatomic parameters.

Avascular necrosis (AVN) of the lunate, also known as Kienbock's disease, is another cause of progressive wrist pain, stiffness and weakness. Various theories exist, however, the exact

etiology remains to be clarified. Negative ulnar variance as a predisposing risk factor was first described by Hulten in 1928.⁹ It was noted at the time that 78% of patients with Kienbock's had negative ulnar variance compared to 23% in the general population; thus, it was theorized that negative ulnar variance leads to increased force transmission across the distal radius, particularly the lunate facet, leading to AVN of the lunate. In a survey of hand surgeons in North America,¹⁰ the majority of the responding surgeons believe ulnar-negative variance to be the sole contributory factor to the development of Kienböck disease. The treatment of Kienbock's disease is based on the Litchman's classification. In the early stages before lunate collapse (stage II or IIIa), treatment is aimed at unloading the lunate fossa. This theory of increased load transmission across the distal radius in patients with negative ulnar variance has led to the common practice of treating Kienbock's disease with a joint leveling procedure such as radial shortening osteotomies, resulting in good clinical outcomes.^{11,12,13,14,15,16,17} However, the magnitude of shortening which leads to optimal clinical outcomes and the effect of radial shortening on distal radius and ulnar loading has not been reported.

As described in Chapter 1 (Section 1.5), earlier biomechanical studies^{18,19,20,21,22,23} on forearm load transmission and simulated radial shortening^{19,24,25} have investigated load sharing at the distal radius and ulna only during static loading of the wrist. Constrained axial loads were applied to the wrist while the wrist was fixed in various positions. The limitation of the methodology was that they did not accurately simulate normal wrist kinematics by reproducing active dynamic wrist motion thus calling into question the clinical applicability of these findings.

The effect of native ulnar variance on loading through the distal forearm is controversial. Previous biomechanical studies have reported that a wrist with a naturally positive ulnar variance have increased loads through the distal ulna when compared to a wrist with negative ulnar variance.^{19,22} However the correlation between ulnar variance and loading at the distal ulna is controversial in recent literature using more physiologically relevant dynamic wrist motion simulators.^{19,26}

The effects of radial length change on axial load transmission during simulated dynamic wrist motion remains to be clarified. Surgeons treating patients with distal radius shortening associated with distal radius fractures and Kienbock's disease require an improved knowledge of the normal forces across the distal radius and how this is altered with radial length changes. This will assist in surgical decision making when considering distal radius osteotomies for malunion or Kienbock's disease. A better understanding of distal forearm loading may also assist in the development of improved arthroplasty designs for the radiocarpal and distal radioulnar joints.

Hence, in order to develop improved evidence-based treatments for distal radial malunions and Kienbock's disease, a biomechanical cadaver-based experimental model was developed to evaluate the effects of radial length change on axial loading through the distal forearm during simulated dynamic wrist motion. Our main objective was to quantify the effects of radial shortening on distal radial and ulnar loading during simulated dynamic wrist motion. Our secondary objective was to clarify the relationship between native ulnar variance and distal ulnar loading under simulated dynamic wrist motion. Our hypotheses were: 1) distal radial loads will increase and distal ulnar loads will decrease with radial lengthening; 2) distal radial loads will

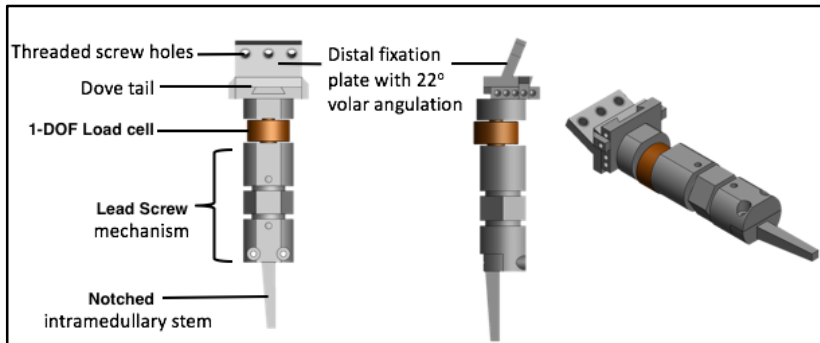
decrease and distal ulnar loads will increase with radial shortening; 3) loading will vary at different wrist positions during simulated dynamic wrist motion; and 4) differences in native ulnar variance will not influence load distribution in the distal radius and ulna.

2.3 METHODS

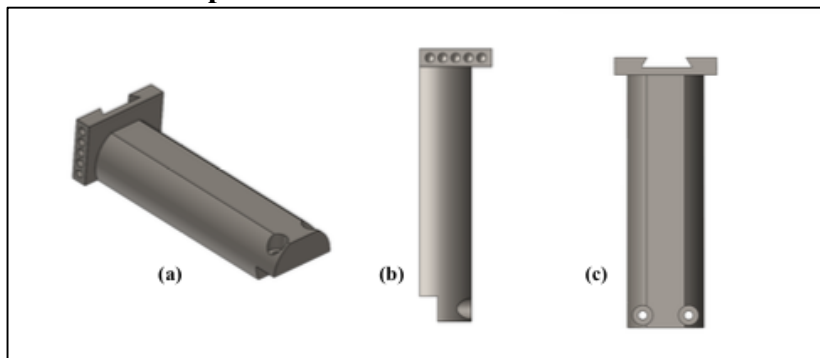
2.3.1 IMPLANT DESIGN

A custom implant was designed to lengthen and shorten the radius using a lead screw mechanism. A one-degree of freedom (1-DOF) load cell (Honeywell® model 11, NJ, USA) was placed distal to the lead screw (Figure 2.1 a) to quantify axial load through the distal radius.

Distally, the radial implant was secured to bone through a locking mechanism by threaded holes in the distal fixation plate to create a fixed angle construct. The distal fixation plate was designed with a 12° volar angulation to match the contour of the volar aspect of the distal radius for flush fit based on previous studies.²⁷ The implant had both a spacer for specimen preparation and the final implant with a load cell and lead screw mechanism for testing. The spacer and load cell were designed similarly with the same length but with a slight width difference; the spacer had a slightly smaller diameter than the final testing implant to facilitate implant insertion and cement fixation. The spacer preserved the native distal radial and ulnar articular height during implant insertion so as not to affect the normal load sharing and native variance of the forearm (Figure 2.1 b). To improve fixation of the distal fragment, the metaphysis was reamed and polymethylmethacrylate (bone cement) was inserted to augment screw purchase. Locking screws were used to provide a rigid fixed angle construct.



a. Radial Custom Implant



b. Radial Spacer Block (a) Isometric (b) Lateral and (c) AP views

Figure 2. 1 Custom Radial Implants

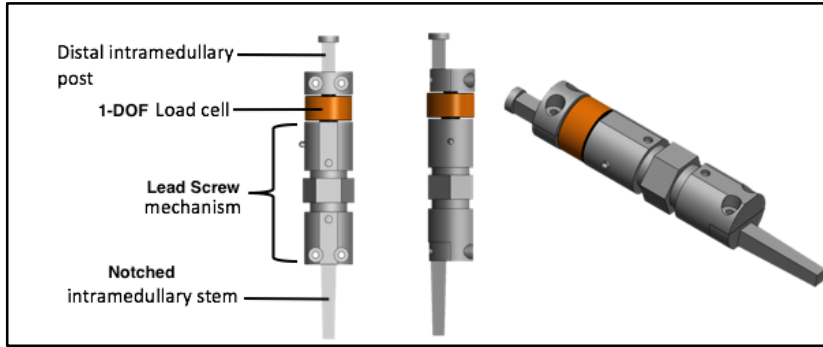
© D Isa, M McGregor

- a. Custom implant for radius. Components include a distal fixation plate with 22 volar angulation, a 1-DOF load cell, lead screw mechanism for length adjustments and a notched proximal stem.
- b. Radial spacer block.

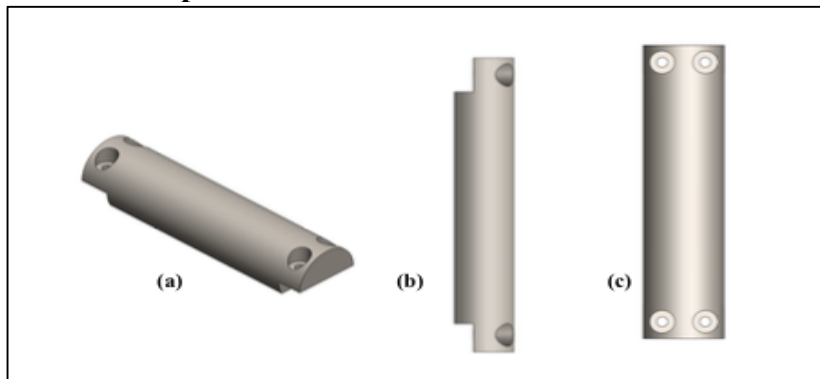
Proximally, the stem was notched and roughened to assist with fixation in the intramedullary canal. An appropriate stem diameter for our study was calculated based on mean intramedullary measurements from cadaveric CT scans. This allowed for a secure fit in the smallest intramedullary canals while also allowing for an adequate cement mantle.

The intermediate components between the proximal and distal components consist of a load cell for axial (tensile and compressive) load measurement and a lead screw mechanism. The lead screw mechanism allowed for length adjustment of the implant. Rotating the central nut caused both threaded eye bolts to be translated in or out simultaneously, thus adjusting the implant length without rotating the thread eye bolts. The thread pitch was such that one third of a full bolt revolution counterclockwise resulted in 1mm of lengthening and one third of a full middle bolt revolution clockwise resulted in 1mm of shortening. The implant was designed to achieve 5 mm of shortening and 5 mm of lengthening each from the native position.

A similar ulnar implant with a 1-DOF load cell (Honeywell® model 11, NJ, USA) was also designed (Figure 2.2 a). The distal component incorporated a rectangular notched stem for cementing into the intramedullary canal of the distal ulna. The intermediate components and proximal stem were designed in a similar fashion to the radial component. The intermediate component between the proximal and distal components consists of a load cell for axial (tensile and compressive) load measurement and a lead screw mechanism. Proximally, the stem was notched and roughened to assist with fixation in the intramedullary canal. The ulnar spacer and custom ulnar implant were designed similarly with the same length but with a slight width difference; the spacer had a slightly smaller diameter than the final testing implant to facilitate maintenance of an intact bone bridge and preserve the native distal ulnar articular surface location during the insertion and cementing process (Figure 2.2 b).



a. Ulnar Custom Implant



b. Ulnar Spacer Block (a) Isometric (b) Lateral (c) AP View

Figure 2. 2 Custom Ulnar Implant

© D Isa, McGregor

- a. Custom implant for ulna. Components include a distal post, a 1-DOF load cell, lead screw mechanism for length adjustments and a notched proximal stem
- b. Ulnar spacer block.

2.3.2 AXIAL LOAD MEASUREMENT

Axial loads measured using the 1-DOF Honeywell® load cell model 11 (NJ, USA) had 0.8% accuracy, 0.1% repeatability. The load cells were zeroed prior to implantation without the application or influence of external loads. The load cells have threaded connections on either side to securely attach to the radial and ulnar custom implants to measure axial (tensile and compressive) forces.

2.3.3 SPECIMEN PREPARATION

Testing was performed on 9 fresh frozen right cadaveric forearm specimens (mean age 74 years; range 60 to 83 years; all male) with no clinical or CT evidence of osteoarthritis. The specimens were amputated at the mid-humeral level and stored at - 20 °C. They were thawed for 18 hours at room temperature (22 °C) and then prepared for mounting.

PA wrist X-rays with the elbow flexed at 90° and forearm in neutral rotation were taken to measure native ulnar variance.

A standard volar flexor carpi radialis (FCR) approach to the distal radius was utilized (Figure 2.3). Skin and subcutaneous tissue was sharply incised. The FCR tendon sheath was then incised and the FCR tendon retracted ulnarly. The floor of the FCR tendon sheath was incised and flexor pollicis longus (FPL) and the contents of the carpal tunnel was retracted ulnarly exposing the pronator quadratus (PQ). The PQ was then subperiosteally elevated off the distal radius in a radial to ulnar direction. Care was taken so as not to disrupt the volar distal radioulnar joint (DRUJ) capsule or interosseous membrane.

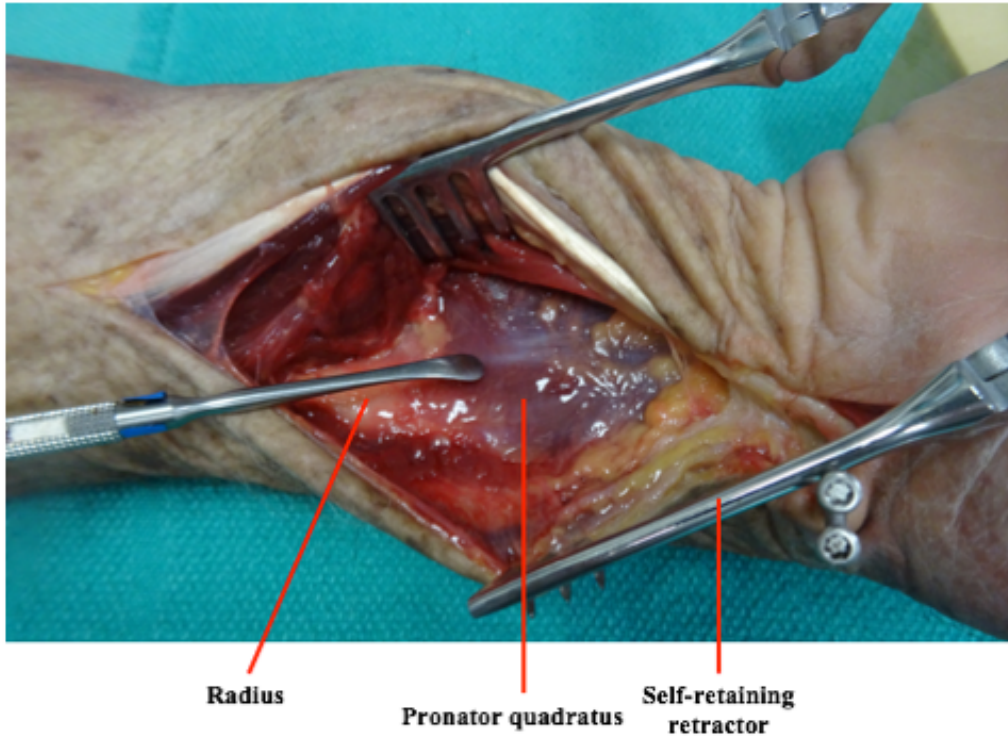


Figure 2. 3 FCR approach. Pronator quadratus over the distal radius.
© D Isa

A 40mm segment of the volar cortex 10 mm proximal to the DRUJ was excised using a cutting guide and a microsagittal saw. The dorsal bone bridge was left intact to maintain the alignment of the radius (Figure 2.4 a-g). The radial implant spacer was then cemented in place (Figure 2.4 h).

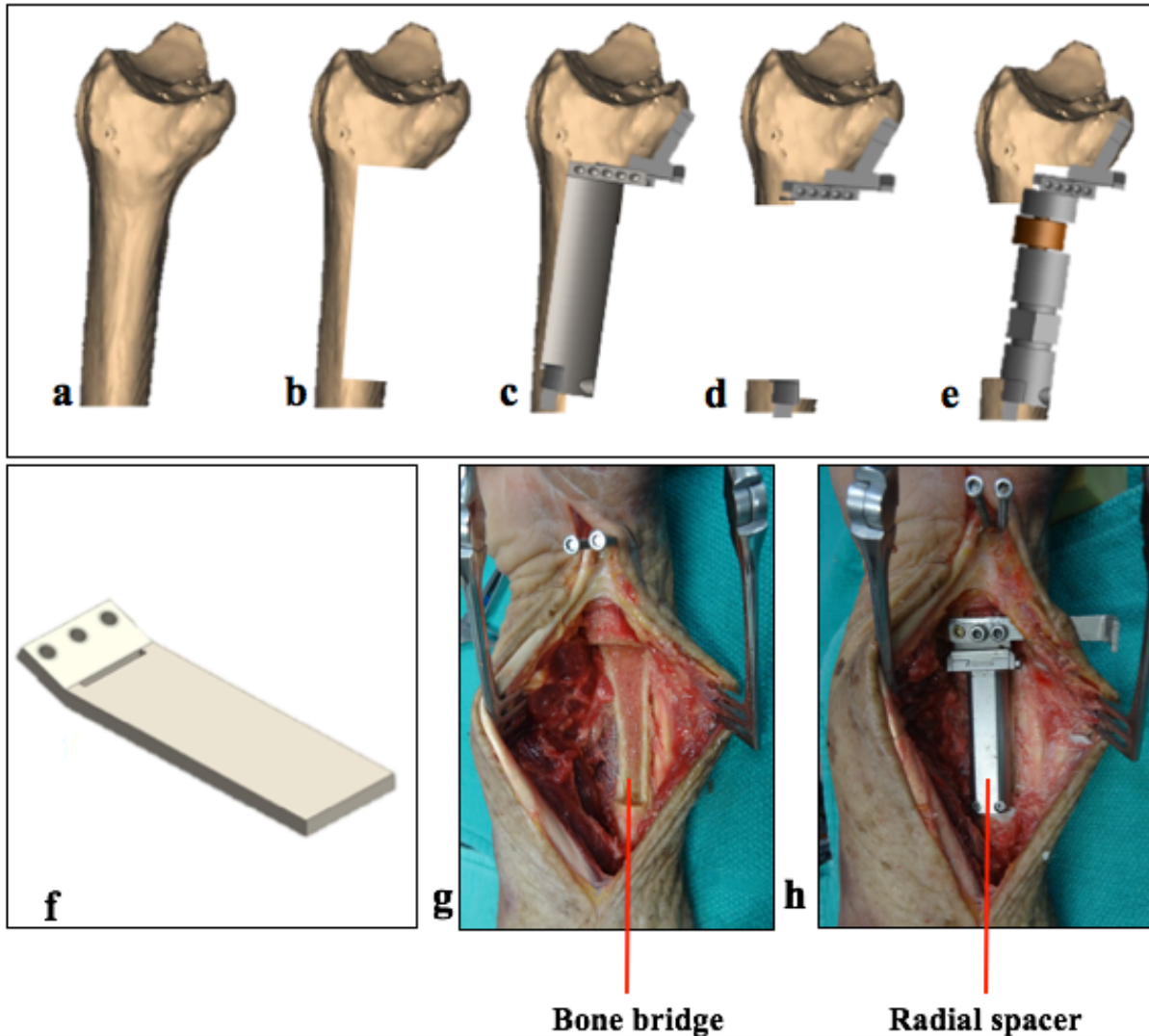


Figure 2. 4 Bone bridge technique radius

© D Isa

(a) – (e) Radial bone bridge technique. Lateral view showing bone bridge left intact dorsally to maintain articular height. The radial spacer is shown inserted. The bone bridge was cut prior to installation of final custom radial implant. (f) Radial Cutting guide (g) Bone Bridge Radius and (h) Cadaver specimen with radial spacer block.

To insert the ulnar implant, the subcutaneous boarder of the ulna was approached using the interval between extensor carpi ulnaris (ECU) and flexor carpi ulnaris (FCU). The extensor

retinaculum was left intact. Using the bone bridge technique, a 40mm segment of bone approximately 10mm proximal to the DRUJ was excised. Utilizing a cutting guide, cuts were made using a microsagittal saw leaving a radially based bone bridge intact. The ulna implant spacer was then cemented in place (Figure 2.5 a-h).

The tendons of the muscle groups contributing the greatest proportion of force for a given motion (prime movers) were exposed and sutured proximal to the extensor retinaculum to allow for simulated active wrist motion.^{28,29}

The tendons of the wrist extensors (extensor carpi radialis longus [ECRL], extensor carpi radialis brevis [ECRB] extensor carpi ulnaris [ECU]), wrist flexors (flexor carpi radialis [FCR], flexor carpi ulnaris [FCU]), pronator teres [PT] and biceps [BI] were sutured using a Spectra extreme braid fishing line (80lbs) using a running locking stitch (Figure 2.6). All sutures (except BI) were tunneled under the skin and passed through alignment guides in the medial and lateral epicondyle to mimic physiologic line of muscle pull. The sutures were then attached to electric servomotors (SMI 2316D-PLS, Animatics, CA) with force transducers (Vishay Precision Group, Raleigh, NC) to control tendon forces.

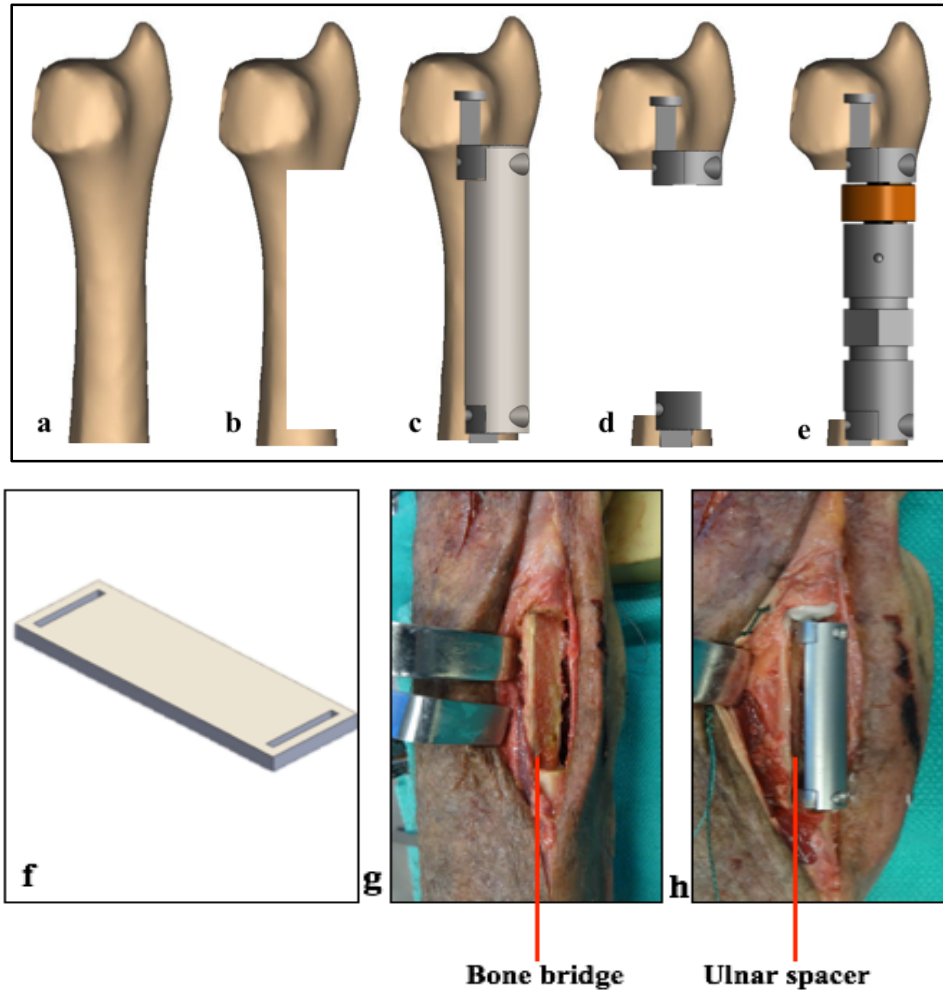


Figure 2. 5 Radial and ulnar spacers in cadaver specimens.

© D Isa

(a) – (e) Ulnar bone bridge technique. AP view showing bone bridge left intact radially to maintain articular height. The ulnar spacer is shown inserted. The bone bridge was cut prior to installation of final custom radial implant. (f) Radial Cutting guide (g) Bone Bridge Radius and (h) Cadaver specimen with radial spacer block.

In order to track joint motion, infrared marker triads were rigidly affixed to the radius, ulna and 3rd metacarpal using custom Delrin® pedestals and wrist motion was tracked using an Optotrak Certus (Northern Digital Inc, Waterloo, Ontario, Canada) motion capture system with a 3D

accuracy of 0.1mm and 0.01mm resolution.³⁰ (Figure 2.7)



Figure 2. 6 Running locking stitch through tendon
© D Isa

All incisions were closed using a nylon zipper to preserve moisture and for ease of accessibility to the radial and ulna implants for length adjustments. The specimens were also kept moist by intermittent saline irrigation of the soft tissues.

Specimens were tested in a simulator capable of producing active wrist motion with simulated muscle loading (Figures 2.7). The humerus was rigidly secured to the simulator by means of a clamp. The elbow was placed at 90° of flexion, neutral varus/valgus and neutral forearm rotation and the ulna was transfixed to a static post on the simulator using two partially threaded steinmann pins at the proximal and middle third of the forearm.

Once the specimen was mounted on the motion simulator, the bone bridge was cut and the radius

and ulnar implant spacers were replaced with the 1 DOF load cells (Figure 2.8).

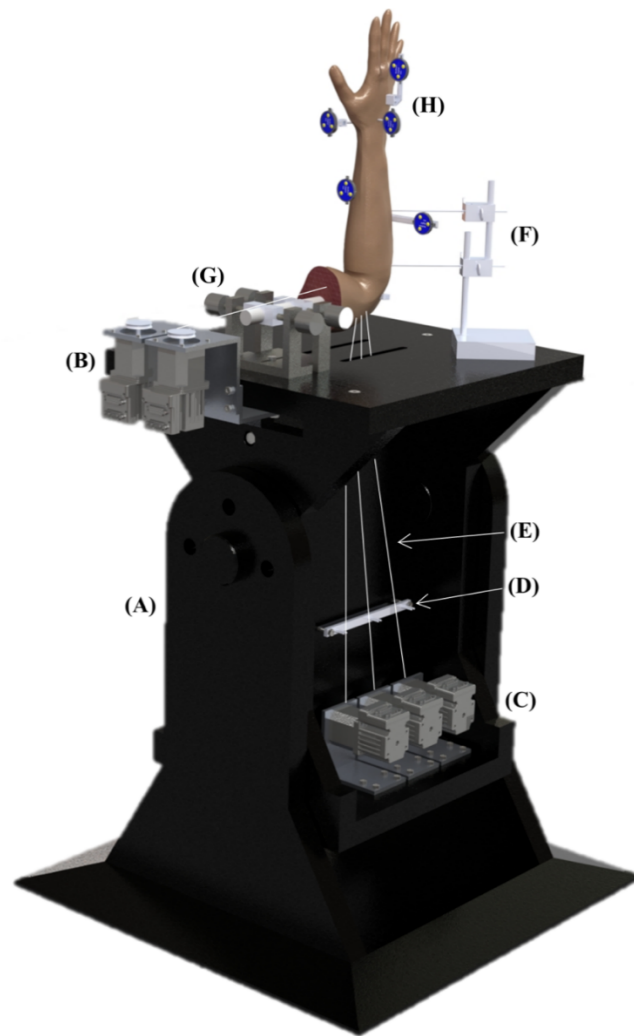


Figure 2. 7 Wrist motion simulator.

© D Iglesias

A wrist motion simulator that utilizes an array of servomotors connected to the tendons of the wrist prime movers was used to apply, maintain and adjust tone loads to achieve simulated active motion. The cadaver arms were mounted on motion simulator with elbow at 90° of flexion and neutral varus/valgus position. Infrared marker triads (“optical tracking markers”) were rigidly affixed to the ulna, radius and third metacarpal using custom Delrin® pedestals.

(a) Delrin® platform (b) & (c) servomotors (motor manifold) (d) Cable guide rail (e) suture attachment to prime movers routed through epicondyle guides (f) Ulnar support tower (g) Humeral clamp (h) Optical tracking markers.

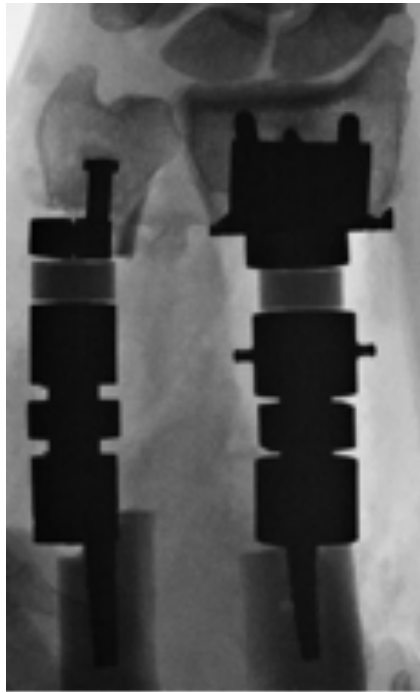


Figure 2. 8 Radiographic image of radial and ulnar implants in-situ.

© D Isa

Radiographic image of the cemented radial and ulna implants in neutral alignment.

2.3.4 SIMULATION OF MOTION AND TESTING PROTOCOL

Our *in-vitro* simulator models the *in-vivo* activation of individual muscles using a force position algorithm to generate reproducible wrist motion pathways.²⁸ Muscle loading protocols are based on electromyographic studies of active wrist motion and theoretical ratios derived from existing data on the cross sectional areas of the muscles of the wrist.³¹ The simulator uses antagonistic muscle pairs to more accurately simulate *in vivo* wrist and forearm motion. A minimum tone load was applied to groups resisting motion (8.9 N to FCU, FCR, ECRL, ECRB and ECU and 15 N to BI and PT). The magnitude of load through the muscle groups enforcing motion increased with the resultant force imbalance moving the wrist in the desired direction. As the wrist moves,

position data from the optical trackers provides feedback to the actuators to alter muscle tensions to achieve the desired motion pathways. The development of this active motion simulator has improved our ability to produce more reproducible motion pathways including flexion, extension, radial and ulnar deviation as well as the dart thrower motions.²⁸ Activation of the BI and PT were used to maintain the forearm in neutral rotation throughout testing.

Before shortening and lengthening of the radius, axial loading data was recorded during simulated dynamic wrist motion at the native radial length. Motions studied included wrist flexion (wrist moved from 50° extended position to 50° of flexion), ulnar deviation (wrist moved from 15° radially deviated position to 10° of ulnar deviation) and dart throw motion (30° of extension and 10° radial deviation to 30° of flexion and 10° ulnar deviation) at a rate of 3° per second (Figure 2.9). All data was collected with the forearm maintained at neutral rotation. Radial shortening and lengthening was simulated by 1 mm intervals with +1, +2 and +3 of lengthening and -1, -2, -3 and -4mm of shortening from native radial length. The ulnar length remained unchanged throughout the testing protocol. We chose a lengthening limit of 3mm as this length was the maximum attainable length due to the intact TFCC.

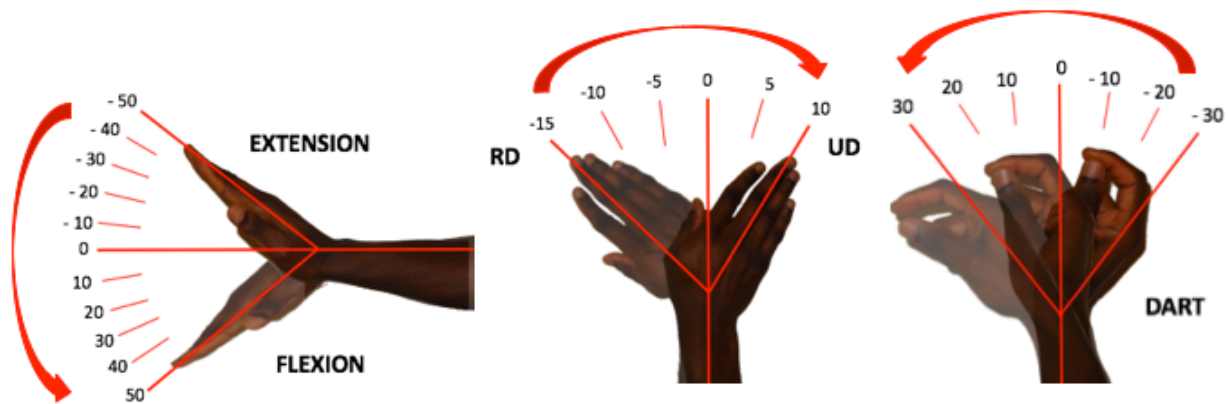


Figure 2. 9 Wrist motions evaluated.

© D Isa

The three primary wrist motions simulated by the wrist motion simulator for purposes of this study: Flexion (from 50° of extension), ulnar deviation [UD] (from 15° of radial deviation [RD]) and multiplanar motion [dart] (from 30° of Extension and 10° of RD).

2.3.5 METHODS AND DATA ANALYSIS

Statistical Analyses

The relationship between radial and ulnar loads and native ulnar variance were calculated using Pearson’s correlation coefficient.

A two-way repeated-measures ANOVA was performed with radial length and joint angle as independent variables and radial and ulnar axial loads as the dependent variables. A Greenhouse-Geisser correction was performed when Mauchly’s test for sphericity was violated. Statistical significance was set at $p < 0.050$. Comparisons were made at interval radial length changes (+3, +2, +1, neutral, -1, -2, -3, -4mm of length change from native length) during simulated dynamic

wrist flexion from 50° of wrist extension to 50° of flexion (-50° to 50°; where -50°, -40°, -30°, -20° and -10° represent wrist extended positions and 10°, 20°, 30°, 40° and 50° represent wrist flexed positions), ulnar deviation from 15° of radial deviation to 10° of ulnar deviation (-15° to 10°; where -15, -10 and -5 are radially deviated positions and 5 and 10 represented ulnarly deviated positions) and dart throw motion from 30° of extension and 10° of radial deviation to 30° of flexion and 10° of ulnar deviation (-30°, -10° to 30°, 10°). Comparisons between flexion angles were done at 10° increments, radial to ulnar deviation at 5° increments and in 10° increments of extension for dart throw motion where -30°, -20° and -10° represent wrist extended positions and 10°, 20°, 30° represent wrist flexed positions. Where interactions were detected between joint angle and radial length, separate ANOVA analyses were undertaken to examine the effect of various radial lengths on distal forearm loading separately. The flexion-extension, radioulnar deviation, and dart-throw motions were sometimes limited in certain cadavers and as a result, 8 specimens were used to evaluate flexion, 7 specimens for ulnar deviation and 6 specimens for dart throw motion.

2.4 RESULTS

2.4.1 NATIVE LOADS AND ULNAR VARIANCE

Mean ulnar variance measured on standard PA radiographs was $0.1 \pm 1.7\text{mm}$ (range -3.1mm – 2.3mm). There was no significant correlation between radial ($r = -0.104$, $p = 0.775$) and ulnar ($r = -0.153$, $p = 0.673$) loads and native ulnar variance.

2.4.2 FLEXION

Radial and ulnar axial loads during simulated active flexion (from the 50° extended position to 50° of flexion) were compared at 10° flexion intervals for each radial length change studied.

There was a significant effect of radial length change on distal radial loads for each millimeter of radial length change ($p < 0.001$) (Figure 2.10 a). With an increase or decrease in radial length, there was an increase or decrease in radial loads respectively (Appendix 2.1): $79 \pm 12\text{N}$ at 3mm, $79 \pm 13\text{N}$ at 2mm, $75 \pm 8\text{N}$ at 1mm of radial lengthening, $72 \pm 8\text{N}$ at native length and $65 \pm 13\text{N}$ at 1mm, $58 \pm 16\text{N}$ at 2mm, $53 \pm 16\text{N}$ at 3mm, $45 \pm 19\text{N}$ at 4mm of radial shortening during wrist flexion. There was an interaction between radial length and joint angle on radial loads ($p = 0.034$).

Post hoc analysis showed significant decrease in radial loads by 10%, 19%, 26% and 38% with 1mm, 2mm, 3mm and 4mm of radial shortening respectively ($p = 0.019$). However, a significant increase in radial loads by 10% occurred only at 3mm of radial lengthening ($p = 0.036$).

Variations in radial loads during wrist flexion with radial length change were statistically significant. In neutral wrist position and in the flexed position (-30° to 50°), with an increase or decrease in radial length, there was a corresponding increase or decrease respectively in radial load (Figure 2.11, $p < 0.001$). However, in the wrist extended positions (-50° to -30°), there was an inverse relationship between length changes and radial loads (Figure 2.11 a); an increase in radial load was observed with radial shortening and a decrease in radial load was observed with radial lengthening ($p = 0.009$).

At each 10° interval of wrist motion from extension to flexion for each millimeter of length change evaluated, there was a significant inverse relationship between ulnar loads and radial length ($p < 0.001$) (Figure 2.11 b). For each millimeter of radial length increase or decrease, there was a corresponding decrease or increase in ulnar loading respectively ($p < 0.001$) (Appendix 2.1): $3 \pm 4\text{N}$ at 3mm, $7 \pm 7\text{N}$ at 2mm, $10 \pm 8\text{N}$ at 1mm of radial lengthening, $12 \pm 6\text{N}$ at native length and $19 \pm 10\text{N}$ at 1mm, $22 \pm 11\text{N}$ at 2mm, $25 \pm 9\text{N}$ at 3mm, $31 \pm 11\text{N}$ at 4mm of radial shortening. There was a 17%, 42% and 75% decrease in ulnar loads from neutral radial length at 1mm, 2mm and 3mm of radial lengthening respectively. There was a 58%, 83%, 108% and 158% increase in ulnar loads compared to neutral length at 1mm, 2mm, 3mm and 4mm of radial shortening respectively.

The effect of joint angle was also significant with greater ulnar loads observed with the wrist in extension compared to neutral and flexed positions for each interval of length change ($p < 0.001$) (Figure 2.10 b). There was no interaction between radial length and joint angle on ulnar loads ($p = 0.084$).

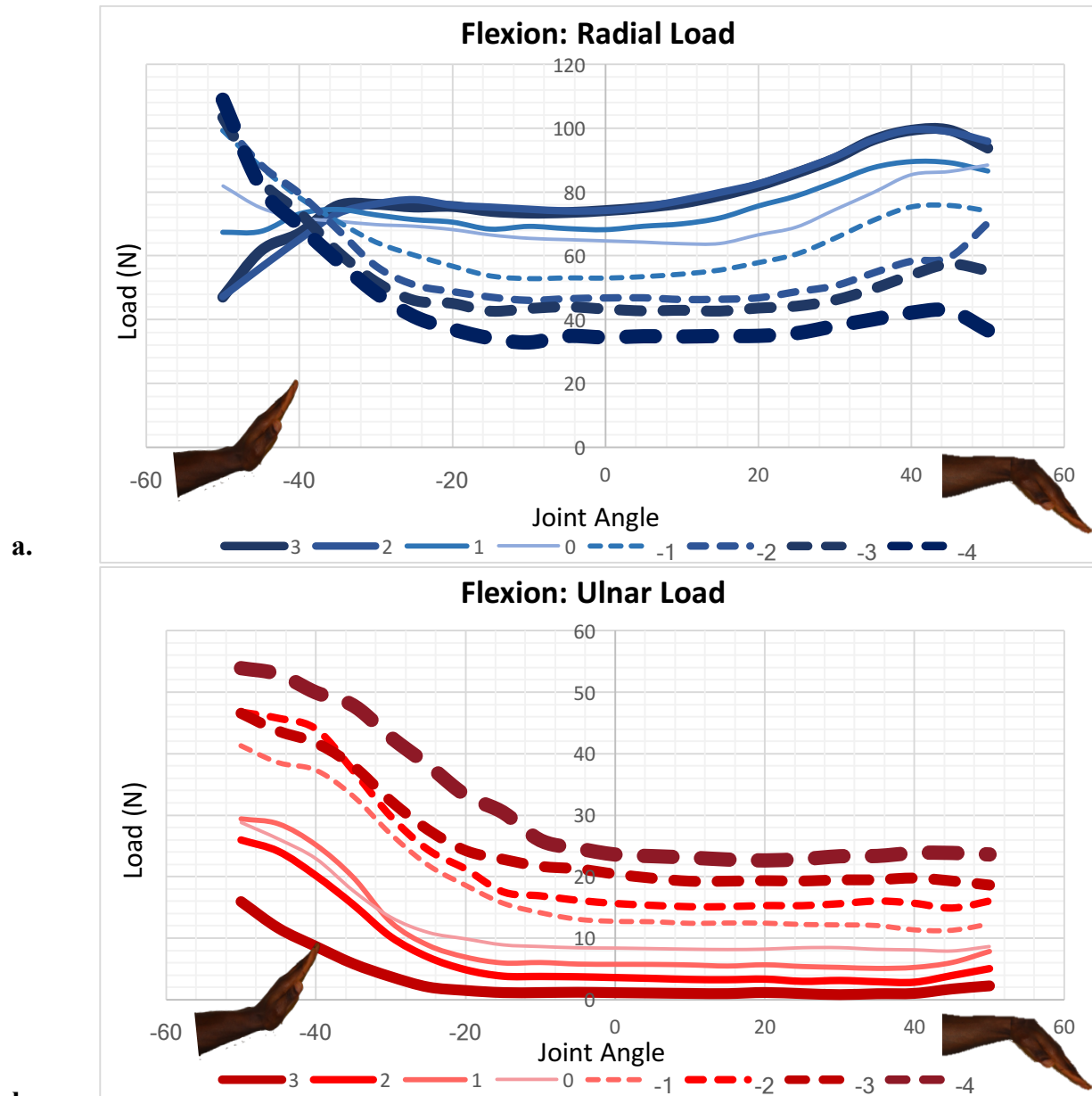


Figure 2. 10 Radial and ulnar loads during wrist flexion n=8.

(In order to facilitate the interpretation of the data, the lines were constructed with increasing thickness to represent lengthening and shortening. Lengthening is solid, and shortening is dashed. The same format is employed for all other related graphs in this chapter.)

- a. Graph showing radial loads at 3mm, 2mm and 1mm of radial lengthening (3, 2, 1), native length (0) and 1mm, 2mm, 3mm and 4mm of radial shortening (-1, -2, -3, -4) during wrist flexion. Flexion motion started with the wrist in 50° of extension (-50) to 50° of flexion (50).
- b. Graph showing ulnar loads at 3mm, 2mm and 1mm of radial lengthening (3, 2, 1), native length (0) and 1mm, 2mm, 3mm and 4mm of radial shortening (-1, -2, -3, -4) during wrist flexion. Flexion motion started with the wrist in 50° of extension (-50) to 50° of flexion (50).

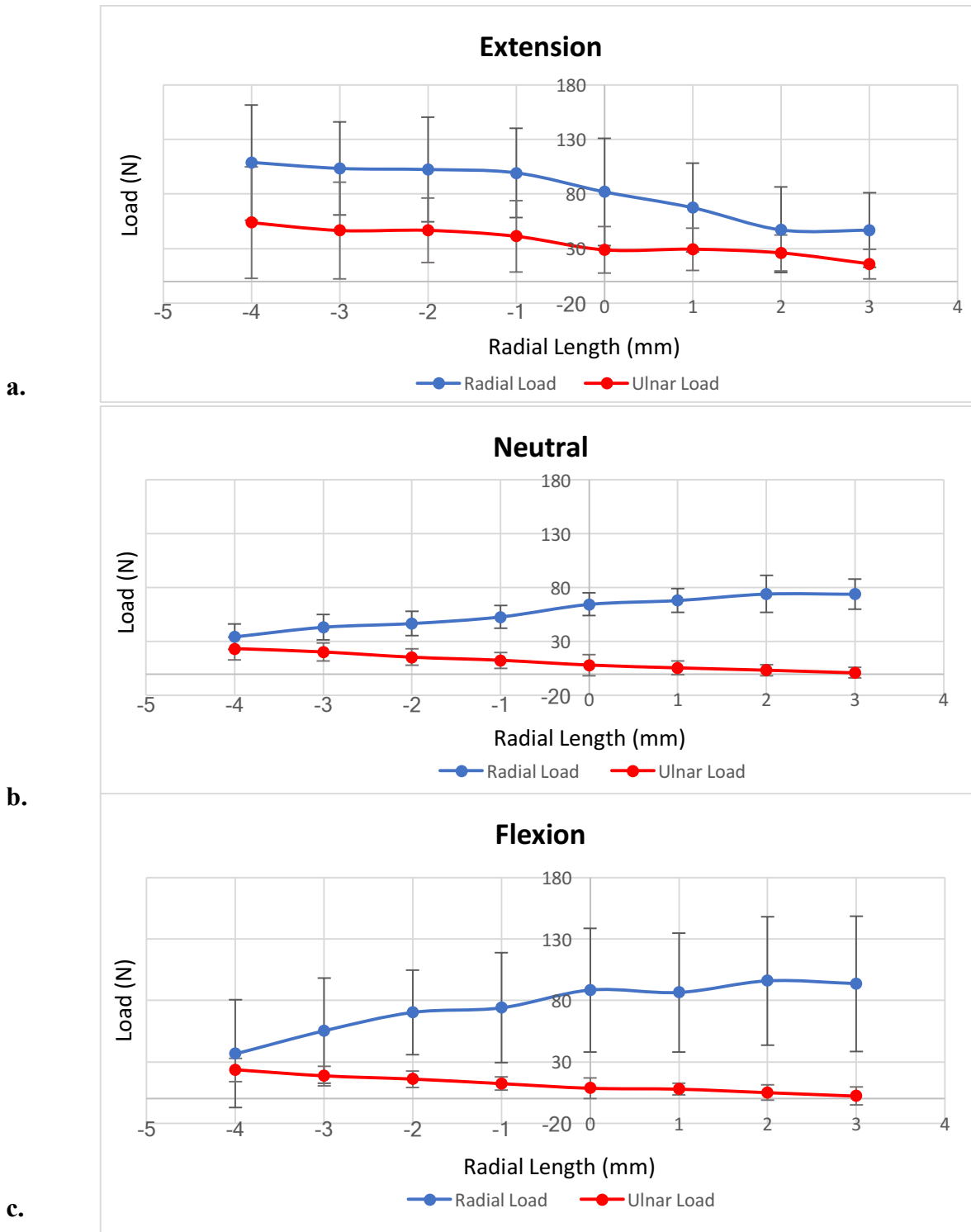


Figure 2. 11 Radial and ulnar loads with radial length change during simulated wrist motion from extension to flexion n = 8.

© D Isa

Radial and ulnar loads at 3mm, 2mm and 1mm of radial lengthening (+3, +2, +1), native radial length (0) and 4mm, 3mm, 2mm and 1mm of radial shortening (-4, -3, -2, -1) in (a) extension, (b) neutral and (c) flexion. Mean \pm 1 SD are shown.

2.4.3 ULNAR DEVIATION

At each 5° interval of ulnar deviation evaluated, radial and ulnar axial load measurements during simulated active ulnar deviation (RUD) from the 15° radially deviated position to the 10° ulnarly deviated position were compared at each interval of radial length change.

Overall, there was a significant relationship between radial loads and radial length change for each millimeter of length change evaluated ($p < 0.001$) (Figure 2.12 a). With an increase or decrease in radial length, there was a decrease in radial loads (Appendix 2.2): $78 \pm 26\text{N}$ at 3mm, $82 \pm 23\text{N}$ at 2mm, $81 \pm 21\text{N}$ at 1mm of radial lengthening (3, 2, 1), $85 \pm 17\text{N}$ at native length (0) and $71 \pm 14\text{N}$ at 1mm, $66 \pm 16\text{N}$ at 2mm, $61 \pm 13\text{N}$ at 3mm, $56 \pm 13\text{N}$ at 4mm of radial shortening (-1, -2, -3, -4) during wrist ulnar deviation. During simulated dynamic ulnar deviation, variation in radial loads based on wrist position were significant ($p = 0.021$) with peak radial loads observed in the radial deviated wrist position for each interval of radial length change (Figure 2.13 a). There was an interaction between joint angle and radial length on radial loads ($p < 0.001$).

Post hoc analysis showed there was a 16%, 22%, 28% and 34% decrease in radial loads compared to native length at 1mm, 2mm, 3mm and 4mm of radial shortening respectively. ($p = 0.002$). Although there was a trend towards decreased radial loads with radial lengthening, changes in radial loads up to 3mm (8% decrease) did not reach statistical significance ($p=0.053$). In the radially deviated wrist position (-15°), post hoc analysis also showed the increase and

decrease in radial load with radial lengthening and shortening respectively was significant (Figure 2.13 a), however, in the neutral (0°) and in ulnarly deviated positions (5° and 10°), peak loads were observed at native length regardless of radial length change ($p < 0.001$) (Figure 2.13 b and c).

With regards to distal ulnar loads, there was a significant inverse relationship between ulnar loads and radial length for each millimeter of length change evaluated ($p = 0.037$) (Figures 2.12 b and 2.13 a, b, c): $7 \pm 7\text{N}$ at 3mm, $10 \pm 7\text{N}$ at 2mm, 13 ± 7 at 1mm of radial lengthening (3, 2, 1), $14 \pm 8\text{N}$ at native length (0) and $18 \pm 7\text{N}$ at 1mm, $21 \pm 7\text{N}$ at 2mm, $25 \pm 8\text{N}$ at 3mm, $30 \pm 10\text{N}$ at 4mm of radial shortening (-1, -2, -3, -4) (Appendix 2.2). There was a 7%, 29% and 50% decrease in ulnar loads from native length at 1mm, 2mm and 3mm of radial lengthening respectively and a 29%, 50%, 79% and 114% decrease in ulnar loads compared to native length at 1mm, 2mm, 3mm and 4mm of radial shortening respectively. Peak loads in the ulna were observed in ulnar deviation at 10° ($p = 0.034$) for each interval of radial length change (Figure 2.13 c). There was no interaction between radial length and joint angle ($p = 0.583$).

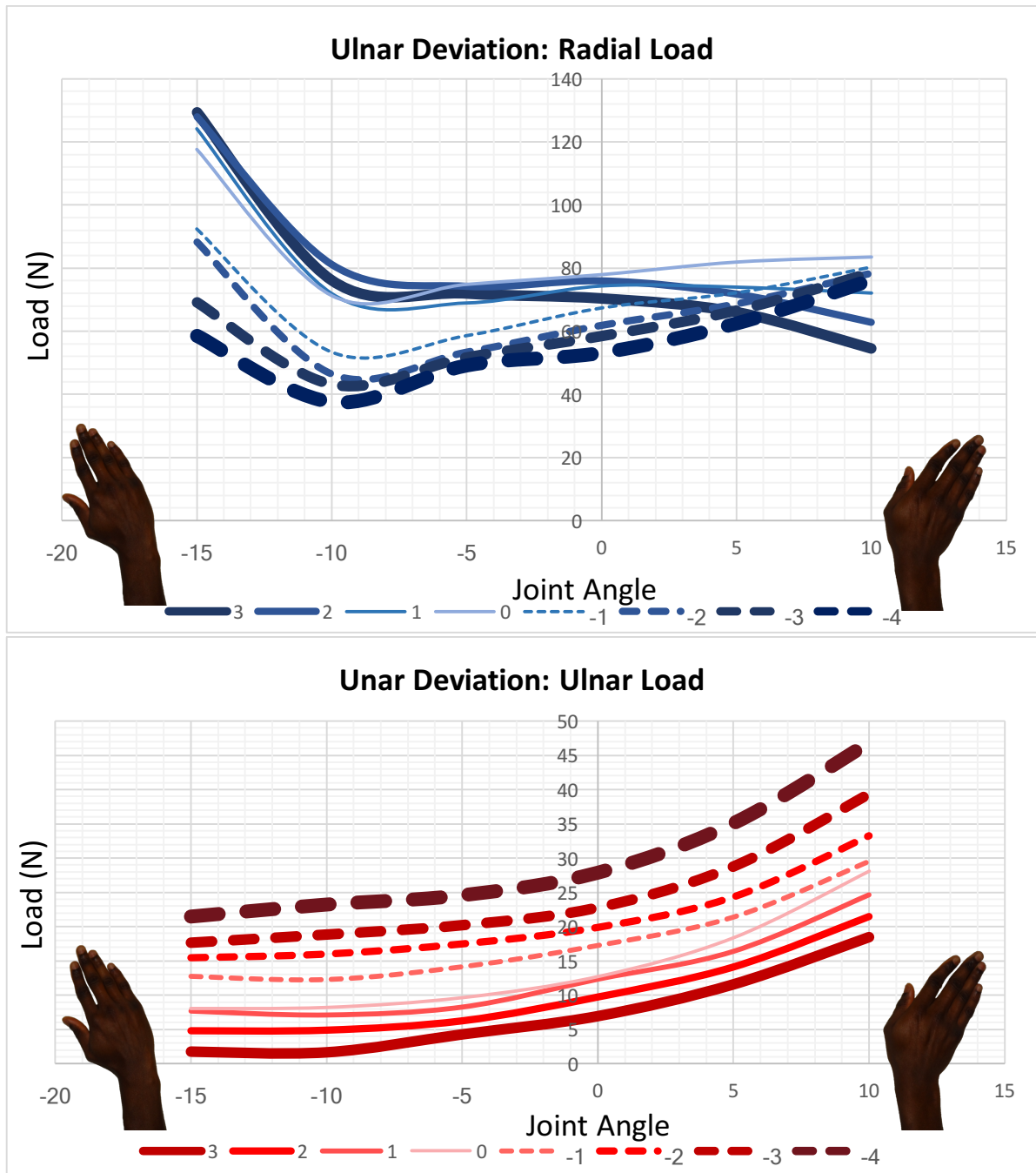


Figure 2. 12 Radial and ulnar loads during wrist ulnar deviation n = 7.

- a. Graph showing radial loads at 3mm, 2mm and 1mm of radial lengthening (3, 2, 1), native length (0) and 1mm, 2mm, 3mm and 4mm of radial shortening (-1, -2, -3, -4) during wrist ulnar deviation. Ulnar deviation started with the wrist in 15° of radial deviation (-15) to 10° of ulnar deviation (10).
- b. Graph showing ulnar loads at 3mm, 2mm and 1mm of radial lengthening (3, 2, 1), native length (0) and 1mm, 2mm, 3mm and 4mm of radial shortening (-1, -2, -3, -4) during wrist flexion. Ulnar deviation started with the wrist in 15° of radial deviation (-15) to 10° of ulnar deviation (10).

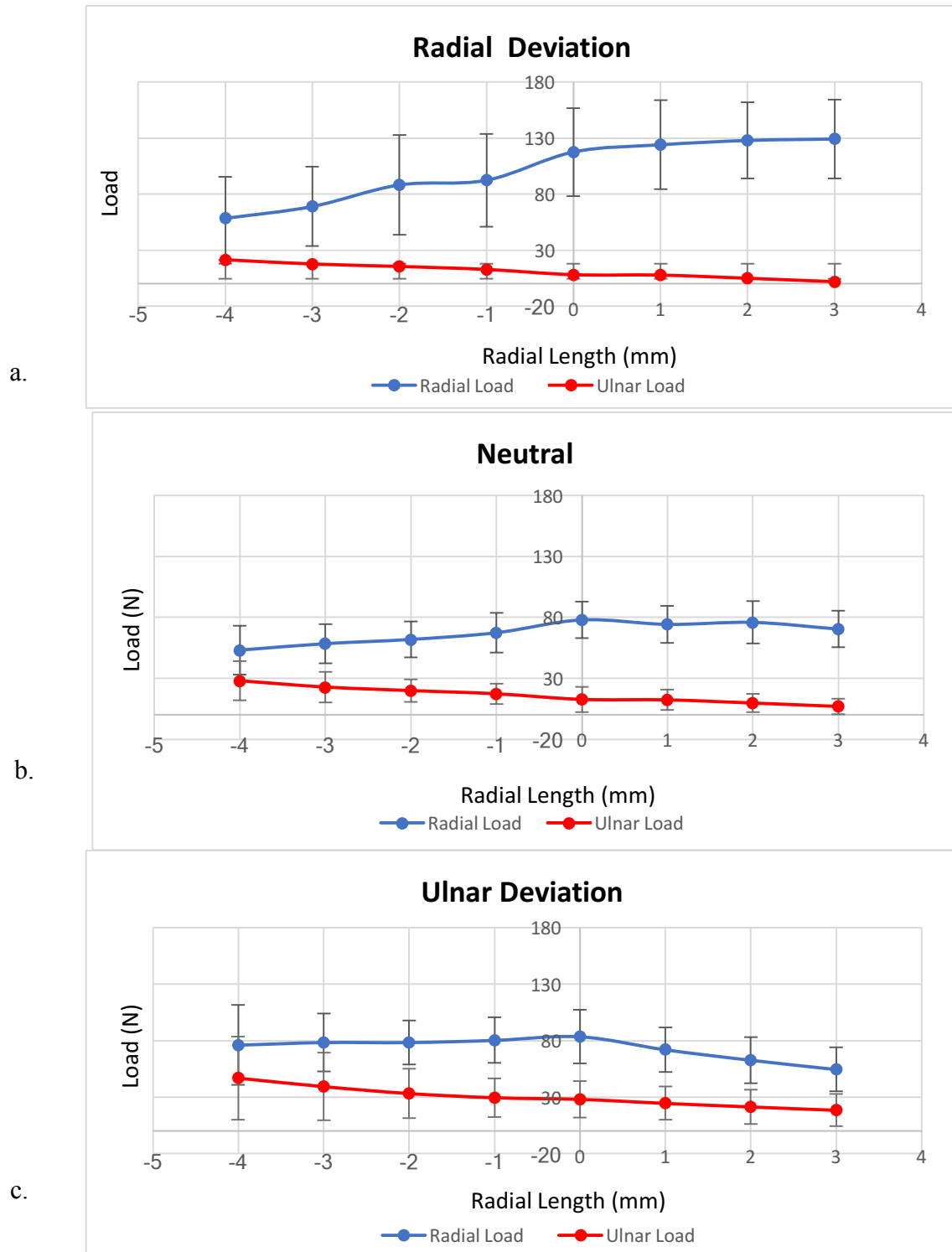


Figure 2. 13 Radial and ulnar loads with radial length change during simulated wrist motion from radial to ulnar deviation n = 7.

© D Isa

Radial and ulnar loads at 3mm, 2mm and 1mm of radial lengthening (+3, +2, +1), native radial length (0) and 4mm, 3mm, 2mm and 1mm of radial shortening (-4, -3, -2, -1) in (a) extension, (b) neutral and (c) flexion. Mean \pm 1 SD are shown.

2.4.4 DART THROW MOTION

Radial and ulnar axial loads during simulated active dart throw (from the 30° extended and 10° radially deviated position to the 30° flexed and 10° ulnarly deviated position) were compared at 10° flexion intervals for each radial length change studied.

Although there was a slight decrease in radial loads with radial lengthening and also, a decrease in radial loads with radial shortening, these changes did not reach statistical significance ($p=0.243$) (Appendix 2.3): $72 \pm 22\text{N}$ at 3mm, $76 \pm 7\text{N}$ at 2mm, $69 \pm 13\text{N}$ at 1mm of radial lengthening (3, 2, 1), $76 \pm 16\text{N}$ at native length (0) and $57 \pm 3\text{N}$ at 1mm, $53 \pm 6\text{N}$ at 2mm, $51 \pm 3\text{N}$ at 3mm, $45 \pm 4\text{N}$ at 4mm of radial shortening (-1, -2, -3, -4) during ulnar deviation. There was a significant change in radial loads with wrist position ($p = 0.003$) with peak radial loads observed at initiation of dart throw with the wrist in extension and radial deviation (- 30° and - 10°) (Figure 2.14 a).

There was an interaction between radial load and joint angle ($p < 0.001$). There was a 5% decrease in radial loads with 3mm of lengthening and 41% decrease in radial loads with 4mm of shortening. However, post hoc analysis showed the decreases in radial loads with radial lengthening up to 3mm ($p = 0.931$) and decreases in radial loads with shortening up to 4mm ($p=0.111$) were not statistically significant.

With regards to distal ulnar loads, there was an inverse relationship between ulnar loads and radial length for each millimeter of length change evaluated ($p < 0.001$) (Figure 2.14 b): $3 \pm 4\text{N}$ at 3mm, $5 \pm 3\text{N}$ at 2mm, $10 \pm 4\text{N}$ at 1mm of radial lengthening, $14 \pm 8\text{N}$ at native length (0) $17 \pm$

4N at 1mm, 20 ± 5 N at 2mm, 24 ± 6 N at 3mm, 29 ± 6 N at 4mm of radial shortening (-1, -2, -3, -4) (Appendix 2.3). An increase in ulnar load was observed with decreasing radial length and vice versa (Figure 2.15 a, b and c). There was a 29%, 64% and 79% decrease in ulnar loads from native radial length at 1mm, 2mm and 3mm of radial lengthening respectively and a 21%, 43%, 71% and 107% decrease in ulnar loads compared to native length at 1mm, 2mm, 3mm and 4mm of radial shortening respectively. During dart throw motion, variation in ulnar loads based on wrist position were significant ($p = 0.001$) with peak ulnar loads observed in the flexed and ulnarly deviated position (10° to 30°). For each interval of radial length change, peak loads in the ulna were observed in terminal dart throw (30° and 10°) ($p = 0.001$) (Figure 2.14 b). At 3mm of radial lengthening, tensile forces were observed in the ulna at initiation of dart throw (-30°) ($p < 0.001$) (Figure 2.15 a). There was no interaction between radial length and joint angle ($p = 0.218$).

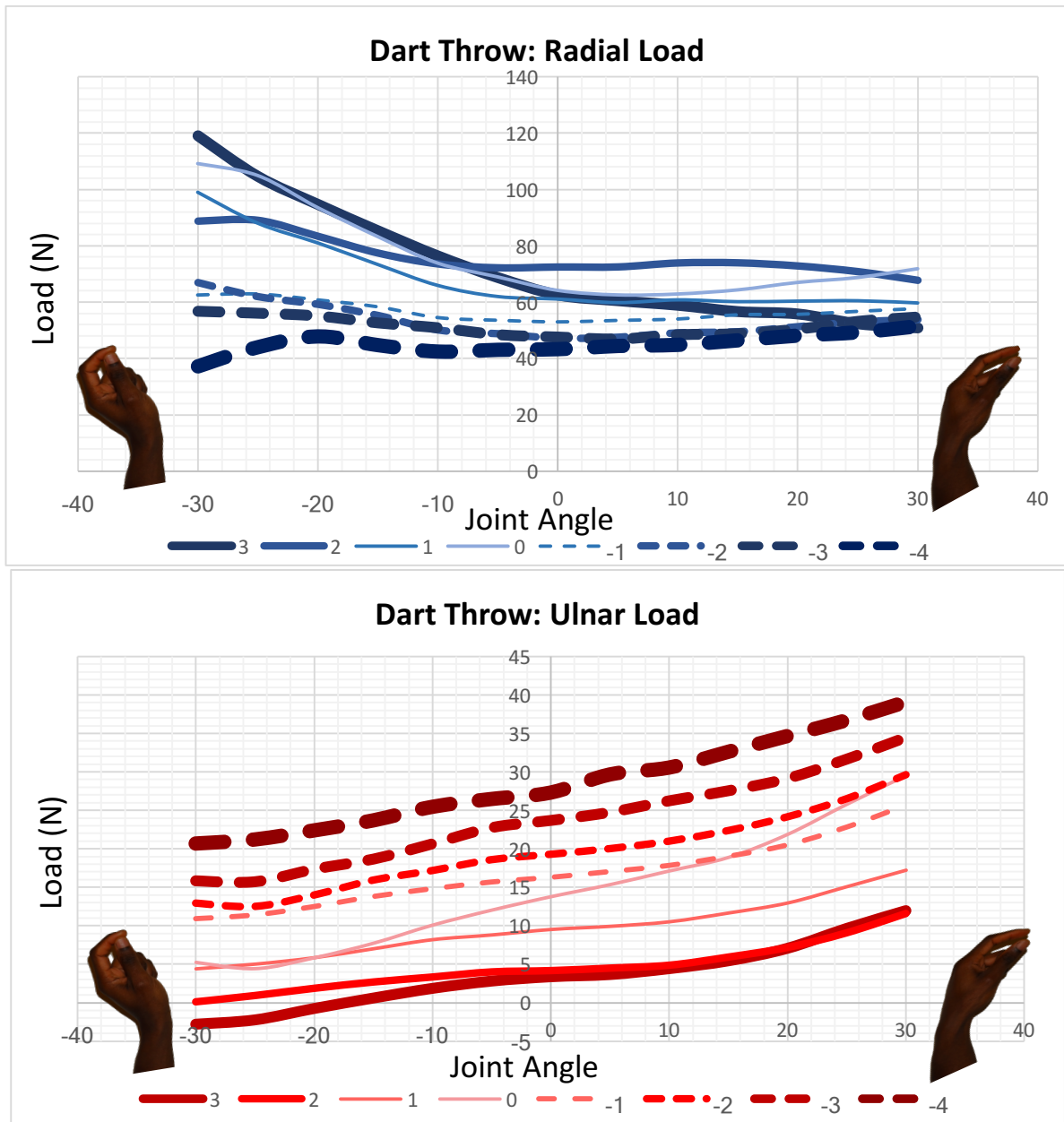


Figure 2. 14 Radial and ulnar loads with radial length change during simulated wrist dart throw motion n = 6.

- a. Graph showing radial loads at 3mm, 2mm and 1mm of radial lengthening (3, 2, 1), native length (0) and 1mm, 2mm, 3mm and 4mm of radial shortening (-1, -2, -3, -4) during dart throw. Dart motion started with the wrist in 30° of extension and 10° of radial deviation (-30, -10) to 30° of flexion and 10° or ulnar deviation (30, 10).
- b. Graph showing ulnar loads at 3mm, 2mm and 1mm of radial lengthening (3, 2, 1), native length (0) and 1mm, 2mm, 3mm and 4mm of radial shortening (-1, -2, -3, -4) during dart throw. Dart motion started with the wrist in 30° of extension and 10° of radial deviation (-30, -10) to 30° of flexion and 10° or ulnar deviation (30, 10).

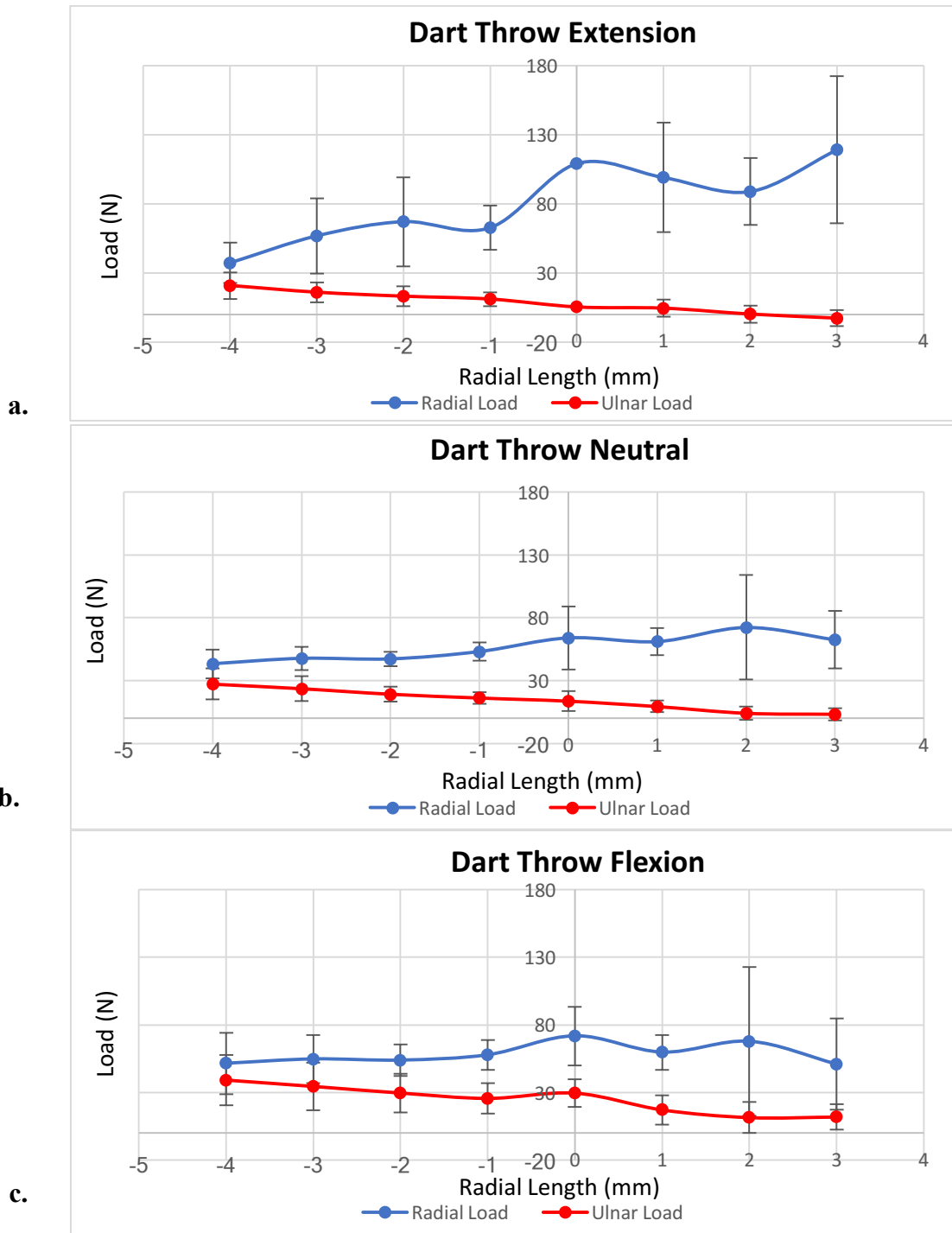


Figure 2. 15 Radial and ulnar loads with radial length change during simulated wrist dart throw motion n = 6.

© D Isa

Radial and ulnar loads at 3mm, 2mm and 1mm of radial lengthening (+3, +2, +1), native radial length (0) and 4mm, 3mm, 2mm and 1mm of radial shortening (-4, -3, -2, -1) in (a) extension (30° extension and 10° radial deviation), (b) neutral and (c) flexion (30° flexion and 10° ulnar deviation). Mean ± 1 SD are shown.

2.5 DISCUSSION

This study demonstrated that axial loading through the distal forearm is complex and dependent on radial length and joint position. During radial length changes, there was more variability in radial loads during simulated wrist motion as compared to ulnar loads which occurred in a more predictable fashion. There was no correlation between native ulnar variance and distal forearm loading.

Our current understanding of forearm loading have been based on observations made from previous studies on the biomechanics of the distal forearm whereby static axial loads were applied to the wrist.^{18,19,20,21,22,23,32} Static wrist loading may not accurately simulate normal distal radius and ulna loading during *in-vivo* wrist motion whereby loading is applied to the wrist by tendons used to achieve motion and by the effects of gravity.

The relationship between native ulnar variance and distal forearm loading remains controversial.^{19,26} Although Bu et al¹⁹ observed wrists with positive native ulnar variance had more load through the distal ulna than wrists with ulnar negative variance, Harley et al²⁶ did not observe a correlation between ulnar variance and distal forearm loading. We did not observe a correlation between native ulnar variance and distal forearm loading consistent with the results observed by Harley et al.²⁶ This can be attributed to the inverse relationship between TFCC thickness and ulnar variance.²⁰ The load bearing characteristics and compensatory thickness of the TFCC likely accommodates axial load differences. Our sample size may have precluded observing significant changes in axial loads with variation in native ulnar variance.

Our study demonstrated an average of 86:14 load sharing between the distal radius and ulna during flexion and ulnar deviation and 84:16 during dart throw. This is comparable to results observed by Harley et al²⁶ with 14% axial loads borne by the distal ulna during quasi-static loading and Greenberg et al³⁴ under static loading. In a static loading study, Ekenstram et al³³ demonstrated 85:15 load sharing between the radius and ulna with no significant change in load sharing from 50° of flexion to 50° extension. Trumble et al¹⁸ demonstrated 17% of the axial load passed through the distal ulna in neutral wrist position under static loading with peak ulnar loads of 24% seen in extension. Harley et al²⁶ observed peak ulnar loads of 17% at 20° in flexion during simulated dynamic motion. The distal ulnar loads in our study findings were similar to Trumble et al¹⁸ with peak mean distal ulna loads of 26% observed when the wrist was in the extended position .

With regards to radial loading, although there were no significant changes in the extended and flexed positions at native length, this changed with radial length change during simulated dynamic flexion: In the extended wrist position, at each interval of radial length increase, there was a trough in radial loads and with radial length decrease, peak radial loads were observed. To our knowledge, our study is the first reporting these variations in radial loads. Peak ulnar loads were observed in extension for each interval of radial length change evaluated in our study.

Pogue et al²⁵ observed significant changes in lunate contact area with 2mm of radial shortening from 13% to 16%. In a cadaveric study by Shepard and Markolf et al,³⁵ an estimated increase in distal ulnar loads of 10% per millimeter of radial shortening was observed (60% increase in distal ulnar force after 6 mm of distal radial shortening). In our study, much greater differences were observed, with radial shortening, 58%, 83%, 108% and 158% increase in ulnar loads were observed at 1mm, 2mm, 3mm and 4mm respectively during flexion; 29%, 50%, 79% and 114%

increases in ulnar deviation and 21%, 43%, 71% and 107% increases with dart throw. A computational study using two-dimensional rigid body spring model predicted a 45% decrease in radiolunate load with 4mm of radial shortening.³⁶ Our study observed similar changes with a 38%, 34% and 41% reduction in radial loads during simulated dynamic flexion, ulnar deviation and dart throw motion respectively with 4mm of radial shortening. We likely observed greater differences from Shepard and Markolf³⁵ due to the employment of dynamic loading with application of greater tendon loads that more closely simulate *in-vivo* wrist kinematics.

Although radial shortening causes a decrease in axial radial loads, our study shows excessive shortening caused a paradoxical increase in distal radial loads (from loads at native length) when the wrist is in extension. When initiating flexion from an extended wrist position, the ECU and FCU exert a greater amount of force to bring the wrist out of the extended position when the radius is shortened. This increased tendon loads across the wrist may explain the rise in axial loads. Consequently, caution should be exercised when performing distal radial shortening osteotomy for Kienbock's disease as excessive shortening may result in not only in ulnocarpal impaction, but also excessive loading of the distal radius during activities that involve wrist extension. Calfee et al³⁷ demonstrated good clinical outcomes with 2mm of radial shortening for Kienbock's disease. Thus, we propose shortening by 2mm to sufficiently reduce distal radial loading for treatment of Kienbock's disease.

The variation in radial loads during simulated radial length change observed in our study (especially in wrist extension) may be explained by the changes in tendon loads that occur with radial length change. In our study, with each interval of radial shortening, we observed an increase in tendon loads in ECU and FCU in the extended wrist position. When initiating flexion

from an extended wrist position, these ulnar sided wrist tendons work harder to bring the wrist out of the extended position when the radius is shortened. In addition to TFCC pathology and ulnocarpal impaction, this may also be another explanation as to why following distal radial fractures, even with minimal shortening, ulnar sided wrist pain is so common. Previous biomechanical studies^{38,39} have observed a decrease in moment arm of the flexors and extensors and a change in their center of rotation with radial shortening/simulated distal radius deformity. This decrease in moment arm and increase in tendon loads may explain the variation in loads during simulated motion with radial length change/simulated distal radius deformity. Tang et al⁴⁰ observed the majority of the principal wrist movers either had an increase in wrist extension moment arm or a decrease in wrist flexion moment arm during simulated distal radius malunion thus possibly increasing the biomechanical consequences for wrist prime movers. Biomechanical changes that occur in surrounding soft tissues during simulated motion are complex and likely play a role in axial load variation with radial length change. The clinical consequences of these changes with subtle deformities remain to be clarified as tendons are capable of adapting to changes in moment arms and excursion such that normal joint torque production is maintained near normal levels.⁴¹

Markolf et al³² observed 4mm of radial shortening resulted in equal load sharing between the radius and ulna. In a biomechanical study,⁴² shortening of the radius using a -4 mm metallic radial head implant increased the mean distal ulnar force from 29% of the applied wrist force to 52% with the elbow in varus alignment. In our study, we observed distal radial loads of 59%, 65% and 61% of total forearm bone loads during flexion, UD and dart throw respectively at 4mm of radial shortening (Appendices 2.12 – 2.14). We did not observe equal load sharing. Radial loads were consistently higher than ulnar loads at even at 4mm of radial shortening for all

three motions evaluated. Percentage radial loads at +3mm, +2mm, +1mm, 0, -1mm, -2mm and -3mm of length change were 96%, 91%, 88%, 86%, 78%, 72% and 68% respectively during flexion, 91%, 89%, 86%, 85%, 80%, 76% and 71% respectively during ulnar deviation and 95%, 94%, 88%, 84%, 77%, 73% and 68% respectively during dart throw (Appendices 2.12 – 2.14). This may be due to differences in muscle loading utilized. Dynamic loading may influence axial bone loads and more closely simulate in-vivo conditions over static loading employed in previous studies. Also, in our protocol, the elbow was placed in neutral position. Previous studies have shown load-sharing at the wrist changes based on the on the varus-valgus positioning of the elbow.^{32,43}

A static loading study by Bu et al⁴⁴ evaluated the effects of sequential radial length change on distal ulnar loading in wrists with inherent differences in ulnar variance. In wrists with ulnar positive variance ($\geq +2\text{mm}$), a decrease in distal ulnar loads from 31% to 8% of total wrist load at 3mm of radial lengthening and an increase to 56% with 4mm of shortening.⁴⁴ The current study observed a decrease in distal ulnar loads from 14% to 3% during flexion and to 9% during ulnar deviation and an increase to 41% during flexion and to 35% during ulnar deviation throw at 3mm of lengthening and 4mm of shortening respectively. During dart throw, a decrease in percentage distal ulnar loads from 16% to 5% and an increase to 39% was observed at 3mm of lengthening and 4mm of shortening respectively. In addition to differences in loading protocols (dynamic versus static), differences may also be explained by the native variance of the wrists utilized.

During simulated dynamic radioulnar deviation, our study showed peak radial loads seen during radial deviation and peak ulnar loads seen with ulnar deviation. This is consistent with previous

biomechanical studies.^{18,26,33,45} This can be attributed to the force vector and tendon loading changes within the radiocarpal joint during ulnar deviation. In our study, increase in radial loads can be attributed to the peak tendon loads in radial sided prime movers (ECRL and FCU) in the radially deviated position whereas increase in ulnar loads in ulnar deviation can be attributed to peak tendon loads in the ulnar sided prime movers (ECU and FCU) in the ulnarly deviated position.

Dart throw motion has been shown to be an important functional motion in performing most activities of daily living.⁴⁶ Greenberg et al³³ observed a mean ulnar load of 18% and a peak ulnar load of 26% during simulated dynamic dart throw motion. No comments were made on the phase of the dart throw at which peak ulnar loads were observed. We observed a mean ulnar load of 16% of total bone load during dart throw at native length (Appendix 2.14). In our analysis of absolute loads, peak radial loads (120% increase) were observed at initiation of dart throw and peak ulnar loads (25% increase) observed at terminal dart throw as the wrist moved from an extended and radially deviated position to a flexed and ulnarly deviated position (Figure 2.14). Interestingly, we observed tensile loads in the ulna at initiation of dart throw with 3mm of radial lengthening. This may have clinical implications in arthroplasty designs of the distal ulna as tensile loads may lead to tensile failure of the implant with excessive change in variance. This tension may well arise due to excessive ulnar shortening and changes in tendon loads that occur with radial length change.

Limitations exist for this study. First, biologic remodeling of the ligaments in response to changes in osseous length likely occur over time and cannot be accounted for in a biomechanical study. Some forearms were excluded in analysis as we could not achieve the desired range of motion in all specimens. Caution should be exercised when applying these results clinically as

we may be underpowered with our sample size to show a statistical difference. However, statistical significance was achieved for most comparisons thus we were evidently powered for most of the comparisons of interest. These are inherent limitations of cadaveric studies due to the costly nature of such studies and their limited availability. Nevertheless, this study is important in understanding load transfer in the distal forearm and serves as basis for further clinical studies. In some wrists, radioulnar deviation was limited to 15 degrees of radial deviation and 10 degrees of ulnar deviation thus we chose this range of motion to include all specimens. Second, the action of pronator quadratus was not simulated and thus we did not account for this force vector across the distal radioulnar joint and its role in load sharing. Third, the forearms were mounted vertically with gravity assistance in flexion past neutral, distal forearm loading may vary when forearms are positioned in horizontal plane positioning with different muscle groups working against gravity. Lastly, in addition, the flexion-extension, radioulnar deviation, and dart-throw motions were sometimes limited in certain cadavers and as a result, we excluded certain specimens from the data analysis.

Notwithstanding the limitations, our study has multiple strengths. Firstly, previous biomechanical studies utilized static loading protocols however, we employed the use of a dynamic wrist motion simulator thus closely simulating *in-vivo* kinematics. Secondly, given the paucity of data in the literature investigating dart throw motion on distal forearm loading, we contributed significantly to existing literature on distal forearm loading by investigating the effects of simulated dart throw on distal forearm loading with radial length. Thirdly, the soft tissues overlying the elbow, forearm, and wrist were left intact and low profile load cells were inserted with minimal disruption of soft tissue envelope thus closely representing *in-vivo* conditions when compared to previous studies. Fourthly, the use of a highly accurate and reliable

optical tracking system enabled accurate tracking of joint angles providing precise feedback to the motion simulator during simulated motion. Fifthly, in this study, we analyzed absolute loads, previous studies^{19,21,22,26,32, 43,47,48} have focused on percentage load sharing between the radius and the ulna. The drawback to percentage load sharing between the radius and ulna reported in previous studies is that if percentage loading remains unchanged with radial length change, the actual axial loads may have changed significantly thus rendering the percent irrelevant.

Lastly, to our knowledge, the effects of distal radial length change during simulated dynamic motion studied has not been reported in the literature to date thus giving new insight into distal forearm axial loading.

This study further clarifies that there is no relationship between distal forearm loading and native ulnar variance. With radial length changes, distal forearm loading during simulated dynamic wrist motion is more complex than described by previous static loading studies. The variation in radial loads observed during simulated dynamic wrist motion with radial length change is novel and adds to the existing body of literature. We observed less variation in ulnar loads with radial length change and changes in ulnar loads that occur in response to length change occur in a more predictable fashion. Our study provides new insight into biomechanical changes that occur with radial length change during simulated *in-vivo* wrist motion using a validated wrist motion simulator.

2.6 REFERENCES

1. Amadio PC, Botte MJ. Treatment of malunion of the distal radius. *Hand Clin.* 1987;3(4):541-561.
2. Bushnell BD, Bynum DK. Malunion of the distal radius. *J Am Acad Orthop Surg.* 2007;15(1):27-40. doi:15/1/27 [pii].
3. Fernandez DL. Correction of post-traumatic wrist deformity in adults by osteotomy, bone-grafting, and internal fixation. *J Bone Joint Surg Am.* 1982;64(8):1164-1178.
4. Hove LM, Fjeldsgaard K, Skjeie R, Solheim E. Anatomical and functional results five years after remanipulated Colles' fractures. *Scand J Plast Reconstr Hand Surg.* 1995;29(4):349-355. doi:10.3109/02844319509008971.
5. Kopylov P, Johnell O, Redlund-johnell I, Bengner U. Fractures of the distal end of the radius in young adults: A 30-year follow-up. *J Hand Surg Am.* 1993;18(1):45-49. doi:10.1016/0266-7681(93)90195-L.
6. A L. Fracture of the distal end of the radius: a clinical and statistical study of end results. *Acta Orthop Scand.* 1959;41:1-118.
7. Batra S, Gupta A. The effect of fracture-related factors on the functional outcome at 1 year in distal radius fractures. *Injury.* 2002;33(6):499-502.
8. Leung F, Ozkan M, Chow SP. Conservative treatment of intra-articular fractures of the distal radius--factors affecting functional outcome. *Hand Surg.* 2000;5(2):145-153.
9. Hulten O. Uber anatomische variationen der handgelenkknochen. *Acta Radiol (Old Ser).* 1928;9:155-168.
10. Kolovich GP, Kalu CMK, Ruff ME. Current Trends in Treatment of Kienböck Disease: A Survey of Hand Surgeons. *Hand (N Y).* 2016;11(1):113-118.

doi:10.1177/1558944715616953.

11. Rock MG, Roth JH, Martin L. Radial shortening osteotomy for treatment of Kienbock's disease. *J Hand Surg Am.* 1991;16(3):454-460.
12. Takahara M, Watanabe T, Tsuchida H, Yamahara S, Kikuchi N, Ogino T. Long-term follow-up of radial shortening osteotomy for Kienbock disease. Surgical technique. *J Bone Joint Surg Am.* 2009;91 Suppl 2(Part 2):184-190. doi:10.2106/JBJS.I.00315.
13. Matsui Y, Funakoshi T, Motomiya M, Urita A, Minami M, Iwasaki N. Radial shortening osteotomy for kienbock disease: Minimum 10-year follow-up. *J Hand Surg Am.* 2014;39(4):679-685. doi:10.1016/j.jhsa.2014.01.020.
14. Watanabe T, Takahara M, Tsuchida H, Yamahara S, Kikuchi N, Ogino T. Long-term follow-up of radial shortening osteotomy for Kienbock disease. *J Bone Jt Surg Am.* 2008;90(8):1705-1711. doi:10.2106/JBJS.G.00421.
15. Salmon J, Stanley JK, Trail IA. kienbock's disease: conservative management versus radial shortening. *J Bone Jt Surg Am.* 2000;82(6):820-823.
16. Tatebe M, Koh S, Hirata H. Long-Term Outcomes of Radial Osteotomy for the Treatment of Kienbock Disease. *J Wrist Surg.* 2016;5(2):92-97. doi:10.1055/s-0036-1581099.
17. Raven EEJ, Haverkamp D, Marti RK. Outcome of Kienböck's disease 22 years after distal radius shortening osteotomy. *Clin Orthop Relat Res.* 2007;460(0):137-141. doi:10.1097/BLO.0b013e318041d309.
18. Trumble T, Glisson RR, Seaber A V, Urbaniak JR. Forearm force transmission after surgical treatment of distal radioulnar joint disorders. *J Hand Surg Am.* 1987;12(2):196-202. doi:http://dx.doi.org/10.1016/S0363-5023(87)80270-8.
19. Bu J, Patterson RM, Morris R, Yang J, Viegas SF. The Effect of Radial Shortening on

- Wrist Joint Mechanics in Cadaver Specimens With Inherent Differences in Ulnar Variance. *J Hand Surg Am*. 2006;31(10):1594-1600. doi:10.1016/j.jhsa.2006.09.004.
20. Palmer a K, Glisson RR, Werner FW. Relationship between ulnar variance and triangular fibrocartilage complex thickness. *J Hand Surg Am*. 1984;9(5):681-682. doi:10.1016/S0363-5023(84)80013-1.
 21. Werner FW, Glisson RR, Murphy DJ, Palmer AK. Force transmission through the distal radioulnar carpal joint: effect of ulnar lengthening and shortening. *Handchir Mikrochir Plast Chir*. 1986;18(5):304-308.
 22. Palmer AK, Werner FW. Biomechanics of the Distal Radioulnar Joint. *Clin Orthop Relat Res*. 1984;187:26-35.
 23. Palmer AK. Triangular fibrocartilage complex lesions: A classification. *J Hand Surg Am*. 1989;14(4):594-606. doi:10.1016/0363-5023(89)90174-3.
 24. Adams BD. Effects of radial deformity on distal radioulnar joint mechanics. *J Hand Surg [Am]*. 1993;18(3):492-498. doi:10.1016/0363-5023(93)90098-N.
 25. Pogue DJ, Viegas SF, Patterson RM, et al. Effects of distal radius fracture malunion on wrist joint mechanics. *J Hand Surg [Am]*. 1990;15(5):721-727.
 26. Harley BJ, Pereria ML, Werner FW, Kinney DA, Sutton LG. Force variations in the distal radius and ulna: Effect of ulnar variance and forearm motion. *J Hand Surg Am*. 2015;40(2):211-216. doi:10.1016/j.jhsa.2014.10.001.
 27. Greeley GS, King GJW, Johnson JA. Biomechanics of the distal radioulnar joint with a malaligned distal radius.
 28. Iglesias D, Lockhart J, Johnson J, King GJW. Development of an In-Vitro Passive and Active Motion Simulator for the Investigation of Wrist Function and Kinematics. 2015.

29. Einhorn T, O’Keefe R, Buckwalter J. Form and function of bone. *Orthop Basic Sci Found Clin Pract.* 2007;3rd Editio:129-174.
30. Certus O. Research-Grade Motion Capture. Digital N Inc, ed. *Manuf Manual.* 2011:1-8.
31. Gordon KD, Dunning CE, Johnson JA, King GJW. Influence of the Pronator Quadratus and Supinator Muscle Load on DRUJ Stability. *J Hand Surg Am.* 2003;28(6):943-950. doi:10.1016/S0363-5023(03)00487-8.
32. Markolf KL, Lamey D, Yang S, Meals R, Hotchkiss R. Radioulnar load-sharing in the forearm. A study in cadavera. *J Bone Joint Surg Am.* 1998;80(6):879-888.
33. Greenberg JA, Werner FW, Smith JM. Biomechanical analysis of the distal metaphyseal ulnar shortening osteotomy. *J Hand Surg Am.* 2013;38(10):1919-1924. doi:10.1016/j.jhsa.2013.06.038.
34. Ekenstam FW, Palmer AK, Glisson RR. The load on the radius and ulna in different positions of the wrist and forearm. A cadaver study. *Acta Orthop Scand.* 1984;55(3):363-365.
35. Shepard MF, Markolf KL, Dunbar a M. Effects of radial head excision and distal radial shortening on load-sharing in cadaver forearms. *J Bone Joint Surg Am.* 2001;83-A(1):92-100.
36. Horii E, Garcia-Elias M, Bishop AT, Cooney WP, Linscheid RL, Chao EY. Effect on force transmission across the carpus in procedures used to treat Kienbock’s disease. *J Hand Surg Am.* 1990;15(3):393-400.
37. Calfee RP, Van Steyn MO, Gyuricza C, Adams A, Weiland AJ, Gelberman RH. Joint leveling for advanced Kienb??ck’s disease. *J Hand Surg Am.* 2010;35(12):1947-1954. doi:10.1016/j.jhsa.2010.08.017.

38. Jin Bo Tang, Ryu J, Kish V, Wearden S. Effect of radial shortening on muscle length and moment arms of the wrist flexors and extensors. *J Orthop Res*. 1997;15(3):324-330. doi:10.1002/jor.1100150303.
39. LaRoque ES, Murray WM, Langley S, Hariri S, Levine BP, Ladd AL. Muscle Moment Arms in the First Dorsal Extensor Compartment After Radial Malunion. *J Bone Jt Surgery-American Vol*. 2008;90(9):1979-1987. doi:10.2106/JBJS.G.01015.
40. Tang JB, Ryu J, Omokawa S, Han J, Kish V. Biomechanical evaluation of wrist motor tendons after fractures of the distal radius. *J Hand Surg [Am]*. 1999;24(1):121-132. doi:10.1053/jhsu.1999.jhsu24a0121.
41. Koh TJ, Herzog W. Increasing the moment arm of the tibialis anterior induces structural and functional adaptation: Implications for tendon transfer. *J Biomech*. 1998;31(7):593-599.
42. Markolf KL, Tejwani SG, O'Neil G, Benhaim P. Load-Sharing at the Wrist Following Radial Head Replacement with a Metal Implant. *J Bone Jt Surg Am*. 2004;86-A(5):1023-1030.
43. Markolf KL, Dunbar AM, Hannani K. Mechanisms of load transfer in the cadaver forearm: Role of the interosseous membrane. *J Hand Surg Am*. 2000;25(4):674-682. doi:10.1053/jhsu.2000.8640.
44. Bu J, Patterson RM, Morris R, Yang J, Viegas SF. The Effect of Radial Shortening on Wrist Joint Mechanics in Cadaver Specimens With Inherent Differences in Ulnar Variance. *J Hand Surg [Am]*. 2006;31(10):1594-1600. doi:10.1016/j.jhsa.2006.09.004.
45. Ekenstam FW, Palmer AK, Glisson RR. The load on the radius and ulna in different positions of the wrist and forearm. A cadaver study. *Acta Orthop Scand*. 1984;55(3):363-

- 365.
46. Brigstocke GHO, Hearnden A, Holt C, Whatling G. In-vivo confirmation of the use of the dart thrower's motion during activities of daily living. *J Hand Surg Eur Vol.* 2014;39E(4):373-378. doi:10.1177/1753193412460149.
 47. Werner FW, Palmer AK, Fortino MD, Short WH. Force transmission through the distal ulna : Effect of ulnar variance , lunate fossa angulation , and radial and palmar tilt of the distal radius. *J Hand Surg Am.* 1992.
 48. Markolf KL, Tejwani SG, Benhaim P. Effects of wafer resection and hemiresection from the distal ulna on load-sharing at the wrist: a cadaveric study. *J Hand Surg [Am]*. 2005;30(2):351-358. doi:10.1016/j.jhsa.2004.11.013.

Chapter 3

3. THE EFFECT OF ULNAR LENGTH CHANGE AND TFC INTEGRITY ON DISTAL FOREARM LOADING DURING SIMULATED WRIST MOTION

3.1 OVERVIEW

This chapter reports on an in-vivo cadaveric study examining the relationship between change in ulnar length and wrist joint forces during simulated wrist motion via load cells in the distal radius and ulna during simulated active motion. Also, the presence and absence of the triangular fibrocartilage (TFC) was evaluated to examine the effects of the TFC on load distribution during ulnar length change.

3.2 INTRODUCTION

Ulnocarpal impaction also known as ulnar impaction or ulnocarpal abutment, is caused by ulnar head abutment against the ulnar side of the carpus. This leads to erosion and perforation of the triangular fibrocartilage (TFC) and/or lunotriquetral ligament, lunate chondromalacia, and ulnar sided degenerative arthritis.^{1,2,3}

Although ulnocarpal impaction is more commonly associated with wrists demonstrating ulnar positive variance, it may also occur in wrists with ulnar negative or neutral variance.⁴ Ulnocarpal impaction may also be seen in distal radius malunion with radial shortening, radial head excision

with subsequent proximal migration of the radius, congenital positive ulnar variance, premature physeal closure of the radius, overgrowth of the ulna due to trauma, Madelung's deformity, infection or tumor.

Changes in ulnar variance with forearm position and grip has been described accounting for subtle variations on radiographs.^{5,6,7} An increase in ulnar variance of up to 2.5mm can occur on pronated grip view.⁷ This dynamic positive ulnar variance causes increased ulnocarpal load and may explain why patients with ulnocarpal impaction syndrome have pain with the ulnocarpal stress test.⁸ The ulnocarpal stress test⁹ places the wrist in ulnar deviation while passively rotating the forearm with an axial load.

Current treatment for symptomatic ulnar impaction include ulnar shortening osteotomy, wafer resection of the ulnar head,⁸ a hemiresection interposition arthroplasty or an excisional arthroplasty¹⁰. All of these procedures are aimed at decreasing load transmission through the distal ulna¹¹ and have been shown to provide satisfactory pain relief.^{12,13,14,15} A limiting factor with ulnar shortening osteotomy is DRUJ arthrosis which has been reported in long-term follow-up studies evaluating the outcome of this procedure.^{16,17} Ulnar shortening osteotomy is also used in the treatment of DRUJ instability as it tightens the ulnocarpal ligaments, DRUJ capsule and TFC. The TFC also functions in load sharing between the radius and ulna.^{18,19} In a biomechanical study by Palmer et al,²⁰ excision of the TFC resulted in a decrease in distal ulnar loads to 8% from 18%.

The optimal amount of ulnar shortening to relieve the symptoms of ulnocarpal impaction

remains unknown. A previous biomechanical study demonstrated a decrease in load transmission through the distal ulna from 18% to 4% by 2.5mm of ulnar shortening¹⁸ thus concluding shortening of only 2.5 mm is sufficient to decompress the ulnocarpal joint. Both wafer removal and hemiresection have been shown to significantly decrease mean distal ulnar loads regardless of ulnar variance.¹¹ These studies were conducted by application of a constant force to cadaveric wrists; this method of static wrist loading may not accurately simulate distal radius and ulna loading during *in-vivo* wrist motion. In a simulated dynamic study by Greenberg et al,²¹ distal ulnar metaphyseal shortening osteotomies were performed with a mean change in ulnar variance of 2.8mm. Significant decreases in ulnar load during flexion-extension, radioulnar deviation and dart thrower's motion were noted after shortening. However, this study did not examine the effect of sequential ulnar length change on distal loading and the effects of TFC sectioning on these loads.

An inverse correlation between ulnar variance TFC thickness exists with greater thickness of the TFC observed in wrists with negative ulnar variance.^{22,23} An earlier study using constrained axial loading by Palmer et al¹⁸ demonstrated resection of the TFC resulted in a reduction in distal ulnar load from 40% to 5% of total wrist load. A subsequent study showed excision of the TFC reduced ulnar load from 18% to 8%.²⁰ However, these studies were conducted under static loading conditions and may not accurately simulate normal wrist mechanics.

The effects of ulnar length change on axial load transmission during simulated dynamic wrist motion and the effect of TFC sectioning on these loads remains to be clarified. A better understanding of distal forearm loading will aid in surgical decision making and provide insight into the treatment of ulnocarpal impaction, TFC injuries and DRUJ instability.

The primary objective of this study was to determine the relationship between ulnar length change and distal forearm axial loading during simulated dynamic wrist motion. Our secondary objective was to evaluate the effect of TFC excision on distal radial and ulnar loads with ulnar length change during simulated dynamic wrist motion. Our hypotheses were: 1) distal ulnar loads will increase and distal radial loads will decrease with ulnar lengthening; 2) distal ulnar loads will decrease and distal radial loads will increase with ulnar shortening; 3) loading will vary at different wrist positions during simulated dynamic wrist motion; and 4) TFC sectioning will have a significant effect on distal forearm loading.

3.3 METHODS

3.3.1 IMPLANT DESIGN

As described in Chapter 2 (Section 2.3.1), a custom implant which incorporates a load cell was designed to lengthen and shorten the ulna using a lead screw mechanism (Figure 2.2 a). The distal component was designed with a rectangular notched stem for cementing into the intramedullary canal of the distal ulna. Stem diameter was calculated based on intramedullary measurements of cadaveric CTs to fit even the smallest intramedullary canals while allowing room for an adequate cement mantle. The purpose of the stem diameter selection and stem notching was to assist with implant fixation in addition to mitigating the risk of implant loosening.

Between the proximal and distal components consists of a load cell for axial (tensile and

compressive) load measurement and a lead screw mechanism. The lead screw mechanism was designed to adjust the implant length by rotating the central nut thus causing both threaded eye bolts to be translated in or out simultaneously without rotating the thread eye bolts. The thread pitch was designed such that one third of a full bolt revolution counterclockwise and clockwise results in 1mm of lengthening and shortening respectively. The implant was designed to achieve 5 mm of shortening and 5 mm of lengthening each from the native position.

The implant had a spacer for specimen preparation while the final implant with a load cell and lead screw mechanism was used for testing. The ulnar spacer (Figure 2.2 b) and custom ulnar implant were designed with the same length. However, the spacer had a slightly smaller diameter than the final testing implant to facilitate maintenance of an intact bone bridge and preserve the native distal ulnar articular surface location during the insertion and cementing process. Again, the stem was notched proximally and roughened to assist with fixation in the intramedullary canal. An appropriate stem diameter for our study was obtained through calculations based on intramedullary measurements from cadaveric CT scans. This was to allow for a secure fit in even the smallest intramedullary canals while allowing for an adequate cement mantle. A one-degree of freedom (1-DOF) Honeywell® load cell model 11 (NJ, USA) cell was placed distal to the lead screw to quantify distal ulnar axial loads.

A similar radial implant including a load cell was also designed (Figure 2.1 a). The distal fixation locking plate was designed with a 22° volar angulation to match the contour of the volar metaphyseal flare of the distal radius. The intermediate components and proximal stem were designed in a similar fashion to the ulnar component with a load cell for axial load measurement and a lead screw mechanism. Proximally, the stem was notched and roughened to assist with fixation in the intramedullary canal. The radial spacer (Figure 2.1 b) and custom radial implant

were designed similarly with the same length but the spacer had a slightly smaller diameter than the final testing implant to facilitate maintenance of an intact bone bridge and preserve the native distal radial articular surface location during the insertion and cementing process. Cutting guides were also designed to guide cuts and ensure reproducible cuts (Figures 2.4 f and 2.5 f)

3.3.2 AXIAL LOAD MEASUREMENT

Axial load was measured using 1-DOF Honeywell® load cell model 11 (NJ, USA) 0.8% accuracy, 0.1% repeatability. The load cells were zeroed prior to implantation without the application or influence of external loads. The threaded connections on either side of the load cells securely attach to the radial and ulnar custom implants to measure axial (tensile and compressive) forces.

3.3.3 SPECIMEN PREPARATION

Testing was performed on 9 fresh frozen right cadaveric forearm specimens (mean age 74 years; range 64 to 83 years; all Caucasian male) with no clinical or CT evidence of osteoarthritis. The specimens were amputated at the mid-humeral level and stored at - 20 °C. They were thawed for 18 hours at room temperature (22 °C) and then prepared for mounting.

An approach to the subcutaneous border of the ulna was utilized initially. The skin and subcutaneous tissue was sharply incised and the interval between extensor carpi ulnaris (ECU)

and flexor carpi ulnaris (FCU) was incised down to the ulna (Figure 3.1). The extensor retinaculum was left intact. Retractors were then placed.

Using the bone bridge technique as described in Chapter 2 (Section 2.3.3), cuts were made using a microsagittal saw leaving a radial bone bridge intact. A 40mm segment of bone was removed approximately 10 mm proximal to the DRUJ utilizing a cutting guide. The ulnar spacer was then cemented in place (Figure 3.4 a).

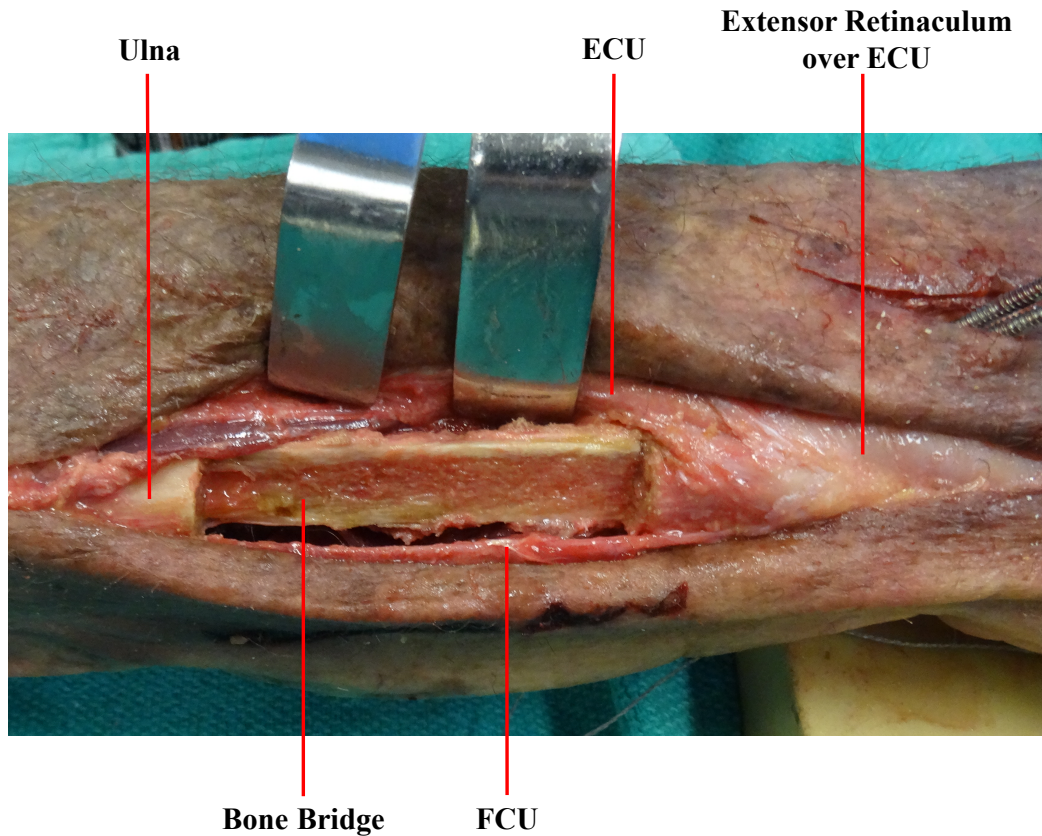


Figure 3. 1 Approach to Subcutaneous Border of the Ulna demonstrating Bone Bridge.
© D Isa

As described in Chapter 2 (Section 2.3.3), the radial spacer was implanted using the volar FCR

approach (Figure 2.2). After incision of the skin and subcutaneous tissue, the FCR tendon sheath was incised and the FCR tendon retracted ulnarly. The floor of the FCR tendon sheath was incised and the contents of the carpal tunnel were retracted ulnarly exposing the pronator quadratus (PQ). The PQ was then subperiosteally elevated off the distal radius carefully to avoid disruption of the volar distal radioulnar joint (DRUJ) capsule or interosseous membrane during this process.

Using the bone bridge technique, a 40mm segment of volar cortex was excised 10mm proximal to the DRUJ. The dorsal bone bridge was left intact to maintain the alignment of the radius during specimen preparation and mounting. The radial implant spacer was then cemented in place (Figure 2.3).

As discussed in Chapter 2 (Section 2.3.3), the tendons of the prime movers were then sutured: The tendons of the wrist extensors proximal to the extensor retinaculum (extensor carpi radialis longus [ECRL], extensor carpi radialis brevis [ECRB] extensor carpi ulnaris [ECU]), wrist flexors (flexor carpi radialis [FCR], flexor carpi ulnaris [FCU]), pronator teres [PT] and biceps [BI] were sutured using a Spectra extreme braid fishing line (80lbs) using a running locking stitch. To mimic physiologic line of pull, all sutures (except BI) were tunneled under the skin and passed through alignment guides in the medial and lateral epicondyle. Tendon forces were controlled by attachment of the sutures to electric servomotors (SMI 2316D-PLS, Animatics, CA) with force transducers (Vishay Precision Group, Raleigh, NC) to control tendon forces.

Infrared marker triads were rigidly affixed to the radius, ulna and 3rd metacarpal using custom Delrin® pedestals to track joint angles and wrist motion was tracked using an Optotrak Certus (Northern Digital Inc, Waterloo, Ontario, Canada) motion capture system with a 3D accuracy of

0.1mm and 0.01mm resolution.²⁴

Nylon zippers were used to close the incisions in order to preserve moisture and for ease of accessibility to the radial and ulna implants for length adjustments. Saline irrigation of the specimen's soft tissues was done intermittently to keep the specimens moist during testing.

Once the specimen was mounted on the motion simulator, the radial and ulnar bone bridges were cut after the spacers were removed and the final implants fixed in place.

3.3.4 SIMULATION OF MOTION AND TESTING PROTOCOL

As discussed in Chapter 2 (Section 2.3.4), the motion simulator utilized in this study simulates *in-vivo* behavior using a force position algorithm that simulates dynamic/active motion based on electromyographic studies on active wrist and forearm motion and ratios derived from existing anatomic data detailing the cross sectional areas of the muscles of the wrist (Figure 2.6).²⁵ Loads are applied to antagonistic muscle pairs to more accurately simulate an *in vivo* wrist with a minimum tone load applied to groups resisting motion (8.9 N to FCU, FCR, ECRL, ECRB and ECU and 15 N to BI and PT). The magnitude of load through the muscle groups enforcing motion increased with the resultant force imbalance moving the wrist in the desired direction. Activation of the BI and PT were used to maintain the forearm in neutral rotation throughout testing.

The motions evaluated in this study included wrist flexion (wrist moved from 50° extended position to 50° of flexion), ulnar deviation (wrist moved from 15° radially deviated position to

10° of ulnar deviation) and dart throw motion (30° of extension and 10° radial deviation to 30° of flexion and 10° ulnar deviation) at a rate of 3° per second (Figure 2.8). All data was collected with the forearm maintained at neutral forearm rotation. The effect of ulnar length change of 1mm, 2mm and 3mm of lengthening and 1mm, 2mm, 3mm and 4mm of shortening on distal forearm loading was studied. The radial length remained unchanged throughout the testing protocol.

The TFC was then excised. A 4cm longitudinal incision centered over the DRUJ was utilized. The extensor digiti minimi (EDM) was exposed and the interval between EDM and the fourth extensor compartment to expose the capsule distal to the extensor retinaculum. The capsule was then incised distal to the TFC to expose the TFC. The TFC was visualized and excised. The dorsal and volar radioulnar ligaments were left intact. After the TFC was excised, the testing protocol was then repeated. Complete excision of the TFC was confirmed at the end of the testing protocol by disarticulating the wrist.

3.3.5 METHODS AND DATA ANALYSIS

Statistical Analyses

A three-way repeated-measures ANOVA was performed to investigate the effect of ulnar length, joint angle and TFC status on axial loads. A Greenhouse-Geisser correction was performed when Mauchly's test for sphericity was violated. Ulnar length, joint angle and TFC status were the

independent variables and axial load the dependent variable. Statistical significance was set at $P < .050$. Comparisons were made at various ulnar lengths (+3, +2, +1, neutral, -1, -2, -3, -4mm of length change) during simulated dynamic wrist flexion from 50° of wrist extension to 50° of flexion (-50° to 50°; where -50°, -40°, -30°, -20° and -10° represent wrist extended positions and 10°, 20°, 30°, 40° and 50° represent wrist flexed positions), ulnar deviation from 15° of radial deviation to 10° of ulnar deviation (-15° to 10°; where -15, -10 and -5 are radially deviated positions and 5 and 10 represented ulnarly deviated positions) and dart throw motion from 30° of extension and 10° of radial deviation to 30° of flexion and 10° of ulnar deviation (-30°, -10° to 30°, 10°). Comparisons between flexion angles were done at 10° increments, radial to ulnar deviation at 5° increments and in 10° increments of flexion for dart throw motion (Figure 2.8).

Where interactions were detected between joint angle, ulnar length and/or TFC status, separate ANOVA analyses were undertaken to examine the effect of various ulnar lengths on distal forearm loading. The flexion-extension, radioulnar deviation, and dart-throw motions were limited in certain cadavers and as a result, 8 specimens were used to evaluate flexion, 7 specimens for ulnar deviation, and 6 specimens for dart thrower's motion.

3.4 RESULTS

3.4.1 FLEXION

For the TFCC intact and sectioned states, radial and ulnar axial loads during simulated active flexion (from the 50° extended position to 50° of flexion) were compared at 10° flexion intervals for each ulnar length change studied.

Changes in ulnar loads with ulnar length change were significant ($p < 0.001$) (Figure 3.2). With ulnar lengthening, there was an increase in ulnar loads and vice versa; $27 \pm 10\text{N}$ at 3mm, $24 \pm 10\text{N}$ at 2mm, $18 \pm 8\text{N}$ at 1mm of ulnar lengthening, $12 \pm 6\text{N}$ at native length and $7 \pm 6\text{N}$ at 1mm, $3 \pm 5\text{N}$ at 2mm, $-1 \pm 3\text{N}$ at 3mm, $-3 \pm 2\text{N}$ at 4mm of ulnar shortening during wrist flexion (Appendix 2.5). There was a 50%, 100% and 125% increase in ulnar loads from neutral ulnar length at 1mm, 2mm and 3mm of ulnar lengthening respectively. Conversely, there was a 42%, 75%, 108% and 125% decrease in ulnar loads compared to native length at 1mm, 2mm, 3mm and 4mm of ulnar shortening respectively with tensile loads were observed at 3 and 4mm of ulnar shortening. During simulated wrist flexion, variation in loading was observed with peak loads observed in the -50° extended wrist position for each millimeter change in ulna length investigated ($p = 0.006$) (Figure 3.3). There was no interaction between TFC status, ulnar length and joint angle ($p = 0.324$) and no interaction between ulnar length and joint angle ($p = 0.325$) on distal ulnar loads.

There was no significant change in radial loads with ulnar length change ($p = 0.324$) (Figure 3.2): $61 \pm 15\text{N}$ at 3mm, $67 \pm 12\text{N}$ at 2mm, $69 \pm 7\text{N}$ at 1mm of ulnar lengthening, $72 \pm 8\text{N}$ at native length and $66 \pm 6\text{N}$ at 1mm, $60 \pm 8\text{N}$ at 2mm, $64 \pm 6\text{N}$ at 3mm, $59 \pm 16\text{N}$ at 4mm of ulnar shortening (Appendix 2.5). There was no interaction between TFC status, ulnar length and joint angle ($p = 0.282$); however, there was a significant interaction between joint angle and ulnar length ($p = 0.002$) on radial loads.

Post hoc analysis showed the variation in radial loads seen in the extended wrist position (-50° to -30°) during simulated dynamic wrist flexion with each millimeter change in ulnar length ($p < 0.05$). More specifically, during flexion, with each millimeter increase in ulna length, peak radial loads were seen in the -50° position and with each millimeter decrease in ulna length, lowest radial loads were seen in the -50° extended position (Figure 3.2 a). Radial and ulnar loads followed similar trends in the extended wrist position (Figure 3.2 a).

Effect of TFC excision

Distal radial and ulnar axial loads during simulated active flexion with the TFC excised were compared to the TFC intact state. At each 10° interval of wrist flexion evaluated from -50° to 50° . There was no effect of TFC sectioning on distal ulnar loads ($p = 0.342$). However, there was a decrease in radial loads ($p = 0.027$) when the TFC was sectioned during simulated dynamic flexion. (Figure 3.3).

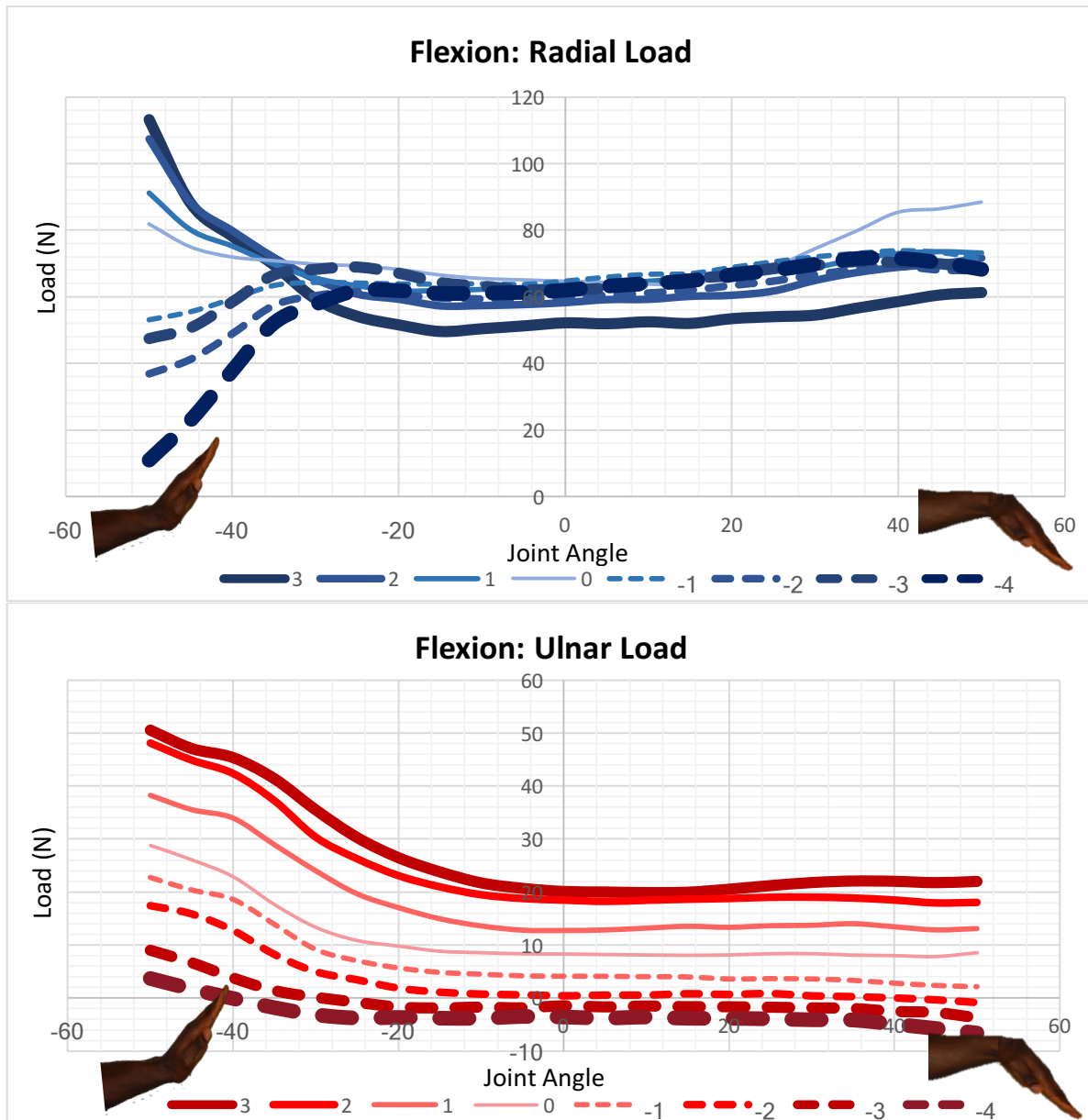


Figure 3. 2 Radial and ulnar loads during wrist flexion n = 8.

(In order to facilitate the interpretation of the data, the lines were constructed with increasing thickness to represent lengthening and shortening. Lengthening is solid, and shortening is dashed. Mean are loads reported. The same format is employed for all other related graphs in this chapter.)

- c. The radial loads at 3mm, 2mm and 1mm of ulnar lengthening (3, 2, 1), native length (0) and 1mm, 2mm, 3mm and 4mm of ulnar shortening (-1, -2, -3, -4) during wrist flexion. Flexion motion started with the wrist in 50° of extension (-50) to 50° of flexion (50).*
- d. The ulnar loads at 3mm, 2mm and 1mm of ulnar lengthening (3, 2, 1), native length (0) and 1mm, 2mm, 3mm and 4mm of ulnar shortening (-1, -2, -3, -4) during wrist flexion. Flexion motion started with the wrist in 50° of extension (-50) to 50° of flexion (50).*

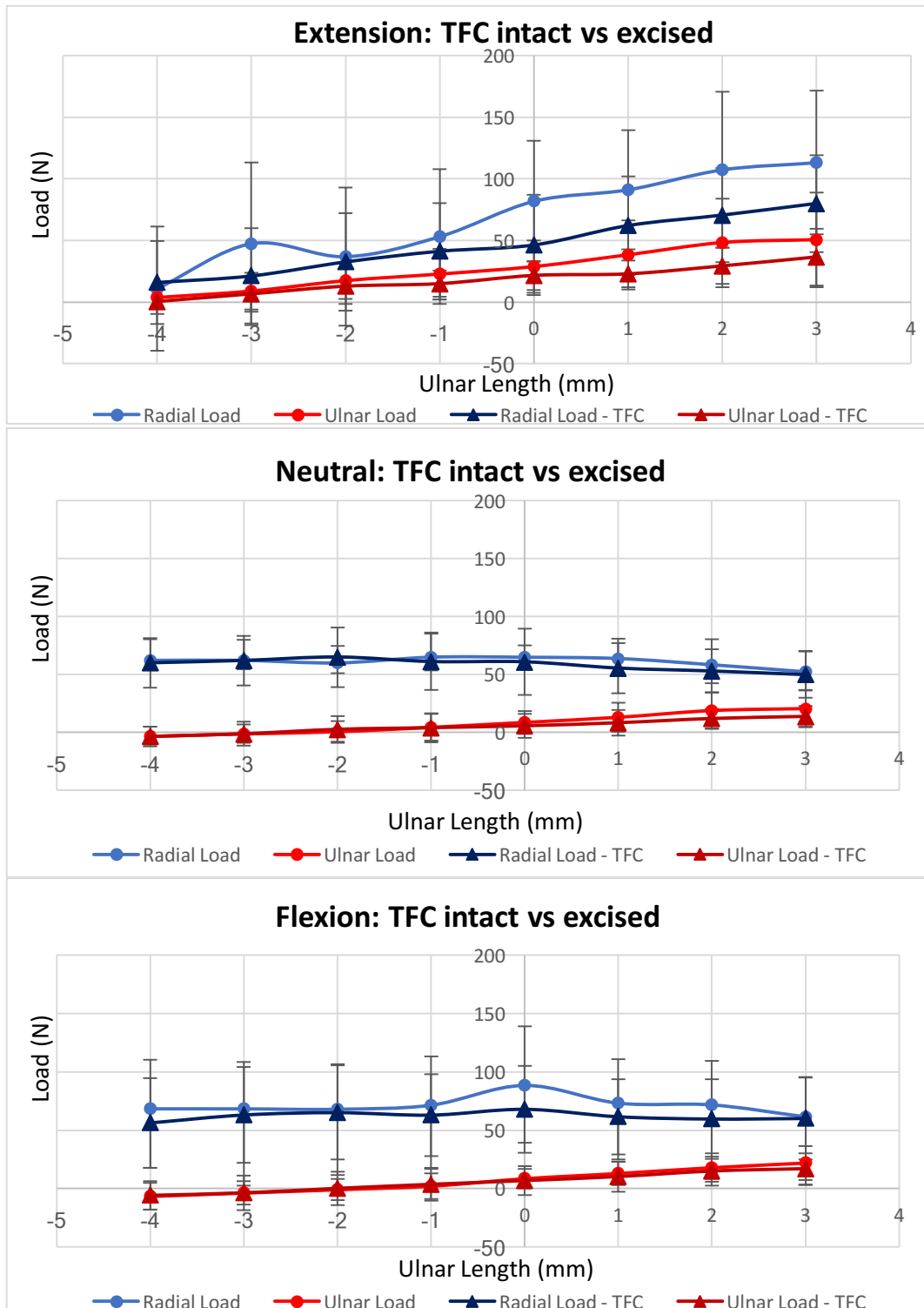


Figure 3. 3 Radial and ulnar loads with ulnar length change during simulated wrist flexion with and without the TFC intact n = 8.

Radial and ulnar loads at 3mm, 2mm and 1mm of ulnar lengthening (+3, +2, +1), native radial length (0) and 4mm, 3mm, 2mm and 1mm of ulnar shortening (-4, -3, -2, -1) in (a) extension, (b) neutral and (c) flexion. Mean \pm 1 SD are shown.

3.4.2 ULNAR DEVIATION

For the TFCC intact and sectioned states, radial and ulnar axial loads during simulated active UD (from the 15° of radial deviation to 10° of UD) were compared at 5° intervals for each ulnar length change studied.

Changes in ulnar loads with ulnar length change were significant ($p < 0.001$) (Figure 3.4). With ulnar lengthening, there was an increase in ulnar loads and vice versa: $27 \pm 10\text{N}$ at 3mm, $24 \pm 10\text{N}$ at 2mm, $20 \pm 8\text{N}$ at 1mm of ulnar lengthening (3, 2, 1), $14 \pm 8\text{N}$ at native length (0) and $10 \pm 7\text{N}$ at 1mm, $7 \pm 6\text{N}$ at 2mm, $3 \pm 5\text{N}$ at 3mm, $-1 \pm 4\text{N}$ at 4mm of ulnar shortening (-1, -2, -3, -4) during wrist UD (Appendix 2.6). There was a 43%, 71% and 93% increase in ulnar loads from neutral ulnar length at 1mm, 2mm and 3mm of ulnar lengthening respectively and a 29%, 50%, 79% and 107% decrease in ulnar loads compared to neutral length at 1mm, 2mm, 3mm and 4mm of ulnar shortening respectively. Tensile loads were observed at 4mm of ulnar shortening.

Variation in distal ulnar loads during simulated dynamic UD were observed (Figure 3.5) with peak ulnar loads observed in ulnar deviation for each millimeter of ulnar length change ($p = 0.003$). There was no significant interaction between TFC status, ulnar length, and joint angle ($p = 0.536$) and no significant interaction between ulnar length and joint angle ($p = 0.297$) on distal ulnar loads.

Changes in radial loads with ulnar length change were significant ($p = 0.008$) with a decrease in radial loads with both ulnar lengthening and shortening (Figure 3.5 a, b, c); $68 \pm 13\text{N}$ at 3mm, 74

$\pm 13\text{N}$ at 2mm, $74 \pm 12\text{N}$ at 1mm of ulnar lengthening (3, 2, 1), $85 \pm 17\text{N}$ at native length (0) and $69 \pm 9\text{N}$ at 1mm, $68 \pm 17\text{N}$ at 2mm, $67 \pm 18\text{N}$ at 3mm, $65 \pm 21\text{N}$ at 4mm of ulnar shortening (-1, -2, -3, -4) (Appendix 2.6). There was no interaction between TFC status, ulnar length, and joint angle ($p = 0.646$); however, there was an interaction between joint angle and ulnar length ($p = 0.006$) on radial loads.

Post hoc analysis showed decreases in radial loads of 20% occurred at 3mm of ulnar lengthening ($p = 0.012$). Meanwhile, there was a 19% decrease in radial loads at 1mm of ulnar shortening ($p = 0.024$) (Appendix 2.5). However, there was no change in radial loads from 1 to 2mm, 2 to 3mm and 3 to 4mm of ulnar shortening ($p = 0.222$, $p = 0.450$ and $p = 0.107$ respectively).

Variation in distal radial loads during simulated dynamic UD were significant with peak radial loads (50% increase from neutral wrist position) observed in radial deviation for each millimeter of ulnar length change ($p = 0.001$) (Figure 3.4).

Effect of TFC excision

Radial and ulnar axial loads in the TFC excised state were compared to the TFC intact state at 5° interval of simulated dynamic wrist UD evaluated from 15° of radial deviation (-15°) to 10° of ulnar deviation (10°). There was no effect of TFC excision on distal ulnar and radial loads ($p = 0.249$ and $p = 0.109$ respectively). (Figure 3.5 a-c).

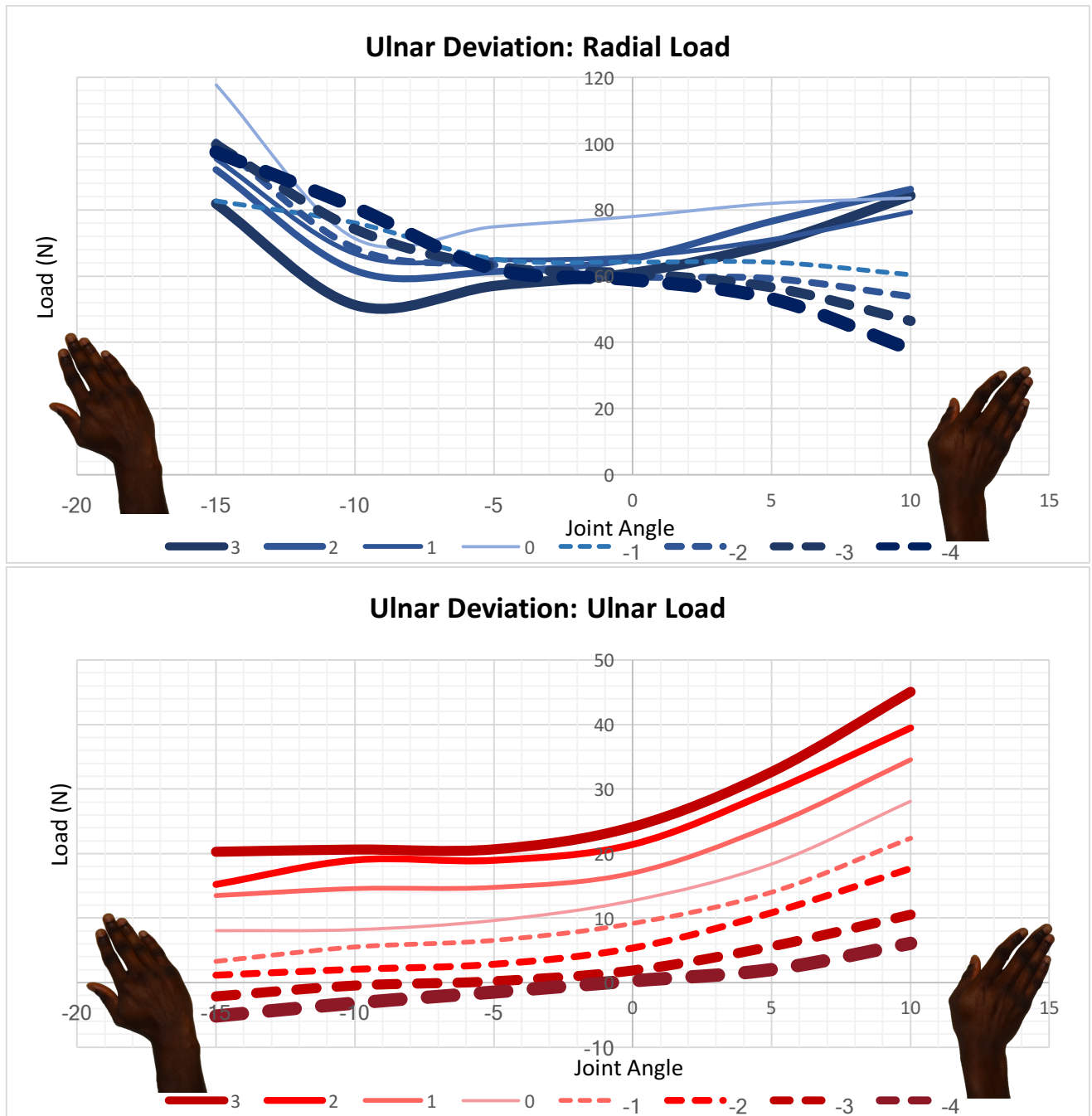


Figure 3. 4 Radial and ulnar loads during ulnar deviation n = 7.

- Graph showing radial loads at 3mm, 2mm and 1mm of ulnar lengthening (3, 2, 1), native length (0) and 1mm, 2mm, 3mm and 4mm of ulnar shortening (-1, -2, -3, -4) during wrist ulnar deviation. Ulnar deviation started with the wrist in 15° of radial deviation (-15) to 10° of ulnar deviation (10).
- Graph showing ulnar loads at 3mm, 2mm and 1mm of ulnar lengthening (3, 2, 1), native length (0) and 1mm, 2mm, 3mm and 4mm of ulnar shortening (-1, -2, -3, -4) during wrist flexion. Ulnar deviation started with the wrist in 15° of radial deviation (-15) to 10° of ulnar deviation (10).

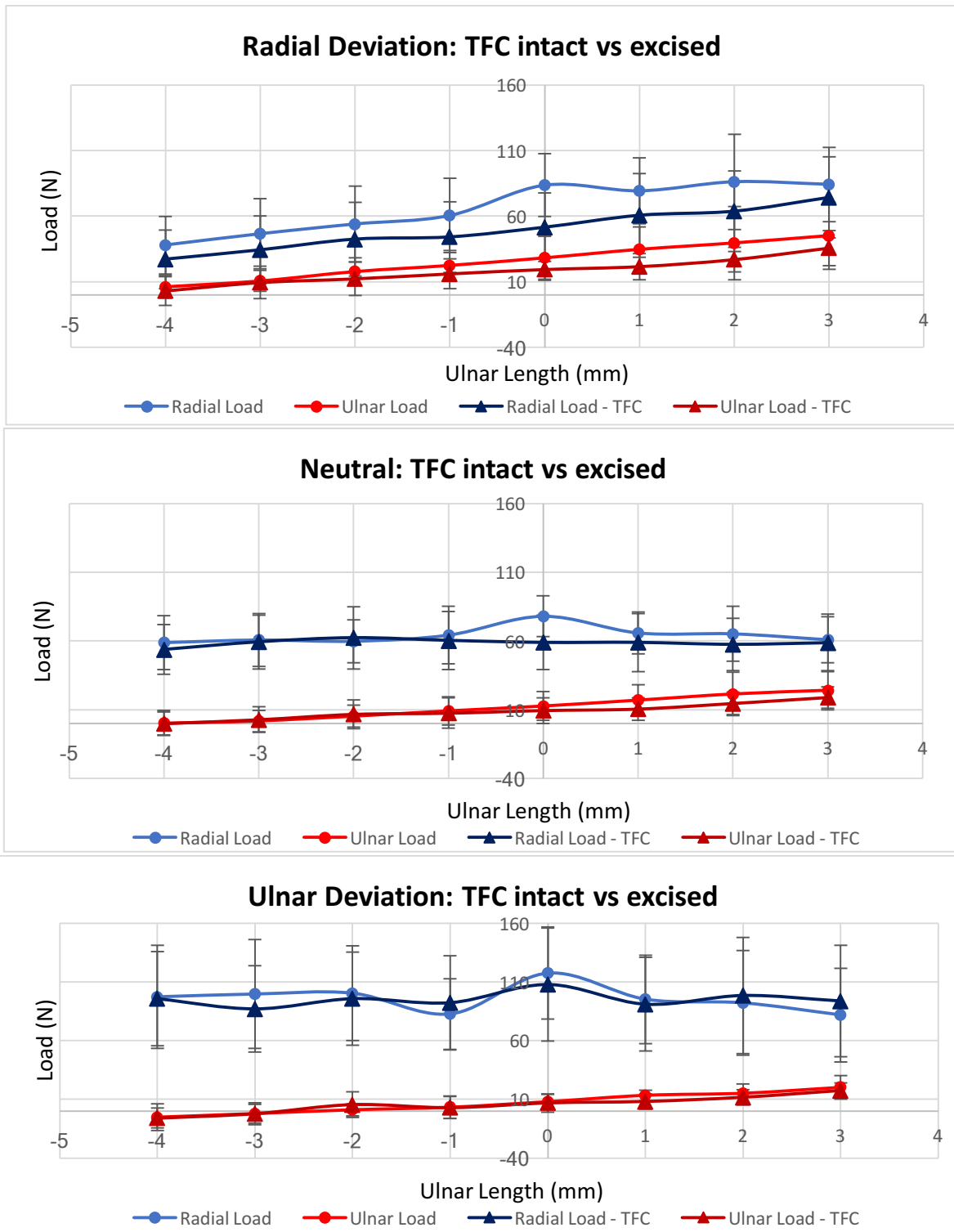


Figure 3. 5 Radial and ulnar loads with ulnar length change during simulated ulnar deviation with and without the TFC intact n = 7.
Radial and ulnar loads at 3mm, 2mm and 1mm of ulnar lengthening (+3, +2, +1), native radial length (0) and 4mm, 3mm, 2mm and 1mm of ulnar shortening (-4, -3, -2, -1) in (a) radial deviation (b) neutral and (c) ulnar deviation. Mean \pm 1 SD are shown.

3.4.3 DART THROW

Radial and ulnar axial loads were compared at each millimeter change in ulnar length from neutral variance for the TFC intact and sectioned states at each 10° interval of simulated active flexion during dart throw (from 30° of extension and 10° radial deviation to 30° of flexion and 10° of ulnar deviation).

Changes in ulnar loads with ulnar length change were significant ($p < 0.001$) (Figure 3.11). With ulnar lengthening, there was an increase in ulnar loads (Figure 3.6): $21 \pm 7\text{N}$ at 3mm, $18 \pm 6\text{N}$ at 2mm, $13 \pm 5\text{N}$ at 1mm of ulnar lengthening (3, 2, 1), $14 \pm 8\text{N}$ at native length (0). Conversely, ulnar loads decreased with ulnar shortening: $2 \pm 6\text{N}$ at 1mm, $-2 \pm 5\text{N}$ at 2mm, $-6 \pm 6\text{N}$ at 3mm, $-10 \pm 6\text{N}$ at 4mm of ulnar shortening (-1, -2, -3, -4) during wrist ulnar deviation (Appendix 2.7). There was a 7%, 29% and 50% increase in ulnar loads from neutral ulnar length at 1mm, 2mm and 3mm of ulnar lengthening, respectively and a 86%, 114%, 143% and 171% decrease in ulnar loads compared to neutral length at 1mm, 2mm, 3mm and 4mm of ulnar shortening respectively. Tensile loads were observed at 2mm, 3mm and 4mm of ulnar shortening. Variation in distal ulnar loads during simulated dynamic dart throw were significant with peak ulnar loads observed in 30° of extension and 10° of radial deviation (-30) for each millimeter of ulnar length change ($p = 0.017$) (Figure 3.6 a). There was no interaction between TFC status, ulnar length, and joint angle ($p = 0.240$) and no interaction between ulnar length and joint angle ($p = 0.206$) on distal ulnar loads.

Furthermore, there were no significant changes in radial loads with ulnar length change ($p = 0.232$). (Figure 3.7 a, b, c); $58 \pm 7\text{N}$ at 3mm, $67 \pm 10\text{N}$ at 2mm, $67 \pm 12\text{N}$ at 1mm of ulnar lengthening (3, 2, 1), $76 \pm 16\text{N}$ at native length (0) and $68 \pm 15\text{N}$ at 1mm, $71 \pm 18\text{N}$ at 2mm, $67 \pm 19\text{N}$ at 3mm, $69 \pm 21\text{N}$ at 4mm of ulnar shortening (-1, -2, -3, -4) (Appendix 2.7). Peak radial loads were observed at initiation of dart throw (30° of extension and 10° of ulnar deviation) for each millimeter change in ulnar length ($p = 0.049$) (Figure 3.6 a). There was no interaction between TFC status, ulnar length, and joint angle ($p = 0.667$) and no interaction effect between joint angle and ulnar length ($p = 0.111$) on radial loads.

Effect of TFC excision

At each 10° interval of dart throw evaluated, radial and ulnar axial loads in the TFC excised state were compared to the TFC intact state. There was no change in distal ulnar loads ($p = 0.240$); however, there was a decrease in radial loads (0.037) when the TFC was excised. (Figure 3.7 a-c).

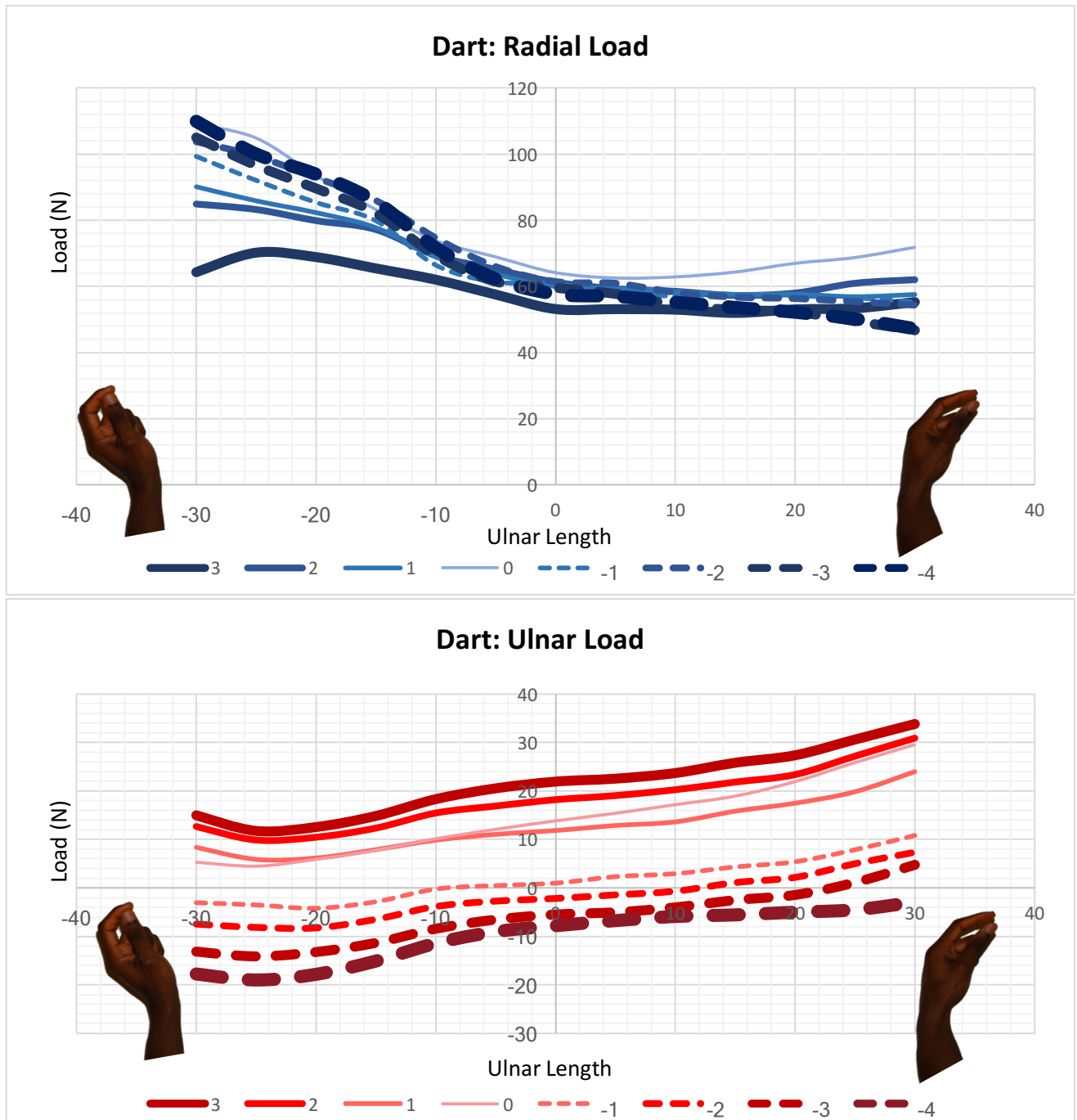


Figure 3. 6 Radial and ulnar loads during dart throw n = 6.

- a. Graph showing radial loads at 3mm, 2mm and 1mm of ulnar lengthening (3, 2, 1), native length (0) and 1mm, 2mm, 3mm and 4mm of ulnar shortening (-1, -2, -3, -4) during dart throw. Dart motion started with the wrist in 30° of extension and 10° of radial deviation (-30, -10) to 30° of flexion and 10° or ulnar deviation (30, 10).
- b. Graph showing ulnar loads at 3mm, 2mm and 1mm of ulnar lengthening (3, 2, 1), native length (0) and 1mm, 2mm, 3mm and 4mm of ulnar shortening (-1, -2, -3, -4) during dart throw. Dart motion started with the wrist in 30° of extension and 10° of radial deviation (-30, -10) to 30° of flexion and 10° or ulnar deviation (30, 10).

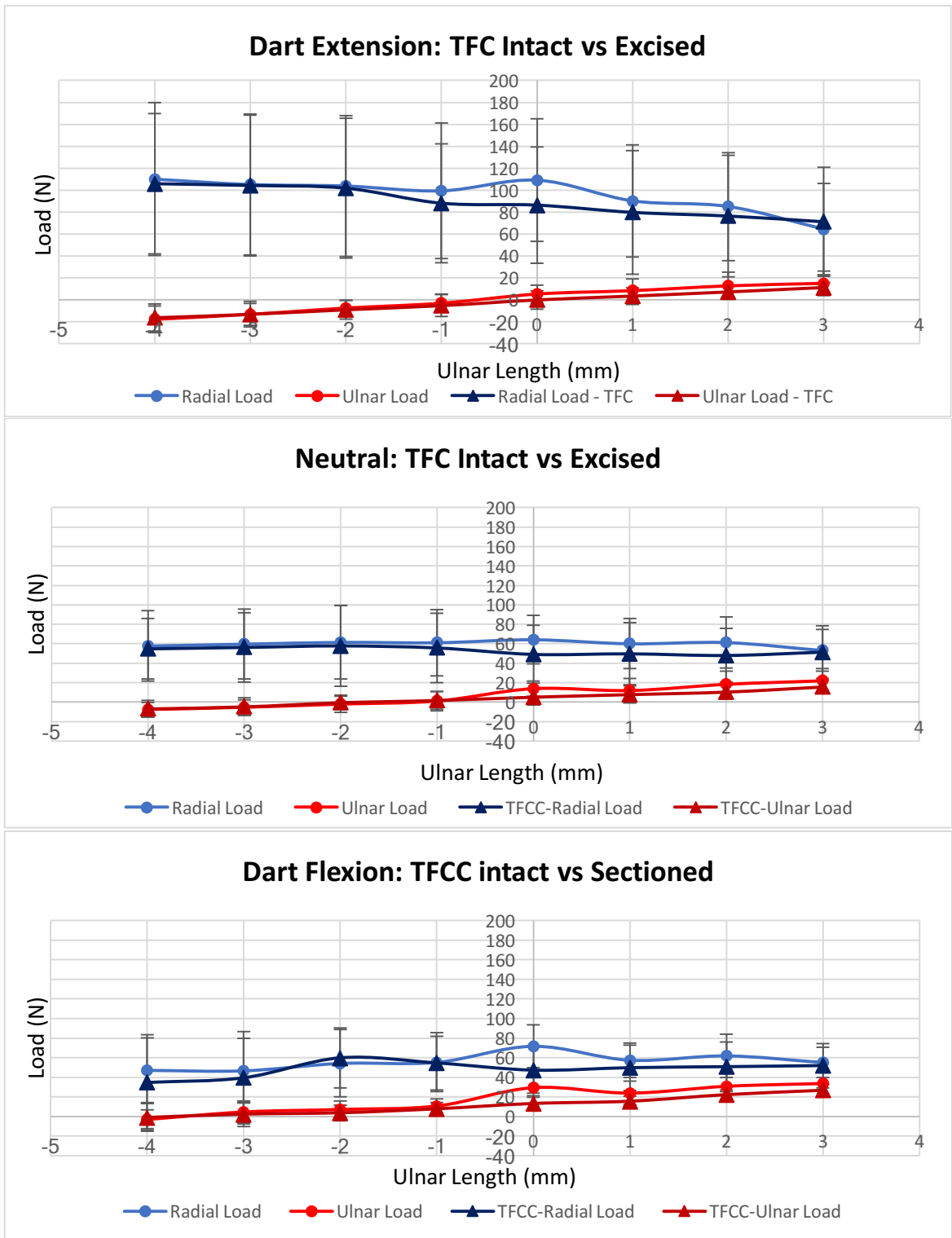


Figure 3. 7 Radial and ulnar loads with ulnar length change during simulated dart throw motion with and without the TFC intact n = 6.
 Radial and ulnar loads at 3mm, 2mm and 1mm of ulnar lengthening (+3, +2, +1), native radial length (0) and 4mm, 3mm, 2mm and 1mm of ulnar shortening (-4, -3, -2, -1) in (a) dart extension (b) neutral and (c) dart flexion. Mean \pm 1 SD are shown.

3.5 DISCUSSION

This biomechanical study was designed to investigate the effects of ulnar length change and TFC integrity on distal forearm loading during simulated wrist motion. Quantifying changes in the forces through the distal radius and ulna with ulnar shortening osteotomies for ulnocarpal impaction or ulnar lengthening osteotomies for Kienbock's disease will provide surgeons useful data to guide their treatment.

The load distribution between the distal radius and ulna varies based on changes in radial length relative to the ulna as a result of surgical osteotomies or distal radius malunion. Earlier studies by Palmer and Werner^{1,26,27,28} investigated the percentage loading by application of a constant force to cadaveric wrists. In a static load sharing study, Palmer and Werner^{27,28} observed when the ulnar length was increased by 2.5 mm, the forearm axial load borne by the distal ulna increased to 42% from 18%. Conversely, when ulnar length was decreased by 2.5 mm, the axial load borne by the ulna decreased to 4%. Greenberg et al²¹ observed a reduction in mean distal ulnar force from 16% to 3% of total wrist load during dynamic motion from 50° of flexion to 50° of extension, 24% to 4% during radial deviation and 18% to 3% during dart throw when a distal metaphyseal osteotomy with an average ulnar shortening of 2.8mm. Herein we evaluated 1mm sequential changes in ulnar length with up to 3mm of lengthening and 4mm of shortening. With regards to absolute loads, we observed a 75%, 50% and 114% reduction in distal ulnar loads during flexion, UD and dart throw at 2 mm of ulnar shortening. Tensile loads were observed in the ulna with a reduction in distal ulnar loads of 108%, 79%, 143% at 3mm of ulnar shortening and at 4mm of shortening, 125%, 107% and 171% decrease in ulnar loads during flexion, ulnar deviation and dart throw motion respectively. However, with regards to percentage of total

compressive bone loads for direct comparison to previous studies, at 2mm of shortening, there was a decrease in distal ulnar loads from 14% to 5% during flexion, from 14% to 9% during UD and from 16% to 0% during dart throw and at 3mm of shortening, there was a decrease to 0%, 4% and 0% during flexion, UD and dart throw respectively (Appendices 2.15 – 2.17). Our results show 2mm of shortening was enough to completely offload the distal ulna during dart throw. Our results differ from Palmer et al²⁸ as they used a static loading protocol with application of arbitrary loads. The use of dynamic loading in our protocol allowed for application of tendon loads that closely mimic *in-vivo* wrist kinematics. With sequential shortening, the tensile loads at the distal ulna were presumably due to decreased tendon loads in the ulnar sided prime movers (ECU and FCU) and additionally, ulnar shortening tensions the TFCC thus placing tension on the distal ulna. Differences from Greenberg et al²¹ may also be attributed to differences in location of ulnar osteotomy, reporting changes in absolute loads versus percentage wrist load, and differences in direction of motion evaluated.

A computational study using two-dimensional rigid body spring model by Horii et al²⁹ observed a decrease in radiolunate load by 45% with 4mm of ulnar lengthening and an increase of 45% with radial shortening. The aforementioned study did not evaluate distal ulnar loading. We noted a 15%, 20% and 24% decrease in distal radial loads with 3mm of ulnar lengthening during flexion, ulnar deviation and the dart throw motions respectively. This however did not reach statistical significance. By lengthening the ulnar beyond 3mm, we may have observed more significant decreases in radial loads, however, further lengthening was limited by the tension in the intact soft tissue envelope. These differences from may be explained by their use of a rigid spring body model which does not differentiate between radial shortening and radial lengthening.

This method does not factor in the soft tissue contributions and effects of dynamic tendon loading on distal forearm loading. We utilized a dynamic motion simulator that models the in-vivo activation of individual muscles using a force position algorithm to generate reproducible wrist motion.³⁰

Conversely, we observed that decreases in distal ulnar loads were more significant when the ulnar was shortened compared to radial lengthening. Tensile loads in the ulna were observed with 3 and 4mm of ulnar shortening versus radial lengthening during flexion, ulnar deviation, and dart throw. We postulate that these observations occur as a result of the greater load transfer through the distal radius and larger surface area of the distal radius, thus, requiring a greater amount of force to lengthen. Also, decreases in tendon loads in the ulnar sided prime movers (ECU and FCU) were more significant with ulnar shortening compared to radial lengthening perhaps also explaining the more significant decreases in ulnar loads with ulnar shortening.

During wrist flexion, we observed an increase in radial loads with each millimeter increase in ulnar length and conversely in the extended wrist position. As discussed in Chapter 2, we observed the same trends with radial shortening. Excessive radial shortening caused a paradoxical increase in distal radial loads (from loads at native length) when the wrist was in extension. When initiating flexion from an extended wrist position, the ulnar sided prime movers exert a greater amount of force to bring the wrist out of the extended position when the radius is relatively short as evidenced by the increased tendon loads observed in the extended wrist positions.

The TFC plays an important role in DRUJ stability and load transmission. In a biomechanical

study with sequential TFC excision, Palmer et al²⁰ observed excision of the central two-thirds of the TFC resulted in a decrease in distal ulnar loads to 13% from 18% and excision of the whole TFC resulted in a decrease in distal ulnar loads to 8% from 18%.²⁰ A subsequent study by the same author confirmed these findings with a decrease in distal ulnar loads to 6% (from 18%) observed when the TFC was excised under static loading conditions.²⁸ Wnorowski et al³¹ observed less dramatic decreases in loads of the distal ulna of 5% (from 21% to 16%) with excision of the TFC.³¹ The aforementioned studies examined the effect of TFC excision on load sharing at the distal radius and ulna. Our study observed a decrease in distal ulnar loads from 14% to 13% of total distal forearm bone load during flexion and UD and a decrease from 16% to 8% during dart throw at native ulnar length after TFC excision. The motion simulator utilized enabled us to dynamically evaluate the role of TFC in load transmission. The TFC's role in load transmission was most evident during dart throw. In this study, we also observed the TFC's role in load sharing was more evident as the ulnar was lengthened when we evaluated percentage load sharing (Appendices 2.15 – 2.17). There was no change in percentage load sharing with ulnar shortening. This presumably is because ulnar shortening in itself significantly offloads the distal ulnar such that with ulnar shortening, the TFC may serve no load bearing function. In this study, at 3mm of ulnar shortening, the distal radius already bore 100% of compressive loads through the distal forearm prior to TFC excision. This trend is similar to the observations by Palmer et al²⁰ where with TFC excision, there was a decrease in distal ulnar loads from 3% to 2% with 2.5mm of shortening and 43% to 26% with 2.5mm of lengthening. In another study by Palmer et al,²⁸ there was a decrease in distal ulnar loads from 4% to 3% with 2.5mm of shortening and 42% to 22% with 2.5mm of lengthening. However, we did not observe the same magnitude of change with ulnar lengthening. At 3mm of lengthening, there was a decrease in

distal ulnar loads from 31% to 25% during flexion, 29% to 24% during ulnar deviation and 27% to 23% during dart throw. The use of a dynamic loading protocol which attempts to simulate physiologic loading may account for these differences. Ferreira et al³² studied the effect of TFCC sectioning on distal ulnar loading in wrists with simulated distal radial malalignment (translation and dorsal angulation) during forearm rotation. Although they observed a decrease of 60% in distal ulnar absolute loads when the TFCC was sectioned, their results did not reach statistical significance. In our study, although there was a trend towards decreased distal ulnar absolute loads of 28%, 25% and 67% compared to the TFC intact condition during flexion, ulnar deviation, and dart throw respectively when the TFC was excised, this did not reach statistical significance. Differences from Ferreria et al³² may be explained by differences in the motions evaluated (forearm rotation versus wrist motion) and protocol of soft tissue sectioning (TFCC was divided by detachment of ulnar attachment whereas we only removed the TFC). Also, variation in loads during forearm rotation differ from variations during flexion/extension and RUD.²² Decreases in distal ulnar loading observed in this study may be due to that fact that excising the TFC releases the constraining effect of the TFC on DRUJ contact force thus causing a resultant reduction in distal ulnar loading as forces across the DRUJ relax considerably.³²

As discussed in Chapter 2 section 2.5, limitations to this study exist. First, we may be underpowered with our sample size to show a statistical difference and we may have seen more significant differences on the effect of TFC excision on distal forearm loading with a larger sample size. We however achieved statistical significance for most comparisons thus we were evidently powered for most of the comparisons of interest. Second, biologic remodeling of the soft tissues in response to bone length changes are likely to occur over time and cannot be accounted for in a biomechanical study. Third, range of motion was limited in some wrists and as

a result, we excluded certain specimens from the data analysis. Fourth, we did not account for the force vector of pronator quadratus across the DRUJ and its role in distal forearm load sharing. Fifth, the forearms were mounted vertically with gravity assistance in flexion past neutral. Consequently, distal forearm loading may vary when forearms are positioned in the horizontal plane with different muscle groups working against gravity. In addition, investigating extension, radial deviation and reverse dart motion may have shown different loading patterns than flexion, ulnar deviation, and dart throw. Lastly, in this study, we statistically analyzed absolute loads, whereas previous studies have focused on percentage load sharing between the radius and the ulna making direct comparisons challenging.

It is important to recognize the strengths of this study. A repeated measures experimental design was employed to enhance comparisons within each arm and hence statistical power. This study advances previous research that examined distal forearm loading by application of static loads and further clarifies the effect of ulnar length change on distal forearm loading during simulated dynamic wrist motion. The custom-designed implant with load cell were designed to be low profile without compromising implant integrity. This minimized soft-tissue dissection and excision during implant insertion. As a result of this, we took into account the effect of an intact soft tissue envelope on distal forearm bone loading. Moreover, the use of a highly accurate and reliable optical tracking system enabled us to track joint angles to provide precise feedback to the motion simulator during motion. Despite the challenges of comparing absolute loads to percentage loads in previous studies, reporting percentage load sharing between the radius and ulna may not accurately reflect the changes in axial loads in the distal radius and ulna. Although actual axial loads may change significantly during radial length change, percentage loading may remain unchanged due to symmetric changes in distal radial and ulnar loads. Thus, absolute

loads are a true reflection of the load changes at the distal radius and ulna.

To our knowledge, the effects of sequential distal ulnar length change during simulated dynamic motion studied has not been reported in the literature to date thus giving new insight into distal forearm axial loading. Ulnar length change from 3mm of lengthening to 4 mm of shortening did not cause significant changes in radial loads as it did ulnar loads. Meanwhile, changes in ulnar loads during length changes followed a more predictable pattern. For each millimeter interval change in ulnar length, when the TFCC was excised, significant decreases in distal radial loads were observed and to a lesser extent, a decrease in ulnar loads.

In conclusion, although ulnar length changes do not cause significant changes in radial loads during simulated active wrist motion, ulnar loads were predictably altered. To our knowledge, this is the first study demonstrating tensile loads in the distal ulna with ulnar shortening beyond 2mm. The role of the TFC in load sharing at the distal radius and ulna was evident with ulnar lengthening beyond neutral.

3.6 REFERENCES

1. Palmer AK. Triangular fibrocartilage complex lesions: A classification. *J Hand Surg Am.* 1989;14(4):594-606. doi:10.1016/0363-5023(89)90174-3.
2. Nishiwaki M, Nakamura T, Nagura T, Toyama Y, Ikegami H. Ulnar-Shortening Effect on Distal Radioulnar Joint Pressure: A Biomechanical Study. *J Hand Surg Am.* 2008;33(2):198-205. doi:10.1016/j.jhsa.2007.11.024.
3. Friedman SL, Palmer AK. The ulnar impaction syndrome. *Hand Clin.* 1991;7(2):295-310.
4. Tomaino MM. Ulnar impaction syndrome in the ulnar negative and neutral wrist: Diagnosis and pathoanatomy. *J Hand Surg Eur Vol.* 1998;23(6):754-757. doi:10.1016/S0266-7681(98)80090-9.
5. Friedman SL, Palmer AK, Short WH, Mark Levinsohn E, Halperin LS. The change in ulnar variance with grip. *J Hand Surg Am.* 1993;18(4):713-716. doi:10.1016/0363-5023(93)90325-W.
6. Jung JM, Baek GH, Kim JH, Lee YH, Chung MS. Changes in ulnar variance in relation to forearm rotation and grip. *J Bone Joint Surg Br.* 2001.
7. Tomaino MM. The importance of the pronated grip x-ray view in evaluating ulnar variance. *J Hand Surg Am.* 2000;25(2):352-357. doi:10.1053/jhsu.2000.jhsu25a0352.
8. Feldon P, Terrono AL, Belsky MR. Wafer distal ulna resection for triangular fibrocartilage tears and/or ulna impaction syndrome. *J Hand Surg Am.* 1992;17(4):731-737. doi:10.1016/0363-5023(92)90325-J.
9. Nakamura R, Horii E, Imaeda T, Nakao E, Kato H, Watanabe K. The ulnocarpal stress test in the diagnosis of ulnar-sided wrist pain. *J Hand Surg - Br Vol.* 1997;22(6):719-723.
10. Bowers WH. Distal radioulnar joint arthroplasty: the hemiresection-interposition

- technique. *J Hand Surg Am*. 1985;10(2):169-178.
11. Markolf KL, Tejwani SG, Benhaim P. Effects of wafer resection and hemiresection from the distal ulna on load-sharing at the wrist: a cadaveric study. *J Hand Surg [Am]*. 2005;30(2):351-358. doi:10.1016/j.jhsa.2004.11.013.
 12. Fulton C, Grewal R, Faber KJ, Roth J, Gan BS. Outcome analysis of ulnar shortening osteotomy for ulnar impaction syndrome. *Can J Plast Surg*. 2012;20(1).
 13. Kim BS, Song HS. A comparison of Ulnar shortening Osteotomy alone versus combined Arthroscopic Triangular Fibrocartilage complex Debridement and Ulnar Shortening Osteotomy for Ulnar Impaction Syndrome. *Clin Orthop Surg*. 2011;3(3):184-190. doi:10.4055/cios.2011.3.3.184.
 14. Tomaino MM, Weiser RW. Combined arthroscopic TFCC debridement and wafer resection of the distal ulna in wrists with triangular fibrocartilage complex tears and positive ulnar variance. *J Hand Surg Am*. 2001;26(6):1047-1052. doi:10.1053/jhsu.2001.28757.
 15. Doherty C, Gan BS, Grewal R. Ulnar Shortening Osteotomy for Ulnar Impaction Syndrome. *J Wrist Surg*. 2014;3(2):85-90. doi:10.1055/s-0034-1372519.
 16. Baek GH, Hyuk JL, Hyun SG, et al. Long-term Outcomes of Ulnar Shortening Osteotomy for Idiopathic Ulnar Impaction Syndrome: At Least 5-Years Follow-up. *Clin Orthop Surg*. 2011;3(4):295-301. doi:10.4055/cios.2011.3.4.295.
 17. Minami A, Kato H. Ulnar shortening for triangular fibrocartilage complex tears associated with ulnar positive variance. *J Hand Surg Am*. 1998;23(5):904-908. doi:10.1016/S0363-5023(98)80171-8.
 18. Palmer AK, Werner FW, Eng MM. The triangular fibrocartilage complex of the wrist-

- Anatomy and function. *J Hand Surg Am.* 1981;6(2):153-162. doi:10.1016/S0363-5023(81)80170-0.
19. Rabinowitz RS, Light TR, Havey RM, et al. The role of the interosseous membrane and triangular fibrocartilage complex in forearm stability. *J Hand Surg Am.* 1994;19(3):385-393. doi:10.1016/0363-5023(94)90050-7.
 20. Palmer AK, Werner FW, Glisson RR, Murphy DJ. Partial excision of the triangular fibrocartilage complex. *J Hand Surg Am.* 1988;13(3):391-394. doi:10.1016/S0363-5023(88)80015-7.
 21. Greenberg JA, Werner FW, Smith JM. Biomechanical analysis of the distal metaphyseal ulnar shortening osteotomy. *J Hand Surg Am.* 2013;38(10):1919-1924. doi:10.1016/j.jhsa.2013.06.038.
 22. Harley BJ, Pereria ML, Werner FW, Kinney DA, Sutton LG. Force variations in the distal radius and ulna: Effect of ulnar variance and forearm motion. *J Hand Surg Am.* 2015;40(2):211-216. doi:10.1016/j.jhsa.2014.10.001.
 23. Werner FW, Palmer AK, Fortino MD, Short WH. Force transmission through the distal ulna : Effect of ulnar variance , lunate fossa angulation , and radial and palmar tilt of the distal radius. *J Hand Surg Am.* 1992.
 24. Certus O. Research-Grade Motion Capture. Digital N Inc, ed. *Manuf Manual.* 2011:1-8.
 25. Gordon KD, Dunning CE, Johnson JA, King GJW. Influence of the Pronator Quadratus and Supinator Muscle Load on DRUJ Stability. *J Hand Surg Am.* 2003;28(6):943-950. doi:10.1016/S0363-5023(03)00487-8.
 26. Palmer a K, Glisson RR, Werner FW. Relationship between ulnar variance and triangular fibrocartilage complex thickness. *J Hand Surg Am.* 1984;9(5):681-682.

doi:10.1016/S0363-5023(84)80013-1.

27. Werner FW, Glisson RR, Murphy DJ, Palmer AK. Force transmission through the distal radioulnar carpal joint: effect of ulnar lengthening and shortening. *Handchir Mikrochir Plast Chir.* 1986;18(5):304-308.
28. Palmer AK, Werner FW. Biomechanics of the Distal Radioulnar Joint. *Clin Orthop Relat Res.* 1984;187:26-35.
29. Horii E, Garcia-Elias M, Bishop AT, Cooney WP, Linscheid RL, Chao EY. Effect on force transmission across the carpus in procedures used to treat Kienbock's disease. *J Hand Surg Am.* 1990;15(3):393-400.
30. Iglesias D, Lockhart J, Johnson J, King GJW. Development of an In-Vitro Passive and Active Motion Simulator for the Investigation of Wrist Function and Kinematics. 2015.
31. Wnorowski DC, Palmer AK, Werner FW, Fortino MD. Anatomic and biomechanical analysis of the arthroscopic wafer procedure. *Arthrosc J Arthrosc Relat Surg.* 1992;8(2):204-212. doi:10.1016/0749-8063(92)90038-D.
32. Ferreira LM, Greeley GS, Johnson JA, King GJW. Load transfer at the distal ulna following simulated distal radius fracture malalignment. *J Hand Surg Am.* 2015;40(2):217-223. doi:10.1016/j.jhsa.2014.10.012.

Chapter 4

4. CONCLUSIONS AND FUTURE DIRECTIONS

4.1 OVERVIEW

This chapter reviews the initial objectives and hypotheses presented in Chapter 1 and key conclusions drawn from Chapters 2 and 3. Finally, an outline for future directions and clinical research are also presented.

4.2 OBJECTIVES AND HYPOTHESES

The effects of distal radius and ulna length changes on load transfer between the radius and ulna has been previously reported under static loading conditions, however, this relationship is poorly understood during simulated dynamic wrist motion that attempts to simulate *in-vivo* wrist kinematics. To clarify this relationship, this thesis quantified the loading of the distal radius and ulna under simulated dynamic wrist motion during radial and ulnar length change with and without the TFC intact. An understanding of these relationships will help surgeons develop a biomechanical rationale for clinical decisions related to management of Kienbock's disease, ulnocarpal impaction syndrome, distal radius and ulnar malunions and will have implications in the improvement of wrist implant design.

Objectives

1. To determine the relationship between distal forearm loading at the wrist and changes in radial length during simulated dynamic wrist motion.
2. To determine the relationship between native ulnar variance and distal forearm

loading.

3. To determine the relationship between distal forearm loading at the wrist and changes in ulnar length during simulated dynamic wrist motion.
4. To determine the relationship between the TFC integrity and the force transmission through the distal ulna with ulnar length change.

4.3 EFFECT OF RADIAL LENGTH CHANGE ON DISTAL FOREARM LOADING DURING SIMULATED WRIST MOTION

Our hypotheses were that (1) there will be no relationship between native ulnar variance and distal forearm loading, (2) distal radial loads will increase and distal ulnar loads will decrease with radial lengthening and vice versa and (3) there will be variation in loads at different wrist positions during simulated dynamic wrist motion.

In this study, there was no correlation between native ulnar variance and distal radial and ulnar loading during simulated dynamic motion. The load bearing characteristics and compensatory thickness of the TFC likely accommodates axial load differences.

Our study also confirmed that with an increase or decrease in radial length, there was an increase or decrease in radial loads respectively. However, with sequential shortening in extension, there was a corresponding increase in radial loads and with sequential lengthening, there was a corresponding decrease in radial loads. These changes were due to the increasing tendon loads seen in the ulnar sided prime movers (ECU and FCU) with each millimeter of radial shortening and vice versa with lengthening. Excessive shortening causes a paradoxical increase in distal radial loads (from loads at native

length) when the wrist is in extension. Based on this paradoxical phenomenon, caution should be exercised to avoid excessive radial shortening osteotomies for Kienbock's disease to prevent increases in distal radius loading during wrist extension.

We observed peak radial loads at the initiation of dart throw and radial deviation at native radial length and for each millimeter change in radial height. Peak ulnar loads were observed in wrist extension, ulnar deviation and terminal dart throw. These changes can be attributed to the force vector and tendon loading changes within the radiocarpal joint during dynamic motion: in radial deviation, peak tendon loads were observed in radial sided prime movers (ECRL and FCU) thus causing a peak in radial loads and in ulnar deviation, peak tendon loads were observed in the ulnar sided prime movers (ECU and FCU) thus causing a peak in ulnar loads.

Although changes in distal ulnar loads occurred in a more predictable fashion with radial length change, this study suggests variation in distal radial loads with length change is more complex than previously described. Excessive radial shortening causes an increase in radial loads in extension and thus caution should be exercised to minimize radial shortening when performing osteotomies for Kienbock's disease. Good clinical outcomes have been reported with 2mm of radial shortening. Thus, shortening by 2mm may be adequate to offload the distal radius.

4.4 THE EFFECT OF ULNAR LENGTH CHANGE AND TFC INTEGRITY ON DISTAL FOREARM LOADING DURING SIMULATED WRIST MOTION

In this study, our hypotheses were that (1) distal radial loads will decrease and distal

ulnar loads will increase with ulnar lengthening and vice versa, (2) excision of TFC during ulnar length change will decrease load transmission through the distal ulnar compared to the TFC intact state and (3) there will be positional variation in axial loads with length change. 3) there will be variation in loads at different wrist positions during simulated dynamic wrist motion.

This study gives new insight into the effect of ulnar length change on distal forearm loading during simulated motion. Ulnar length change did not cause significant changes in radial loads as it did with ulnar loads. When initiating flexion from an extended wrist position, the ulnar sided prime movers exert a greater amount of force to bring the wrist out of the extended position when the radius is relatively short as evident by the sequential increases in tendon loads observed in the extended wrist positions with each millimeter of ulnar lengthening.

Changes in distal ulnar loads with ulnar length changes occurred in a predictable fashion with tensile loads in the ulna observed with ulnar shortening beyond 2mm. Ulnar shortening tensions the TFCC and decreases tendon loads in the ECU and FCU to achieve motion both of which account for the sequential decreases in distal ulnar loads thus placing tension on the distal ulna.

For all ulnar length change intervals evaluated, when the TFC was excised, significant decreases in distal radial absolute loads were observed and to a lesser extent, decreases in ulnar loads compared to the TFC intact state. Excising the TFC releases the constraining effect of the TFC on DRUJ contact force thus causing a resultant reduction in distal forearm loading. The role of the TFC in load sharing at the distal radius and ulnar had a

noticeable effect during ulnar lengthening when percentage load sharing was evaluated. We did not observe changes in load sharing with ulnar shortening as shortening in itself significantly offloaded the distal ulnar with 100% of the compressive loads borne by the distal radius with 3 mm of ulnar shortening.

We also observed more significant decreases in radial load with radial shortening versus ulnar lengthening. With radial shortening, we observed a decrease in summed radial loads of 13%, 24%, 29% and 37% at 1mm, 2mm, 3mm and 4mm respectively and a decrease in summed radial loads of 10%, 11% and 20% at 1mm, 2mm and 3mm of ulnar lengthening respectively (Appendices 2.4 and 2.8) during dynamic motion. This study demonstrated radial shortening is more effective in reducing radial loads over ulnar lengthening.

Armistead et al¹ performed ulnar lengthening osteotomies in 20 patients with an average native ulnar variance of 3.1mm (range 0 to -8mm). The ulnar was lengthened to neutral variance. In patients with neutral ulnar variance, the ulnar was lengthened by 2mm with satisfactory clinical results. We observed a reduction in radial loads of 11% at 2mm of ulnar lengthening, however, 2mm of radial shortening produced 24% decrease in radial loads. From a biomechanical standpoint, shortening of radius produces more dramatic decreases in load and may be preferred over ulnar lengthening as a treatment for Kienbock's disease; reducing DRUJ problems by avoiding excessive changes in variance. Changes in variance of more than 4 mm has been shown to cause peak pressures at the DRUJ.² Although ulnar lengthening as a joint leveling procedure is a treatment option for Kienbock's disease,^{1,3} ulnar lengthening has been shown to have a nonunion rate of 15%¹ making it the less popular option over radial shortening osteotomies; furthermore in this biomechanical study we have shown it to be less effective.

In summary, this study suggests that biomechanically, radial shortening is a more effective form of treatment in Kienbock's disease. Ulnar shortening beyond 2mm during distal ulnar arthroplasties places tension on the distal ulna which can result in tensile failure of the implant.

4.5 FUTURE DIRECTIONS

The use of a motion simulator to investigate wrist biomechanics shows great promise. Current understanding of wrist biomechanics is based on static loading studies which do not represent *in-vivo* conditions. As we only examined the effects of radial and ulnar shortening on axial loads, studies on the effects of multiplanar deformities (translation, angulation and shortening) on rotational and bending loads in addition to axial loads can be readily performed under dynamic loading conditions. The effect of extension, radial deviation, reverse dart and forearm rotation on axial loads remain to be clarified as well as the effect of forearm position (horizontal vs vertical orientations) on these loads. A wide range of biomechanical studies can be performed to investigate the effects of multiplanar deformity on distal radial and ulna kinematics. Also, the effects of various surgical reconstructive techniques and wrist arthroplasty on wrist kinematics and biomechanics can be investigated under simulated dynamic conditions.

4.6 REFERENCES

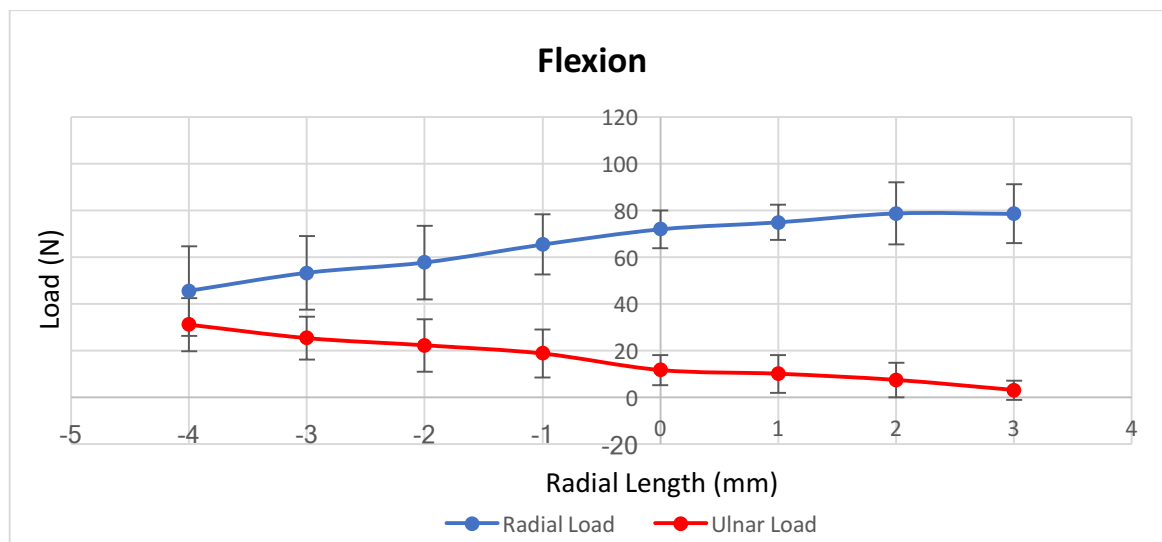
1. Armistead RB, Linscheid RL, Dobyns JH, Beckenbaugh RD. Ulnar lengthening in the treatment of Kienbock's disease. *J Bone Jt Surg Am.* 1982;64(2):170-178.
2. Nishiwaki M, Nakamura T, Nagura T, Toyama Y, Ikegami H. Ulnar-Shortening Effect on Distal Radioulnar Joint Pressure: A Biomechanical Study. *J Hand Surg Am.* 2008;33(2):198-205. doi:10.1016/j.jhsa.2007.11.024.
3. Kawoosa AA, Dhar SA, Mir MR, Butt MF. Distraction osteogenesis for ulnar lengthening in Kienbock's disease. *Int Orthop.* 2007;31(3):339-344. doi:10.1007/s00264-006-0181-0.

APPENDICES

Appendix 1 Glossary of Terms

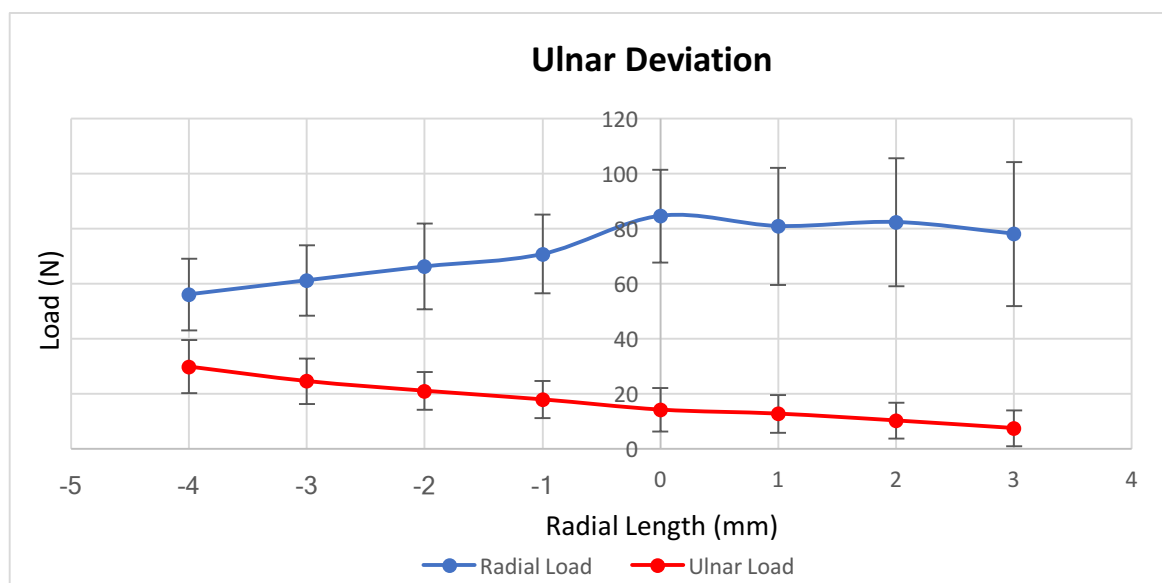
Actuators	Machine component/mechanical device responsible for controlling a system by converting energy into mechanical motion
Axial load	Load applied along the primary/central axis of the bony shaft
Biomechanics	The study of mechanics of a living body, especially of the forces exerted by the musculoskeletal system
Degree of freedom	Number of independent motions
Dynamic loading	Exertion of varying amount of force to achieve a desired motion
Force vector	Having both magnitude and direction
Hydraulic	Operated, moved or effected by the pressure transmitted when fluid is forced through a confined space under pressure
Kinematics	Properties of motion of an object without reference to forces that result in motion
Minimum tone load	Least amount of load required to provide resistance
Motion Simulator	Device that reproduces <i>in-vivo</i> wrist and forearm motion
Newton	SI unit of force
Optical trackers	Monitoring a defined measurement space using two or more cameras
Pneumatic	Operated by gas or pressurized air
Servomotor	An actuator that allows for precise control of an object's velocity
Static loading	Exerting a constant amount of force without causing motion

Appendix 2



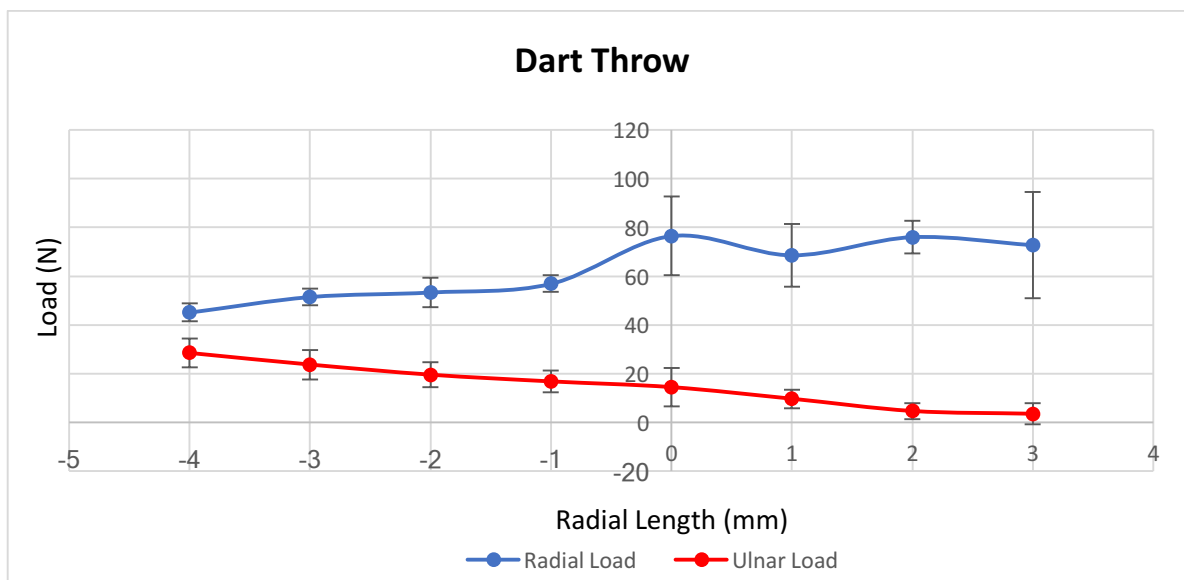
Appendix 2. 1 Graph showing radial and ulnar loads with radial length change during flexion (Mean \pm SD).

With an increase or decrease in radial length, there was an increase or decrease in radial loads respectively ($p < 0.001$). For each millimeter of radial length increase or decrease, there was a corresponding decrease or increase in ulnar loading respectively ($p < 0.001$).



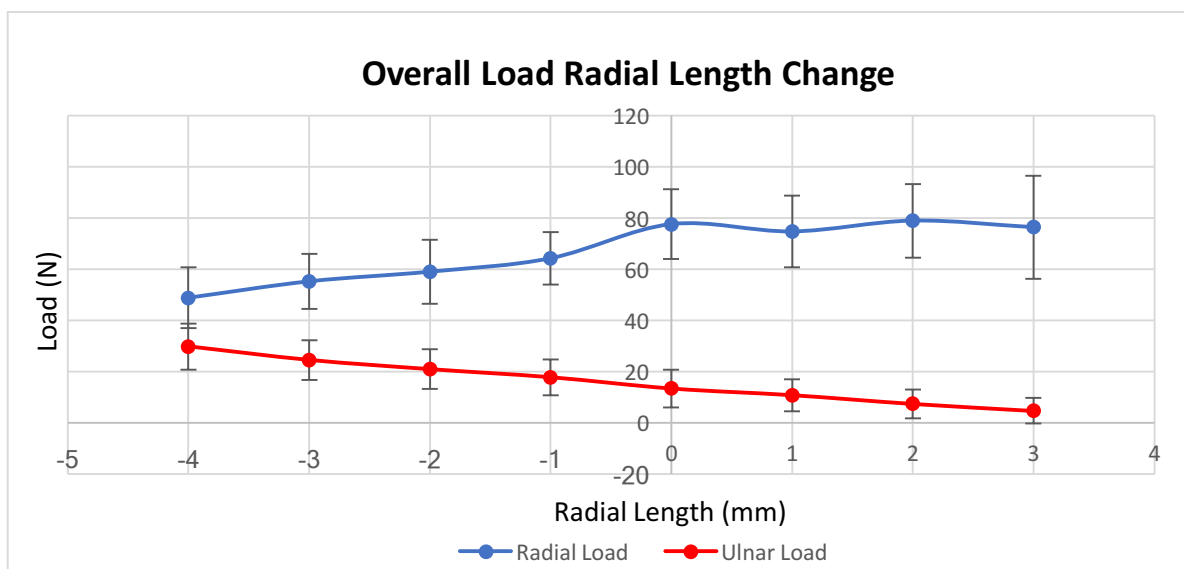
Appendix 2. 2 Graph showing radial and ulnar loads with radial length change during ulnar deviation (Mean \pm SD).

Overall, there was a significant relationship between radial loads and radial length change for each millimeter of length change evaluated ($p < 0.001$). Peak radial loads are seen at native length. For each millimeter of radial length increase or decrease, there was a corresponding decrease or increase in distal ulnar loading respectively ($p = 0.037$).



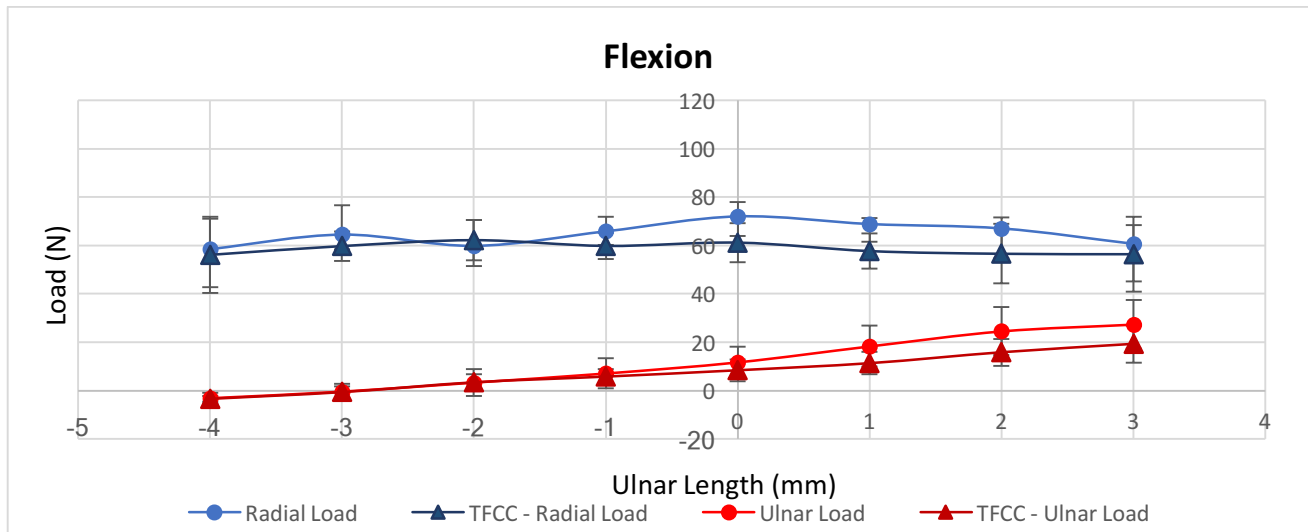
Appendix 2. 3 Graph showing radial and ulnar loads with radial length change during dart throw (Mean \pm SD).

Changes in radial loads during radial height change did not reach statistical significance ($p=0.243$). An inverse relationship between ulnar loads and radial length for each millimeter of length change evaluated was observed ($p < 0.001$). For each millimeter of radial length increase or decrease, there was a corresponding decrease or increase in distal ulnar loading respectively.



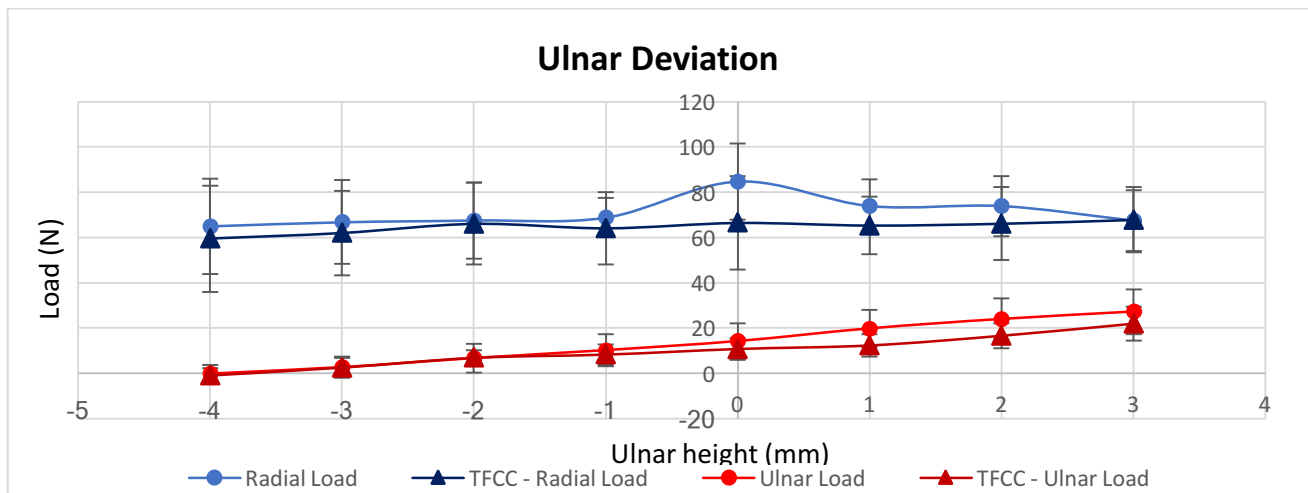
Appendix 2. 4 Graph showing radial and ulnar loads with radial length change during dynamic wrist motion (Mean \pm SD).

Radial lengthening did not produce significant load changes however, each millimeter of radial shortening caused a step wise decrease in radial loads (13%, 24%, 29% and 37% at 1mm, 2mm, 3mm and 4mm of shortening respectively). For each millimeter of radial length increase or decrease, there was a corresponding decrease or increase in distal ulnar loading respectively.



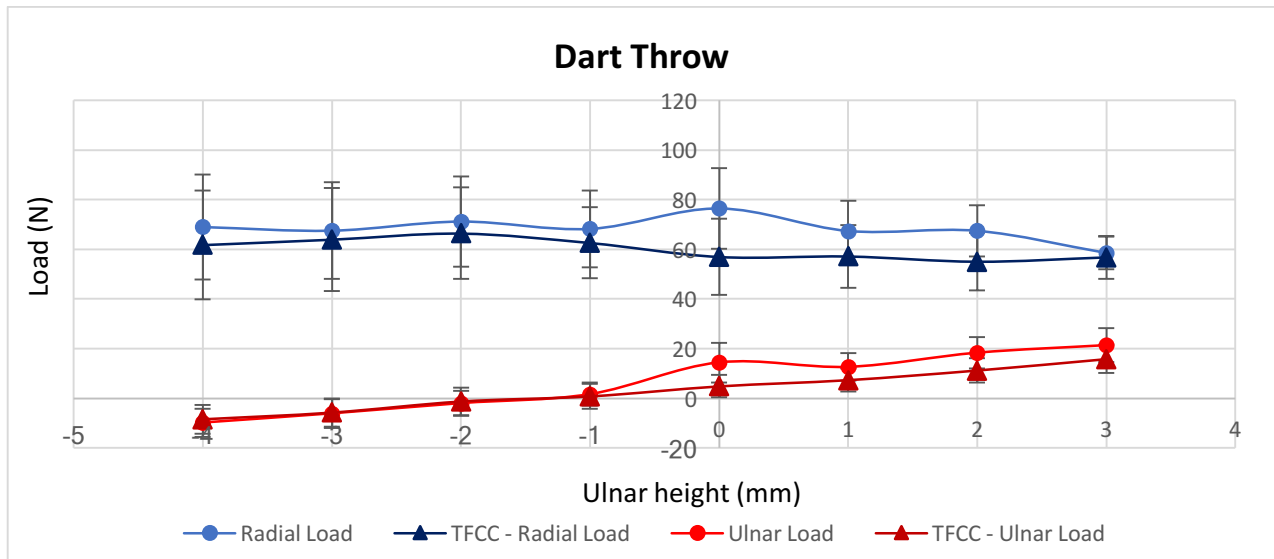
Appendix 2. 5 Graph showing radial and ulnar loads with ulnar length change during flexion with and without the TFC intact (Mean \pm SD).

There was no significant change in radial loads with ulnar length change ($p = 0.324$). With ulnar lengthening, there was an increase in ulnar loads and vice versa ($p < 0.001$). There was a statistically significant decrease in radial loads ($p = 0.027$) when the TFC was excised. There was a trend towards decreased distal ulnar loads when the TFC was excised however, this did not reach statistical significance ($p = 0.342$).



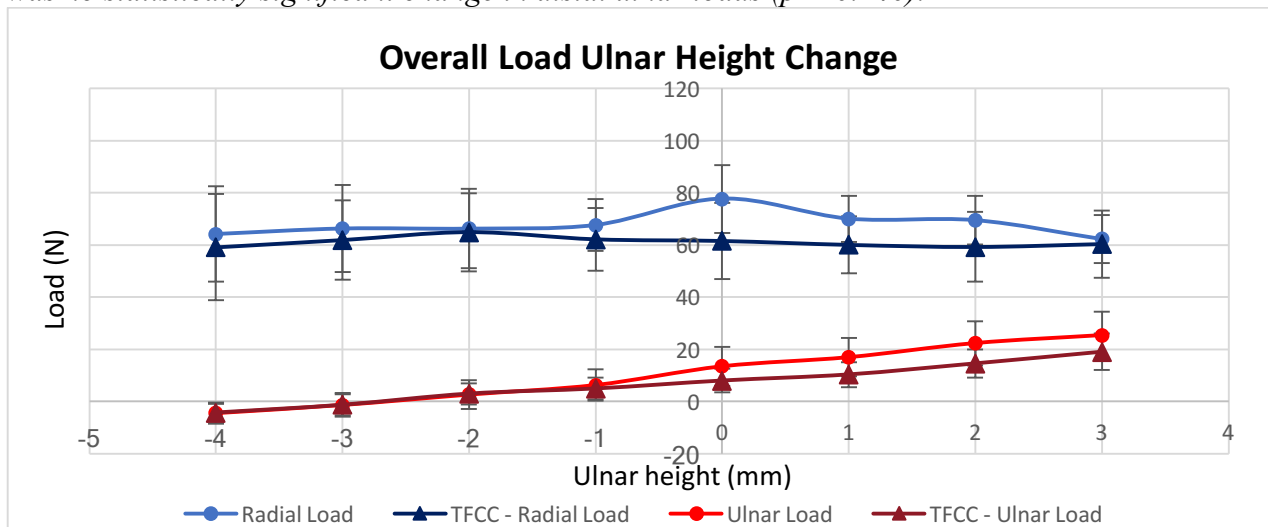
Appendix 2. 6 Graph showing radial and ulnar loads with radial length change during ulnar deviation with and without the TFC intact (Mean \pm SD).

Changes in radial loads with ulnar length change was statistically significant ($p = 0.008$) with a decrease in radial loads with both ulnar lengthening and shortening. with ulnar lengthening, there was an increase in ulnar loads and with shortening, a decrease ($p < 0.001$). There was a trend towards decreased distal ulnar and radial loads when the TFC was excised however, this did not reach statistical significance ($p = 0.249$ and $p = 0.109$ respectively).



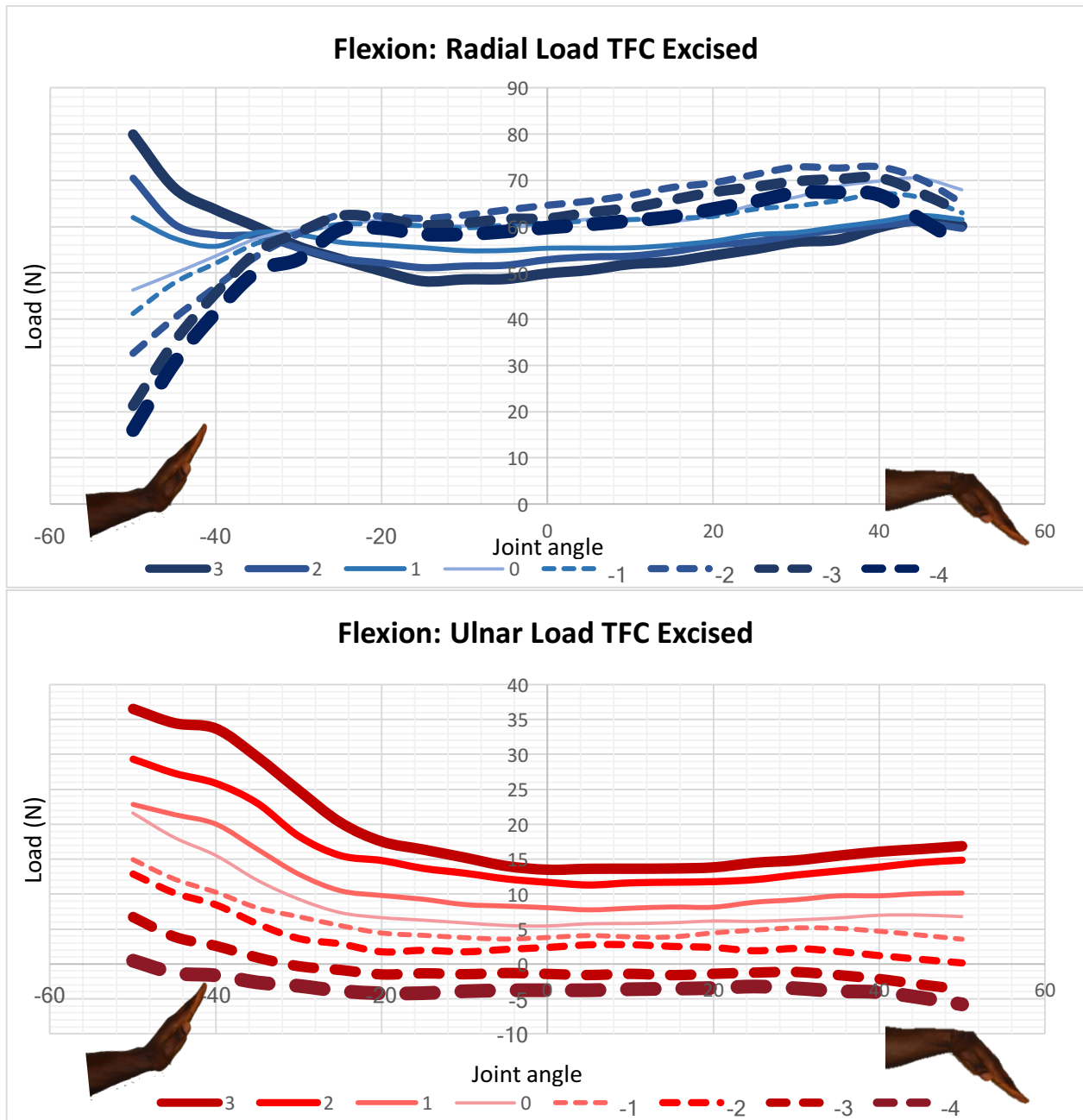
Appendix 2. 7 Graph showing radial and ulnar loads with radial length change during dart throw with and without the TFC intact (Mean \pm SD).

There was no significant change in radial loads with ulnar length change ($p = 0.232$). Changes in ulnar loads with ulnar length change were statistically significant ($p < 0.001$): with ulnar lengthening, there was an increase in ulnar loads and with shortening, a decrease in ulnar loads. There was a decrease in mean radial loads (0.037) when the TFC was excised. However, there was no statistically significant change in distal ulnar loads ($p = 0.240$).



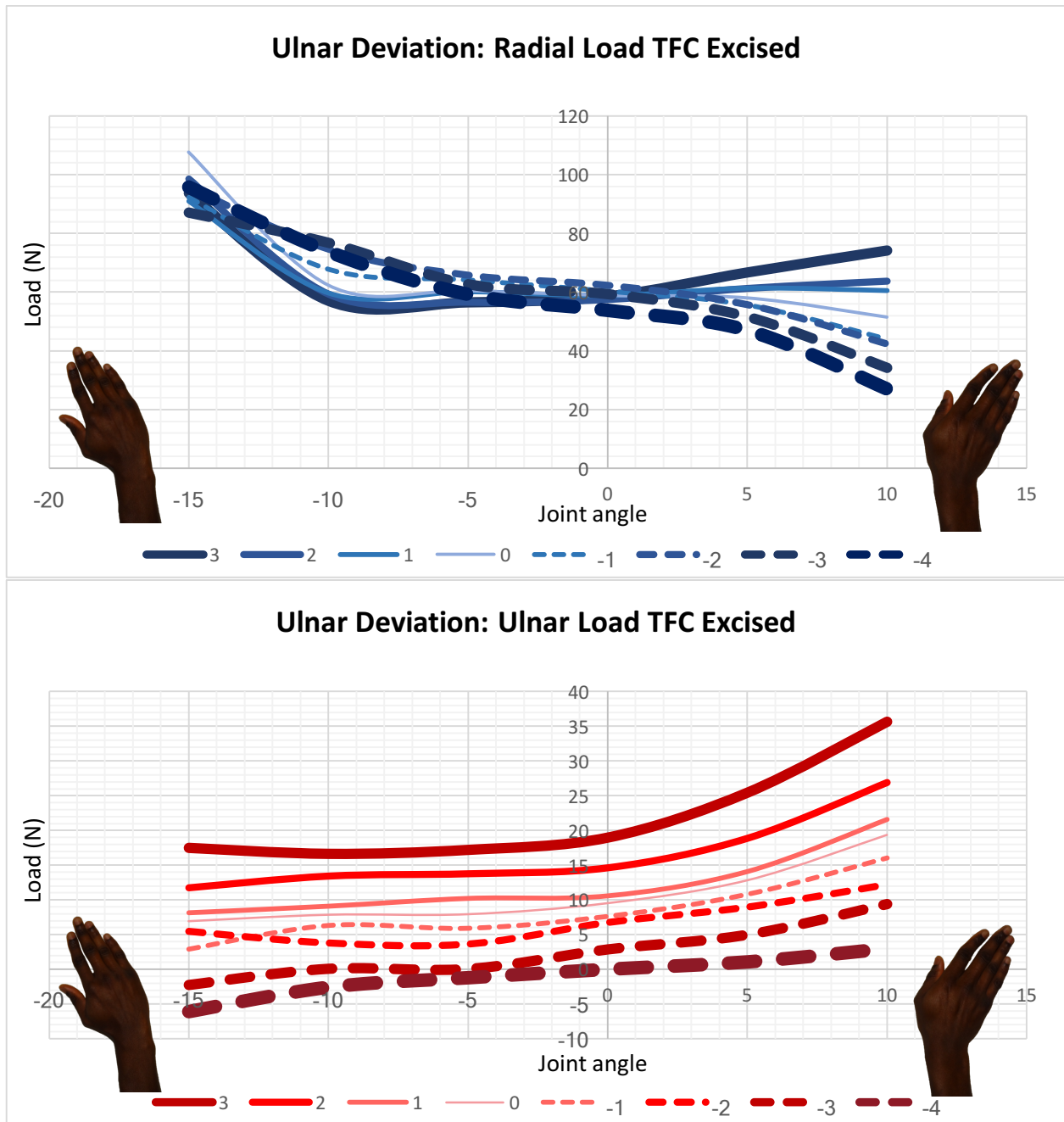
Appendix 2. 8 Graph showing radial and ulnar loads with radial length change during dynamic wrist motion with and without the TFC intact (Mean \pm SD).

No significant change in radial load with radial length change during simulated active motion. For each millimeter of radial length increase or decrease, there was a corresponding decrease or increase in distal ulnar loading respectively. There was a decrease in radial and ulnar loads with TFC excision.



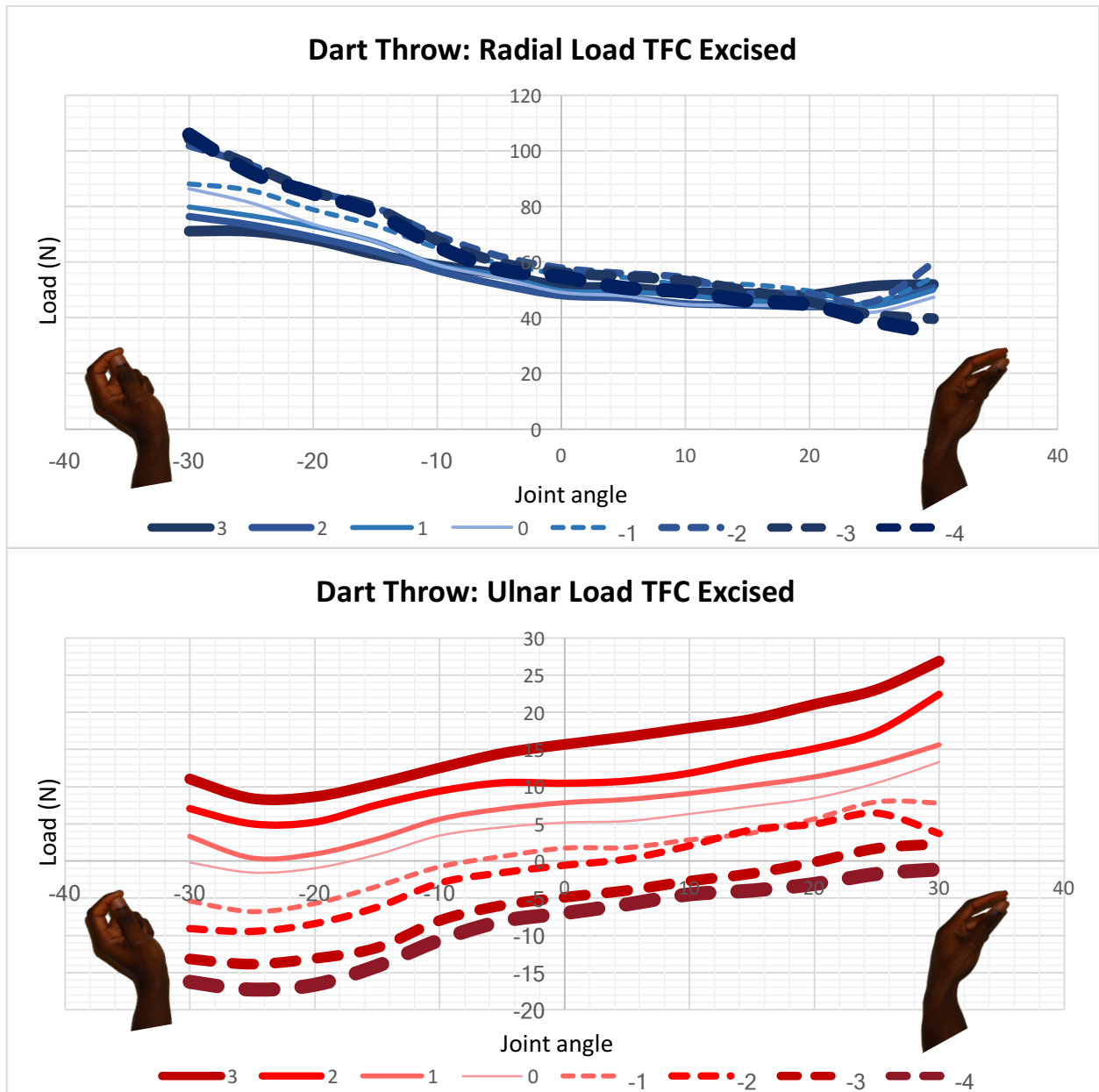
Appendix 2. 9 Radial and ulnar loads during wrist flexion with the TFC excised n = 8.

- a. Graph showing radial loads at 3mm, 2mm and 1mm of ulnar lengthening (3, 2, 1), native length (0) and 1mm, 2mm, 3mm and 4mm of ulnar shortening (-1, -2, -3, -4) during wrist flexion with the TFC excised. Flexion motion started with the wrist in 50° of extension (-50) to 50° of flexion (50).
- b. Graph showing ulnar loads at 3mm, 2mm and 1mm of ulnar lengthening (3, 2, 1), native length (0) and 1mm, 2mm, 3mm and 4mm of ulnar shortening (-1, -2, -3, -4) during wrist flexion with the TFC excised. Flexion motion started with the wrist in 50° of extension (-50) to 50° of flexion (50).



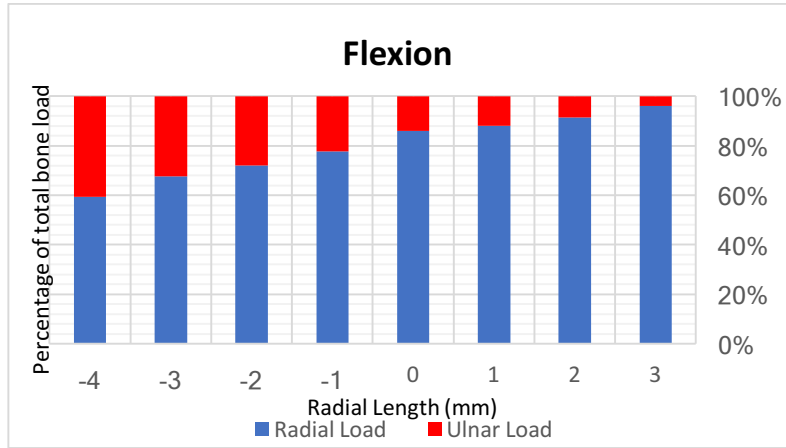
Appendix 2. 10 Radial and ulnar loads during ulnar deviation with the TFC excised n = 7

- Graph showing radial loads at 3mm, 2mm and 1mm of ulnar lengthening (3, 2, 1), native length (0) and 1mm, 2mm, 3mm and 4mm of ulnar shortening (-1, -2, -3, -4) during wrist ulnar deviation with the TFC excised. Ulnar deviation started with the wrist in 15° of radial deviation (-15) to 10° of ulnar deviation (10).
- Graph showing ulnar loads at 3mm, 2mm and 1mm of ulnar lengthening (3, 2, 1), native length (0) and 1mm, 2mm, 3mm and 4mm of ulnar shortening (-1, -2, -3, -4) during wrist flexion with the TFC excised. Ulnar deviation started with the wrist in 15° of radial deviation (-15) to 10° of ulnar deviation (10).

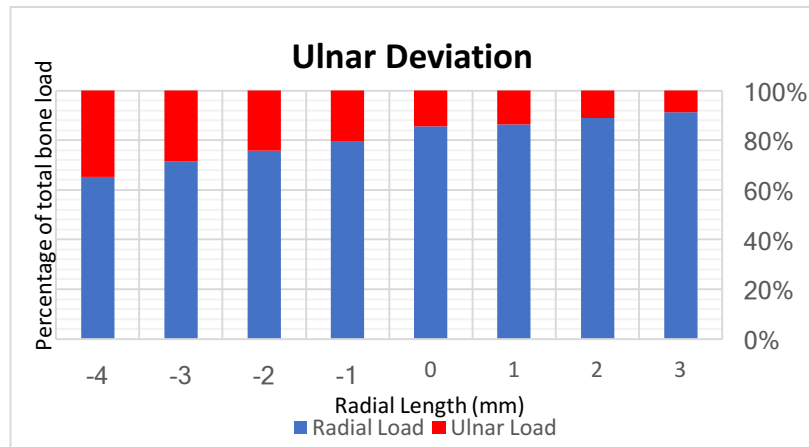


Appendix 2. 11 Radial and ulnar loads during dart throw with the TFC excised n = 6.

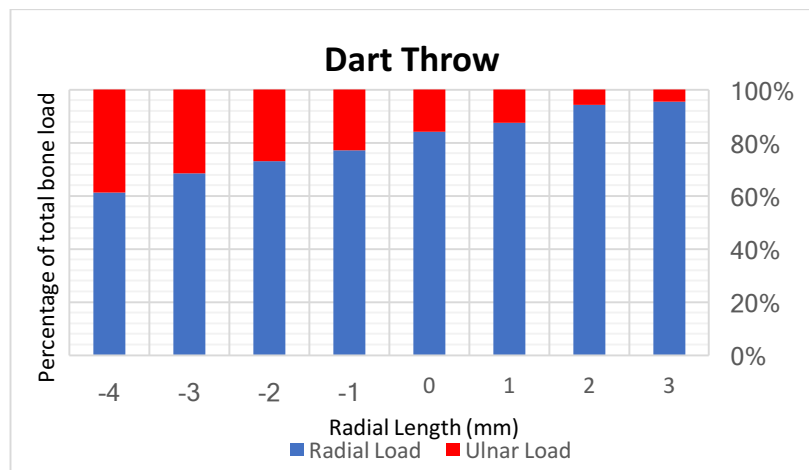
- a. Graph showing radial loads at 3mm, 2mm and 1mm of ulnar lengthening (3, 2, 1), native length (0) and 1mm, 2mm, 3mm and 4mm of ulnar shortening (-1, -2, -3, -4) during dart throw with the TFC excised. Dart motion started with the wrist in 30° of extension and 10° of radial deviation (-30, -10) to 30° of flexion and 10° or ulnar deviation (30, 10).
- b. Graph showing ulnar loads at 3mm, 2mm and 1mm of ulnar lengthening (3, 2, 1), native length (0) and 1mm, 2mm, 3mm and 4mm of ulnar shortening (-1, -2, -3, -4) during dart throw with the TFC excised. Dart motion started with the wrist in 30° of extension and 10° of radial deviation (-30, -10) to 30° of flexion and 10° or ulnar deviation (30, 10).



Appendix 2. 12 Percentage load sharing with radial length change during flexion expressed as a percentage of forearm compressive loads

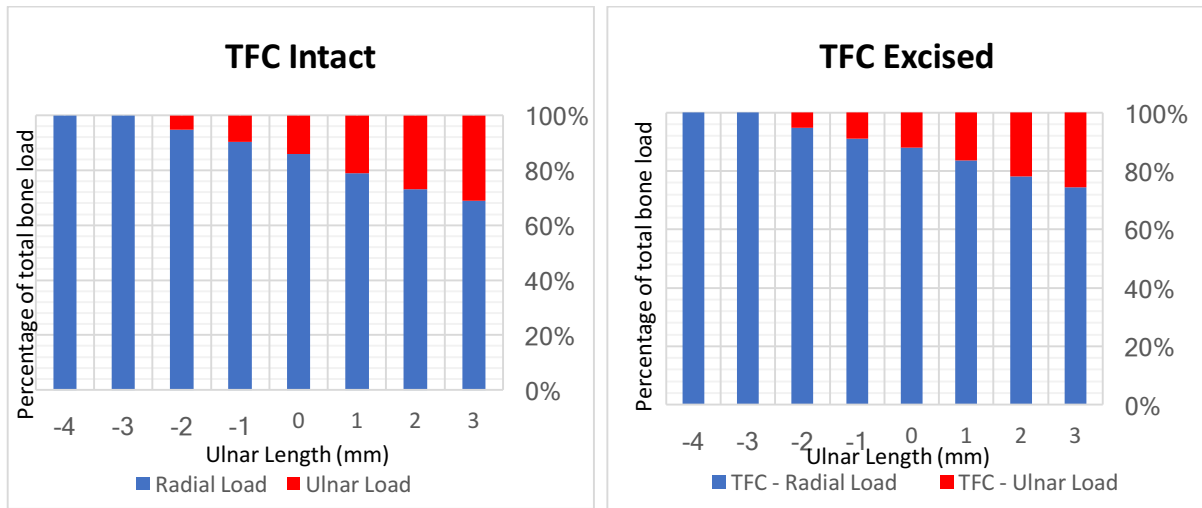


Appendix 2. 13 Percentage load sharing with radial length change during ulnar deviation expressed as a percentage of forearm compressive loads



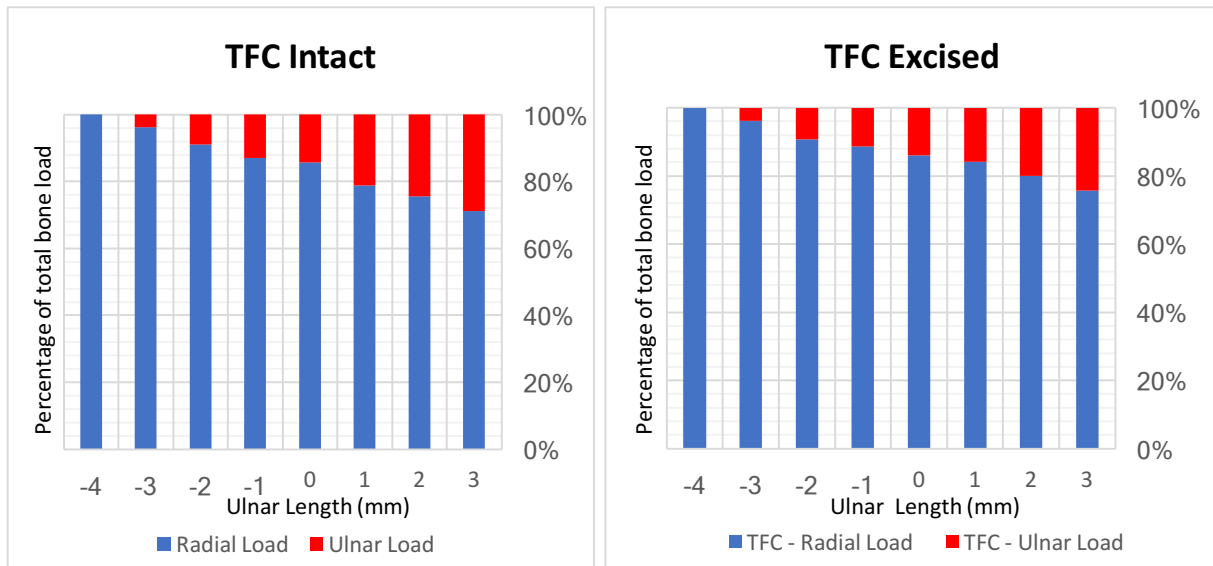
Appendix 2. 14 Percentage load sharing with radial length change during ulnar deviation expressed as a percentage of forearm compressive loads

Flexion – Ulnar Length Change



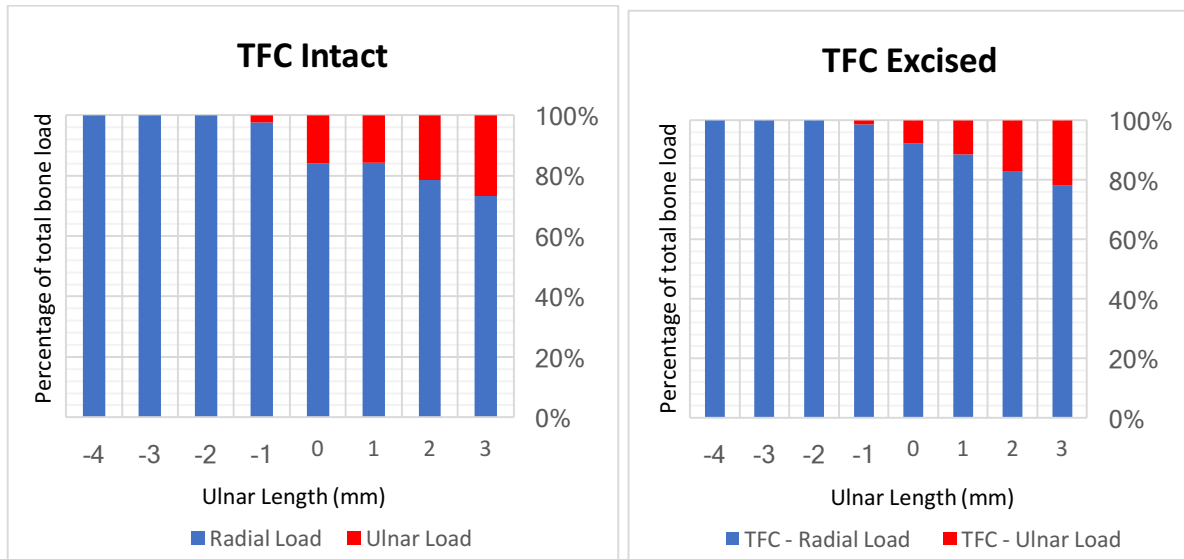
Appendix 2. 15 Percentage load sharing with ulnar length change with and without an intact TFC during flexion expressed as a percentage of forearm compressive loads

Ulnar Deviation – Ulnar Length Change

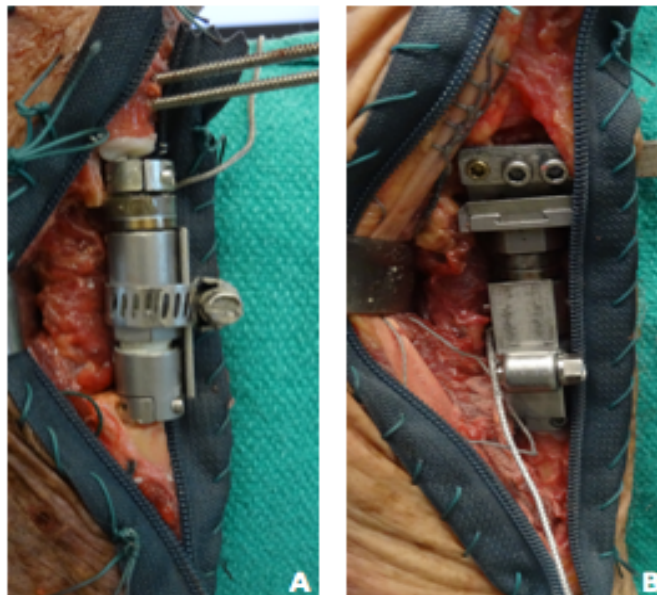


Appendix 2. 16 Percentage load sharing with ulnar length change with and without an intact TFC during ulnar deviation expressed as a percentage of forearm compressive loads

Dart Throw – Ulnar Length Change



Appendix 2. 17 Percentage load sharing with ulnar length change with and without an intact TFC during ulnar deviation expressed as a percentage of forearm compressive loads.



Appendix 2. 18 Ulnar and radial implants in cadaver forearms

- a. *Ulnar Implant in-situ with plate and hose clamp around lead screw to counteract rotational torques.*
- b. *Radial Implant in-situ with plate and hose clamp around lead screw to counteract rotational torques.*

CURRICULUM VITAE

AHAOIZA DIANA ISA MD, FRCSC
Upper Extremity Fellow
Roth | McFarlane Hand and Upper Limb Centre
London, Ontario

Education

Masters of Surgery (MSc) Candidate

The Effect of Radial and Ulnar Length Change on distal forearm loading.

Supervisors: Dr. G. King, Dr. J. Johnson

Site: Bioengineering Lab Roth | McFarlane Hand & Upper Limb Centre, London, Ontario

September 2016 – August 2017

Upper Extremity Fellowship

Location: Roth | McFarlane Hand & Upper Limb Centre, London, Ontario

August 2015 – August 2017

Orthopedic Surgery Residency

Location: Memorial University of Newfoundland (MUN), St. John's, Newfoundland

July 2010 – June 2015

Doctor of Medicine (Honors)

Location: Memorial University of Newfoundland, St. John's, Newfoundland

Received: May 2010

Completion of Phase 1 (Medical Sciences) - (Honors)

Location: International Medical University (IMU), Kuala Lumpur, Malaysia

Twinning program between IMU and Memorial University.

Received: June 2007

PreMed Cambridge A - Levels (Honors)

(Post-secondary GCE Advanced Level qualification offered by educational institutions in England, Wales and Northern Ireland to students completing secondary or pre-university education)

Location: Taylor's University College, Kuala Lumpur, Malaysia

Received: June 2004

Academic Awards and Honors

Award	Reason for award	Location of Tenure	Period held
A. E Shapter Resident Award for Clerkship Teaching in Orthopedic Surgery	Teaching/Education	Memorial University	2011-2012
Charles. E. Frost Award for an Outstanding student in clerkship	Academics	Memorial University	2010
Faculty of Medicine Dean's List	Academics	Memorial University	2010
Faculty of Medicine Phase 1 Dean's List	Academics	International Medical University, Malaysia	2005-2007
Award for High Academic Achievement	Academics	International Medical University, Malaysia	2007
Award for Academic Excellence in Cambridge A-Levels	Academics	Taylor's University College, Malaysia	2003-2004

Examinations and Qualifications

Principles of surgery - Royal College of Physicians and Surgeons Canada 2012
 United States Medical Licensing Examination (USMLE) Step 1 2008
 United States Medical Licensing Examination (USMLE) Step 2 CK 2010
 Licentiate of the Medical Council of Canada (LMCC) Part I 2010
 Licentiate of the Medical Council of Canada (LMCC) Part II 2011
 Royal College of Physicians and Surgeons Orthopedic - Surgery Specialty examination 2015

Publication / Research Record

Functional Outcome of Pediatric Supracondylar Fractures: A 3-5 Year Follow-up
Isa AD, Furey A, Stone C, O’Dea F. Canadian Journal of Surgery (CJOS) 2014

Orthopedic Knowledge Update Chapter 28: Elbow Reconstruction
KJ Faber, **AD Isa**, GA Athwal, GJW King

Arthroscopic Debridement for Primary Elbow Osteoarthritis with and without Capsulectomy: A Comparative Cohort Study
Accepted for publication *Shoulder and Elbow*
AD Isa, GA Athwal, J Macdermid, GJW King, KJ Faber

Diagnostic performance of plain radiographs and 3D CT in evaluating primary elbow osteoarthritis
Manuscript in Review
AD Isa, GJ Puskas, GA Athwal, R Grewal, GJW King, KJ Faber

Conference Presentations

Canadian Orthopedic Association Annual Meeting (COA) (Ottawa, ON) 2017
Arthroscopic Debridement for Primary Elbow Osteoarthritis with and without Capsulectomy: A Comparative Cohort Study (Podium)
AD Isa, GA Athwal, J Macdermid, GJW King, KJ Faber

Orthopedic Trauma Association Annual Meeting (Phoenix, AZ) 2013
Title: Functional Outcome of Pediatric Supracondylar Fractures: A 3-5 Year Follow-up (Poster)
Isa AD, Stone C, O’Dea F, Furey A

Canadian Orthopedic Association Annual Meeting (COA) (Winnipeg, MB) 2013
Title: Functional Outcome of Pediatric Supracondylar Fractures: A 3-5 Year Follow-up (Poster)
Isa AD, Stone C, O’Dea F, Furey A

Canadian Orthopedic Resident Association Annual Meeting (CORA) (Winnipeg, MB) 2013
Title: Functional Outcome of Pediatric Supracondylar Fractures: A 3-5 Year Follow-up (Poster)
Isa AD, Stone C, O’Dea F, Furey A

Work Experience

Locum Orthopedic Surgeon, Moncton, NB: August 2016 and December 2016

Educational Courses/Meetings

Canadian Orthopedic Association Annual Meeting (COA) June 2017
American Academy of Orthopedic Surgeons Annual Meeting (Orange County, FL) March 2016
Canadian Orthopedic Resident Forum (Calgary, AB) April 2015
Sainte-Justine Pediatric Orthopedic Review Course (Montreal, QC) March 2015
Canadian Orthopedic Resident Review in Reconstruction and Pediatrics (Toronto, ON) January 2015
Canadian Orthopedic Resident Review in Trauma (Toronto, ON) November 2014
Current Concepts in Joint Replacement (Las Vegas, Nevada) May 2014
OTA Advanced Fracture Course for Residents (Chicago, IL) April 2014
Orthopedic Trauma Association Annual Meeting (Phoenix, AZ) October 2013
Canadian Orthopedic Association Annual Meeting (COA) (Winnipeg, MB) June 2013
Canadian Orthopedic Resident Association Annual Meeting (CORA) (Winnipeg, MB) June 2013
Advanced Knee Arthroscopy Course (Montreal, QC) November 2012
COA Basic Science Course (Toronto, ON) October 2012
American Academy of Orthopedic Surgeons Annual Meeting (San Francisco, CA) February 2012
AO Basic Fracture Course for Residents (Halifax, NS) May 2010
Stryker Shoulder Arthroscopy Course (St. John's, NL) September 2010
Advanced Trauma Life Support (St. John's, NL) August 2010